

Bestiary of 6D (1, 0) SCFTs: Nilpotent orbits and anomaliesFlorent Baume^{1,*} and Craig Lawrie^{2,†}¹*II. Institut für Theoretische Physik, Universität Hamburg, Luruper Chaussee 149, 22607 Hamburg, Germany*²*Deutsches Elektronen-Synchrotron DESY, Notkestrasse 85, 22607 Hamburg, Germany*

(Received 22 April 2024; accepted 12 July 2024; published 23 August 2024)

Many six-dimensional (1, 0) superconformal field theories (SCFTs) are known to fall into families labeled by nilpotent orbits of certain simple Lie algebras. For each of the three infinite series of such families, we show that the anomalies for the continuous zero-form global symmetries of a theory labeled by a nilpotent orbit O of \mathfrak{g} can be determined from the anomalies of the theory associated to the trivial nilpotent orbit (the parent theory), together with the data of O . In particular, knowledge of the tensor branch field theory is bypassed completely. We show that the known anomalies, previously determined from the geometric/atomic construction, are reproduced by analyzing the Nambu-Goldstone modes inside of the moment map associated to the \mathfrak{g} flavor symmetry of the parent SCFT. This provides further evidence for the physics underlying the labeling of the SCFTs by nilpotent orbits. We remark on some consequences, such as the reinterpretation of the 6D a -theorem for such SCFTs in terms of group theory.

DOI: [10.1103/PhysRevD.110.045021](https://doi.org/10.1103/PhysRevD.110.045021)**I. INTRODUCTION**

In recent years, the study of six-dimensional superconformal field theories (SCFTs) has undergone rapid progress. While such theories were conjectured to exist from an analysis of superconformal algebras [1], the absence of any concrete bottom-up construction led to the widespread doubt of their existence. Such SCFTs can be shown to lack any relevant or marginal (supersymmetry-preserving) parameters [2–6], precluding the existence of a straightforward Lagrangian approach, and rendering the usual weakly coupled perturbative techniques impotent. Instead, it is necessary to develop alternative techniques, often string-theoretic, to both understand the existence of such inherently strongly coupled quantum field theories, and to extract their physical behavior.

It was not until the heyday of string theory that a construction giving rise to an interacting 6D SCFT with maximal supersymmetry was developed. Consider type IIB string theory compactified on an orbifold singularity:

$$\mathbb{C}^2/\Lambda, \quad (1.1)$$

where Λ is a finite subgroup of $SU(2)$. As the orbifold is a noncompact Calabi-Yau twofold, the compactification does not break supersymmetry entirely, but preserves half the supersymmetry in the resulting effective six-dimensional theory. The fundamental degrees of freedom of the compactified theory are tensionless self-dual strings, which arise from the type IIB perspective from D3-branes wrapping the collapsed, zero-volume cycles associated to the orbifold singularity. However, it was shown in [7–9], that these are, in fact, local superconformal field theories, and each tensionless string couples to a self-dual two-form potential which belongs to a tensor multiplet. There is a moduli space of supersymmetric vacua parametrized by the vacuum expectation values of the scalar fields inside of these tensor multiplets; this is the *tensor branch* of the SCFT. At the generic point of the tensor branch all of the self-dual strings are tensionful. The classification of finite subgroups of $SU(2)$ is an ADE-classification; thus, there are two infinite series of 6D (2, 0) SCFTs and three sporadic SCFTs, corresponding to

$$A_{N \geq 1}, \quad D_{N \geq 4}, \quad E_6, \quad E_7, \quad E_8. \quad (1.2)$$

Typically, we use this ADE-classification to label each 6D (2, 0) SCFT by a simple and simply laced Lie algebra. The top-down construction of strongly coupled superconformal field theories, either from string theory or from higher-dimensional field theory, has been extremely powerful over the last thirty years; see [10] for a recent review.

The type IIB string theoretic construction just described yields 6D SCFTs with maximal supersymmetry. It is natural to consider an analogous construction for 6D

*Contact author: florent.baume@desy.de†Contact author: craig.lawrie1729@gmail.com

Published by the American Physical Society under the terms of the [Creative Commons Attribution 4.0 International license](https://creativecommons.org/licenses/by/4.0/). Further distribution of this work must maintain attribution to the author(s) and the published article's title, journal citation, and DOI. Funded by SCOAP³.

SCFTs with minimal supersymmetry. Instead of the orbifold in Eq. (1.1), we can consider the compactification of type IIB string theory on a noncompact Kähler surface which is *not* Calabi-Yau. Naively, this breaks all of the supersymmetry in the effective six dimensional theory, however, it is possible to simultaneously turn on a non-trivial axio-dilaton profile such that one quarter of the supersymmetry is preserved. In this way, we should replace the noncompact Calabi-Yau twofold of Eq. (1.1) with a noncompact elliptically fibered Calabi-Yau threefold, where the elliptic fibration captures the axio-dilaton profile; this puts us squarely in the realm of F-theory [11–13].

The generalization to such Calabi-Yau threefold compactifications has been worked out in [14,15]. Consider a noncompact elliptically fibered Calabi-Yau threefold

$$\pi: Y \rightarrow B, \tag{1.3}$$

where the base of the fibration, B , contains no complex curves of finite volume. The base may be singular, in which case we assume that it has at most one singular point, which we label as b_0 . Further, we assume that $\pi^{-1}(b)$ is an irreducible, possibly degenerate, genus-one curve, for all points $b \in B$; thus [16], we can write the elliptic fibration Y as a Weierstrass model over B . Assume that the Weierstrass model has at most one nonminimal fiber,¹ supported over the point b_0 in B . Then F-theory compactified on Y leads to an interacting 6D (1, 0) SCFT with a single energy-momentum tensor.² Thus, to construct 6D (1, 0) SCFTs, it is necessary to know how to construct Calabi-Yau threefolds satisfying the requisite properties.

We know that for the construction of the 6D (2, 0) SCFTs, the base B takes the form of an orbifold singularity:

$$B = \mathbb{C}^2/\Lambda. \tag{1.4}$$

In [14], it was shown that for any Y that engineers a 6D SCFT, the base must instead be a “generalized orbifold.” These take the same form as in Eq. (1.4), however Λ is now allowed to be particular finite subgroups of $U(2)$, instead of $SU(2)$. We refer the reader to [14] for a review of the generalized orbifolds, in particular the action of the finite group Λ on the coordinates of \mathbb{C}^2 . In the end, there are two families of generalized orbifolds, known as generalized A -type and generalized D -type orbifolds, each parametrized by a pair of integers p, q , and which we write as

$$\mathcal{A}_{(p,q)}, \quad \mathcal{D}_{(p+q,q)}. \tag{1.5}$$

¹The definition of nonminimal is somewhat technical and not particularly illuminating, so we suppress it here. We refer the reader to [17] for a full review of the construction of 6D (1, 0) SCFTs from F-theory.

²The edge-case, where there is neither a singular point in the base, nor a nonminimal singular fiber, leads to a trivial SCFT.

For particular combinations of the parameters, the generalized orbifolds reduce to the standard orbifold singularities. There is no generalization of the standard E -type orbifolds.

Once a generalized orbifold \mathbb{C}^2/Λ has been specified, it is necessary to provide information which captures the nature of the nonminimal singular fiber supported over the orbifold point. In fact, as we review in Sec. II, it is sufficient to encode this data in a choice of (possibly trivial) ADE Lie algebra, \mathfrak{g} . In the end, then, one can obtain the following families of 6D (1, 0) SCFTs:

$$\mathcal{A}_{(p,q)}^{\mathfrak{g}}, \quad \mathcal{D}_{(p+q,q)}^{\mathfrak{g}}, \quad E_6^{\mathfrak{g}}, \quad E_7^{\mathfrak{g}}, \quad E_8^{\mathfrak{g}}. \tag{1.6}$$

This constitutes a natural generalization of the families of 6D (2, 0) SCFTs in Eq. (1.2). Here the possibilities for \mathfrak{g} are constrained by the surface singularity. Similarly, the values of p and q that can appear are constrained as only certain combinations correspond to 6D (1, 0) SCFTs, see [14].

In this paper, we focus on families of theories where the number of tensor multiplets can be taken to be arbitrarily large. As such, we do not consider the E -type bases further here, however, see [18] for an analysis of those SCFTs. Similarly, when the theories $\mathcal{A}_{(p,q)}^{\mathfrak{g}}$ and $\mathcal{D}_{(p+q,q)}^{\mathfrak{g}}$ admit a large N limit in the number of tensors, the combinations (p, q, \mathfrak{g}) are further constrained. In particular, for $\mathcal{A}_{(p,q)}^{\mathfrak{g}}$, they are specified by an integer $N \geq 1$, and two fractions f_L and f_R which belong to the set

$$\left\{ \frac{1}{6}, \frac{1}{5}, \frac{1}{4}, \frac{1}{3}, \frac{2}{5}, \frac{1}{2}, \frac{3}{5}, \frac{2}{3}, \frac{3}{4}, \frac{4}{5}, \frac{5}{6}, 1 \right\}. \tag{1.7}$$

The f_L and f_R are related to the numbers of fractional M5-branes in the M-theory dual descriptions of these 6D (1, 0) SCFTs, as we discuss momentarily. For a choice of (p, q) , specified by fractions f_L and f_R , the choice of algebra \mathfrak{g} must satisfy that

$$\max(\text{denom}(f_L), \text{denom}(f_R)) \leq \frac{n_{\mathfrak{g}}}{2}, \tag{1.8}$$

where $\text{denom}(\cdot)$ is the denominator of the fraction and $n_{\mathfrak{g}} = 2, 4, 6, 8, 12$ for $\mathfrak{g} = \mathfrak{su}(K), \mathfrak{so}(2K), e_6, e_7, e_8$, respectively. Similarly, the $\mathcal{D}_{(p+q,q)}^{\mathfrak{g}}$ theories that exist for large numbers of tensors can be specified by an integer $N \geq 4$, a fraction f belonging to the set in Eq. (1.7), and an ADE Lie algebra \mathfrak{g} which satisfies the analogous condition to Eq. (1.8). We write these theories as

$$\mathcal{A}_{N-1;f_L,f_R}^{\mathfrak{g}}, \quad \text{and} \quad \mathcal{D}_{N;f}^{\mathfrak{g}}. \tag{1.9}$$

for convenience. These are the families of 6D (1, 0) SCFTs that generalize the infinite series of AD-type 6D (2, 0) SCFTs.³

³When $f_L = f_R = 1$ or $f = 1$, then the generalized orbifold is just the standard orbifold. We will use the shorthand $\mathcal{A}_{N-1}^{\mathfrak{g}} = \mathcal{A}_{N-1;1,1}^{\mathfrak{g}}$ and $\mathcal{D}_N^{\mathfrak{g}} = \mathcal{D}_{N;1}^{\mathfrak{g}}$ for convenience.

Here, we have constructed the theories in Eq. (1.9) from type IIB string theory (or its nonperturbative avatar, F-theory). However, each member of these families of theories can also be realized in M-theory. The description of $\mathcal{A}_{N-1}^{\mathfrak{g}}$ in terms of M5-branes is straightforward. It is the 6D (1, 0) SCFT that lives on the world volume of a stack of N M5-branes probing a \mathbb{C}^2/Γ orbifold singularity, where Γ is the finite subgroup of $SU(2)$ with the same ADE-type as \mathfrak{g} . Notice that both the M-theory and F-theory descriptions involve an orbifold, but in the former it is associated to the “fiber data,” \mathfrak{g} , and in the later it is instead associated to the base of the elliptic fibration: A_{N-1} . As we discuss later, when the fractional numbers are different than 1, there are “fractional” M5-branes, and when the base is of generalized D-type, there are orientifold 5-branes in the M-theory description.

The theory $\mathcal{A}_{N-1;f_L,f_R}^{\mathfrak{g}}$, which is known as (fractional) conformal matter [19], typically has a non-Abelian flavor algebra which is

$$\mathfrak{f} = \mathfrak{g}_{f_L} \oplus \mathfrak{g}_{f_R}, \quad (1.10)$$

where \mathfrak{g}_{f_L} and \mathfrak{g}_{f_R} are simple Lie algebras fixed by f_L and f_R . When $\mathcal{A}_{N-1;f_L,f_R} = A_{N-1}$, this theory is simply rank N ($\mathfrak{g}, \mathfrak{g}$) conformal matter, and $\mathfrak{g}_{f_L=1} = \mathfrak{g}_{f_R=1} = \mathfrak{g}$. It has been proposed that giving a nilpotent vacuum expectation value to the moment map associated to the $\mathfrak{g}_{f_L} \oplus \mathfrak{g}_{f_R}$ flavor symmetry triggers a Higgs branch renormalization group flow to a new interacting 6D (1, 0) SCFT [20–22], for N sufficiently large.⁴ Such vacuum expectation values depend only on a choice of nilpotent orbit, rather than the nilpotent element itself, and thus we can consider a family of 6D (1, 0) SCFTs

$$\mathcal{A}_{N-1;f_L,f_R}^{\mathfrak{g}}(O_L, O_R), \quad (1.11)$$

where O_L and O_R are nilpotent orbits of $\mathfrak{g}_{f_L}^L$ and $\mathfrak{g}_{f_R}^R$, respectively. Similarly, the theories $\mathcal{D}_{N,f}^{\mathfrak{g}}$ have only a single non-Abelian flavor factor

$$\mathfrak{f} = \mathfrak{g}_f, \quad (1.12)$$

and again new interacting 6D SCFTs can be obtained via nilpotent Higgsing of that flavor symmetry. Picking O as a nilpotent orbit of \mathfrak{g}_f , we then have the family of theories⁵

$$\mathcal{D}_{N,f}^{\mathfrak{g}}(O). \quad (1.13)$$

Another interesting family of 6D (1, 0) SCFTs that are realized in the geometric F-theory construction are the so-called rank N (e_8, \mathfrak{g}) orbi-instanton theories [19]. From the M-theory perspective, these SCFTs live on the world volume of N M5-branes probing a \mathbb{C}^2/Γ orbifold, where Γ is the finite ADE group corresponding to the simple Lie algebra \mathfrak{g} , and contained inside of an end-of-the-world M9-brane. Furthermore, we can choose an f belonging to the set in Eq. (1.7), such that f and \mathfrak{g} satisfy the analogous condition to that in Eq. (1.8). Let $N \geq 1$, then we can denote this family of theories as

$$\mathcal{O}_{N,f}^{\mathfrak{g}}. \quad (1.14)$$

These theories possess a flavor symmetry which is

$$\mathfrak{f} = e_8 \oplus \mathfrak{g}_f, \quad (1.15)$$

where \mathfrak{g}_f is again fixed by the fraction f . The \mathfrak{g}_f arises from the orbifold singularity in M-theory, and again it is expected that giving a vacuum expectation value to the associated moment map generically triggers a Higgs branch renormalization group flow that leads to a new interacting 6D (1, 0) SCFT. On the other hand, the e_8 flavor symmetry does not arise from the orbifold singularity, but instead from the M9-brane; in particular, it is necessary to pick a choice of boundary conditions, on the S^3/Γ boundary of the \mathbb{C}^2/Γ orbifold, for the E_8 -bundle associated to the M9-brane. Such a boundary condition corresponds to a choice of homomorphism

$$\sigma: \Gamma \rightarrow E_8. \quad (1.16)$$

The e_8 flavor symmetry factor is realized when σ is the trivial homomorphism, and the symmetry is broken to a subalgebra for any other choice of ρ . It is widely believed that there exists a Higgs branch renormalization group flow from the theory with σ trivial to any theory where the homomorphism is nontrivial [29]. That is, there is a family of 6D (1, 0) SCFTs

$$\mathcal{O}_{N,f}^{\mathfrak{g}}(\sigma, O), \quad (1.17)$$

where σ belongs to $\text{Hom}(\Gamma, E_8)$ and O is a nilpotent orbit of \mathfrak{g}_f , which arise via Higgs branch renormalization group flows from $\mathcal{O}_{N,f}^{\mathfrak{g}}$.

It turns out that, once the effective field theory at the generic point of the tensor branch involves a sufficiently large number of tensor multiplets,⁶ every known 6D SCFT

⁴The Higgs branch renormalization group flows triggered by such vacuum expectation values do not exhaust the interacting fixed points on the Higgs branch, in general. For example, there are also flows triggered by giving vevs to so-called end-to-end operators, such as have been studied in [23–28]. We do not study the effects of this “end-to-end Higgsing” in this paper.

⁵The Higgs branch of the $\mathcal{D}_{f,N}^{\mathfrak{g}}(O)$ family of SCFTs is analyzed extensively in [18].

⁶The required number of tensor multiplets is not particularly large.

belongs to one of the families in Eqs. (1.11), (1.13), and (1.17).⁷

We have now discussed, in some detail, a mechanism for constructing 6D (1, 0) SCFTs via the compactification of F-theory on certain noncompact elliptically fibered Calabi-Yau threefolds. However, since these theories are inherently strongly coupled, and cannot be written down in a Lagrangian formulation, it is generally hard to extract the physical properties. Anomalies are by nature topological, and thus it should be possible to determine them without detailed access to the microscopics of the SCFT.

Consider first the 6D (2, 0) SCFTs that are engineered via type IIB string theory compactified on an orbifold singularity, \mathbb{C}^2/Λ . When $\Lambda = \mathbb{Z}_K$, the SCFT has an alternative interpretation as the world volume theory on a stack of K M5-branes in M-theory. The anomalies of the (2, 0) SCFT can then be determined by considering anomaly inflow from the M-theory bulk. The dependence of the anomalies of all 6D (2, 0) SCFTs on the finite group Λ has been determined [31–37]:

$$I_8 = \frac{h_{\mathfrak{g}}^{\vee} d_{\mathfrak{g}}}{24} p_2(N) + \frac{r_{\mathfrak{g}}}{48} (p_2(N) - p_2(T)) + \frac{1}{4} (p_1(T) - p_1(N))^2. \quad (1.18)$$

This is a formal eight-form polynomial in the characteristic classes of the global symmetries of the SCFT. The $p_i(T)$ are the Pontryagin classes of the tangent bundle to the 6D spacetime, this captures the $\mathfrak{so}(1, 5)$ Lorentz group; $p_i(N)$ are the Pontryagin classes of the bundle associated to the $\mathfrak{so}(5)_R$ R-symmetry. The coefficients $h_{\mathfrak{g}}^{\vee}$, $d_{\mathfrak{g}}$, and $r_{\mathfrak{g}}$ are, respectively, the dual Coxeter number, the dimension, and the rank of the ADE Lie algebra \mathfrak{g} of the same ADE-type as the finite group Λ .

Similarly, the anomaly polynomials for the 6D (1, 0) SCFTs can be worked out from the geometric description of the effective tensor branch field theory. Generically, the anomaly polynomial can be written as follows⁸:

⁷There are two subtleties here. First, we are considering only the local operator spectrum of the 6D SCFT; when considering extended operators, each member of the families given here may correspond to multiple SCFTs that differ only in their spectrum of extended operators. Second, there are discretely gauged versions of some members of these families; these are distinct as local SCFTs, however, for the purposes of the anomalies that we consider in this paper, they can be treated as equivalent. For more details on the discretely gauged 6D (1, 0) SCFTs, and especially their Higgs branches, see [30].

⁸Throughout this paper, we typically ignore Abelian flavor symmetries; it is straightforward to generalize the analysis to include the anomalies for such symmetries. Abelian symmetries require additional care due to the presence of ABJ anomalies which does not occur with non-Abelian Lie algebras as their generators are traceless [38,39].

$$I_8 = \frac{\alpha}{24} c_2(R)^2 + \frac{\beta}{24} c_2(R) p_1(T) + \frac{\gamma}{24} p_1(T)^2 + \frac{\delta}{24} p_2(T) + \sum_a \text{Tr} F_a^2 \left(\kappa_a p_1(T) + \nu_a c_2(R) + \sum_b \rho_{ab} \text{Tr} F_b^2 \right) + \sum_a \mu_a \text{Tr} F_a^4. \quad (1.19)$$

Now, $c_2(R)$ is the second Chern class of the bundle associated to the $\mathfrak{su}(2)_R$ R-symmetry; and, $\text{Tr} F_a^2$ and $\text{Tr} F_a^4$ are the one-instanton normalized traces of the curvature, F_a , for each simple non-Abelian factor in the flavor algebra.

On the tensor branch of the SCFT, where the strings become tensionful, the superconformal symmetry is broken, however, the Lorentz symmetry, the R-symmetry, and any flavor symmetry remains unbroken. As the coefficients in the anomaly polynomial in Eq. (1.19) are coefficients of characteristic classes of unbroken symmetry, they are unchanged under the movement onto the tensor branch. Thus, one can determine the anomaly polynomial of the effective field theory at the generic point of the tensor branch, and then use a variant of 't Hooft anomaly matching [40], to determine the anomaly polynomial of the SCFT at the origin of the tensor branch [37,41–43].⁹ In particular, see Algorithm 1 of [43] for a concise and comprehensive algorithm to determine the SCFT anomaly polynomial from any tensor branch configuration in the F-theory construction.

For the 6D (2, 0) SCFTs, we could see precisely how the anomaly coefficients in Eq. (1.18) depended on the data of the F-theory compactification; in this case, the noncompact elliptically fibered Calabi-Yau threefold is the trivial elliptic fibration over the orbifold singularity in Eq. (1.1), and we see directly how the coefficients in Eq. (1.18) depend on Λ . Of course, using the tensor branch effective field theory, it is straightforward to apply 't Hooft anomaly matching to determine the anomaly coefficients *in terms of the data of the tensor branch theory*. In particular, the dependence of the anomaly coefficients on the tensor branch data, such as the number of vector multiplets, hypermultiplets, the Green-Schwarz couplings, etc., has been determined for many of theories studied here, see, for example, [37,43,47–52].

In this paper, we take an orthogonal approach: we would like to know how the anomalies of the theories

$$\mathcal{A}_{N-1;f_L,f_R}^{\mathfrak{g}}(O_L, O_R), \quad \mathcal{D}_{N;f}^{\mathfrak{g}}(O), \quad \mathcal{O}_{N;f}^{\mathfrak{g}}(\emptyset, O), \quad (1.20)$$

where \emptyset represents the trivial homomorphism $\sigma: \Gamma_{\mathfrak{g}} \rightarrow E_{\mathfrak{g}}$, can be determined from a bottom-up SCFT perspective.

⁹Alternatively, one can attempt to determine certain combinations of the 't Hooft anomaly coefficients from the conformal bootstrap; this orthogonal approach has been shown, in certain cases, to recover the anomaly coefficients determined from the F-theory geometry [44–46].

We determine the anomalies of the, so-called, parent, or ultraviolet, theories

$$\mathcal{A}_{N-1;f_L,f_R}^{\mathfrak{g}}, \quad \mathcal{D}_{N;f}^{\mathfrak{g}}, \quad \mathcal{O}_{N;f}^{\mathfrak{g}}, \quad (1.21)$$

from the tensor branch effective field theory. Then, we argue that the anomalies of the infrared theories in Eq. (1.20) can be written in terms of the anomalies of the parent theories in Eq. (1.21) and the nilpotent orbits, without further recourse to the effective field theory on the tensor branch. In particular, we determine the anomalies from the tensor branch, and we show that the resulting anomalies are exactly what one would expect from the bottom-up nilpotent Higgsing of the moment map of an SCFT, where the only modes to decouple in the infrared are the Nambu-Goldstone modes inside of the moment map.

The structure of this paper is as follows. In Sec. II, we review the atomic construction of 6D (1, 0) SCFTs in F-theory, and detail the three infinite series of SCFTs whose anomalies we explore in this paper. We determine the anomaly polynomials for the three infinite series of 6D (1, 0) SCFTs, written in terms of the nilpotent orbit data, that we consider in this paper in Sec. III. In Sec. IV, we compute the contribution to the anomaly polynomial from the Nambu-Goldstone modes inside of the moment map upon Higgsing, and show that the bottom-up approach, captured in Algorithm 1, reproduces the anomaly polynomial known from the tensor branch description. We discuss some consequences and future directions in Sec. V. Finally, in Appendices A–D, we provide a comprehensive review of the necessary data for nilpotent orbits, and enumerate how nilpotent orbits are related to 6D (1, 0) tensor branch geometries.

II. THE BESTIARY OF LONG 6D SCFTS

In Sec. I, we have explained how a noncompact elliptically fibered Calabi-Yau threefold, subject to certain conditions, can give rise to a 6D (1, 0) SCFT via the medium of F-theory. Unfortunately, these elliptic fibrations involve nonminimal fibers supported over points of the base of the fibration, which, *a priori*, renders them challenging to work with directly. Luckily, a method is

known through which such elliptic fibrations can be obtained [14,15].

The general strategy to obtain a 6D (1, 0) SCFT via F-theory is to construct an elliptically fibered Calabi-Yau threefold, \tilde{Y} , with a smooth base \tilde{B} containing a set of curves $\Sigma^i \subset \tilde{B}$, such that the elliptic fibration is minimal. F-theory compactified on this elliptic fibration in fact gives a description of the theory on the generic point of the tensor branch of the SCFT. The conformal fixed point is reached by shrinking all curves in the base to zero volume. The possible \tilde{Y} such that the contraction map leads to a Y which engineers a 6D (1, 0) SCFT are highly constrained. The curves must then have self-intersection $\Sigma^i \cdot \Sigma^i = -n$ with $12 \leq n \leq 1$, and to be able to contract them simultaneously for all curves, their adjacency matrix must furthermore be negative definite:

$$A^{ij} = \Sigma^i \cdot \Sigma^j < 0. \quad (2.1)$$

One can enumerate every elliptically fibered Calabi-Yau threefold \tilde{Y} satisfying the necessary conditions. Collapsing all curves to zero size one can then reach the geometries Y describing any 6D (1, 0) SCFT admitting a construction via F-theory. This was achieved in [14,15], where it was concluded that at the fixed point, all bases are given by a choice of orbifold $B = \mathbb{C}^2/\Lambda$, with Λ a discrete subgroup of $U(2)$. We now review the procedure whereby elliptic fibrations \tilde{Y} , that lead to elliptic fibrations Y that engineer a 6D (1, 0) SCFT, can be constructed.

As is now common in the literature, we denote a curve of self-interaction $(-n)$ with a nontrivial fiber associated with a gauge algebra \mathfrak{g} by:

$$\frac{\mathfrak{g}}{n}. \quad (2.2)$$

When the fiber is trivial, $\mathfrak{g} = \emptyset$, we omit it and only write the curve associated with the tensor multiplet. Furthermore, if two curves intersect, which they can only do with intersection number 1, they are depicted side by side.

The tensor branch of any 6D (1, 0) SCFT can then be constructed from a small number of building blocks associated to non-Higgsable clusters (NHCs) [12,13,53]

$$\begin{matrix} \mathfrak{su}_3 & \mathfrak{so}_8 & \mathfrak{f}_4 & \mathfrak{e}_6 & \mathfrak{e}_7 & \mathfrak{e}_7 & \mathfrak{e}_8 & \mathfrak{su}_2 \mathfrak{q}_2 & \mathfrak{su}_2 \mathfrak{q}_2 & \mathfrak{su}_2 \mathfrak{so}_7 \mathfrak{su}_2 \\ 3, & 4, & 5, & 6, & 7, & 8, & (12), & 2 \ 3, & 2 \ 2 \ 3, & 2 \ 3 \ 2, \end{matrix} \quad (2.3)$$

or to ADE Dynkin diagrams constructed out of (-2) -curves

$$\underbrace{2 \dots 2}_{N-1}, \quad \underbrace{2 \dots 2}_2 \ 2, \quad \underbrace{2}_{22222}, \quad \underbrace{2}_{222222}, \quad \underbrace{2}_{2222222}. \quad (2.4)$$

The fiber over each of these curves may be tuned so that it corresponds to a larger algebra as long as it leads

to a well-defined elliptic fibration. These enhancements may give rise to additional matter fields on these curves, and there may be a flavor symmetry \mathfrak{f} rotating them. We denote the presence of additional flavor symmetries as

$$\frac{\mathfrak{g}}{n}[\mathfrak{f}]. \quad (2.5)$$

Any SCFT is then obtained by gluing non-Higgsable clusters—possibly with enhanced fibers—via (-1) -curves that have a flavor symmetry \mathfrak{f} . For instance, if we consider two curves $\overset{\mathfrak{g}_L}{m}$ and $\overset{\mathfrak{g}_R}{n}$, we can gauge a subalgebra of \mathfrak{f} to obtain a new theory:

$$\overset{\mathfrak{g}_L}{m} \overset{\mathfrak{g}}{1} \overset{\mathfrak{g}_R}{n}, \quad \mathfrak{g}_L \oplus \mathfrak{g}_R \subset \mathfrak{f}. \quad (2.6)$$

Note that when the subalgebra is not maximal, there might be a residual flavor symmetry in the new configuration.

This process can then be repeated as many times as necessary to obtain bases of an elliptic fibration with an arbitrary number of curves subject to the condition that there are only minimal singularities and that the adjacency matrix A^{ij} is negative definite. On the tensor branch, where the curves have finite volume, one can then find the gauge spectrum straightforwardly. In practice, it is done simply by reading off the matter content from tables in the large majority of cases. For a concise review of the tensor branch description of 6D $(1, 0)$ SCFTs we have summarized here and the subtleties that may arise, we defer to [17].

A simple example of this pictorial description of the geometry is that of minimal (e_6, e_6) conformal matter. In the blown-up phase, it is constructed out of two (-1) -curves with trivial fibers intersecting a (-3) -curve with a type-IV fiber corresponding to an \mathfrak{su}_3 algebra. An inspection of the geometry further reveals the presence of two non-compact curves with e_6 fibers, giving rise to two flavor symmetries. The theory on the tensor branch is therefore denoted by:

$$[e_6]1 \overset{\mathfrak{su}_3}{3} 1[e_6]. \quad (2.7)$$

The conformal fixed point is then reached by simultaneously shrinking every curve to zero volume. This example will be used throughout this section to illustrate some of the features of long quivers.

Depictions of the blown-up geometry—or equivalently of the tensor branch of a 6D SCFT—like the one in Eq. (2.7) are called *generalized quivers* (or often simply quivers, for short), dubbed so due to their resemblance with those appearing in usual gauge theories, but where the links symbolizing bifundamental hypermultiplets are now potentially replaced by more complicated objects, generalizing the notion of matter. A quiver describing the generic point of tensor branch of a 6D SCFT is unique in all but a handful of cases; by abuse of language we will often refer to a specific SCFT and its quiver interchangeably.

The possible curve configurations of the generalized quivers are very constrained by demanding that the elliptically fibered Calabi-Yau is well defined, or equivalently by demanding the absence of gauge anomalies of the field theory. When the number of curves—or

TABLE I. ADE classification of minimal conformal matter and the associated nodes of self-intersection $(-n_{\mathfrak{g}})$. Type A conformal matter corresponds to a $(1, 0)$ hypermultiplet transforming in the bifundamental representation of $\mathfrak{su}(K) \oplus \mathfrak{su}(K)$, and is simply denoted by a dot (\cdot) .

\mathfrak{g}	$A_0^{\mathfrak{g}}: [\mathfrak{g}]-[\mathfrak{g}]$	Node $n_{\mathfrak{g}}$
\mathfrak{su}_K	$[\mathfrak{su}_K] \cdot [\mathfrak{su}_K]$	$\overset{\mathfrak{su}_K}{2}$
\mathfrak{so}_{2K}	$[\mathfrak{so}_{2K}] \overset{\mathfrak{sp}_{K-4}}{1} [\mathfrak{so}_{2K}]$	$\overset{\mathfrak{so}_{2K}}{4}$
e_6	$[e_6]1 \overset{\mathfrak{su}_3}{3} 1[e_6]$	e_6
e_7	$[e_7]1 \overset{\mathfrak{su}_2}{2} \overset{\mathfrak{so}_7}{3} \overset{\mathfrak{su}_2}{2} 1[e_7]$	e_7
e_8	$[e_8]12 \overset{\mathfrak{su}_2}{2} \overset{\mathfrak{g}_2}{3} \overset{\mathfrak{f}_4}{15} \overset{\mathfrak{g}_2}{13} \overset{\mathfrak{su}_2}{2} 21[e_8]$	e_8 (12)

equivalently tensor multiplets—is taken to be large enough, it turns out that they must arrange themselves into a long linear spine with repeating patterns, up to possible “decorations” at each side. The constituents of the spine are themselves 6D $(1, 0)$ SCFTs called minimal $(\mathfrak{g}, \mathfrak{g})$ conformal matter [19], of which Eq. (2.7) is an example. In the M-theory picture, these correspond to the world volume theory on a single M5-brane probing a \mathbb{C}^2/Γ singularity, where Γ is a finite subgroup of $SU(2)$. These theories follow an ADE classification and have a $\mathfrak{f} = \mathfrak{g} \oplus \mathfrak{g}$ flavor symmetry, where \mathfrak{g} is of the same ADE type as Γ .

When $\Gamma = \mathbb{Z}_K$, the SCFT is nothing else but a single hypermultiplet transforming in the bifundamental representation of $\mathfrak{su}_K \oplus \mathfrak{su}_K$. For the other types of simply laced algebras, conformal matter can therefore be thought of as a generalization of ordinary bifundamental matter—hence their name—and we will use the following shorthand to depict them:

$$[\mathfrak{g}]-[\mathfrak{g}], \quad (2.8)$$

where the brackets indicate the presence of the two flavor symmetries. The ADE algebra \mathfrak{g} uniquely determines the quiver of minimal conformal matter, and is summarized in Table I.

The interpretation of minimal conformal matter as a generalization of bifundamental hypermultiplets does not simply come from their flavor symmetries, but as simple building blocks of more involved theories. Indeed, we can “glue” two minimal conformal matter theories together to obtain a larger SCFT through a procedure called *fusion* [22], which generalizes the usual notion of gauging. Indeed, while in four dimensions gauging a flavor symmetry by introducing a vector multiplet to mediate the interaction is sufficient, this is not always the case in six dimensions, and the new theory may still be plagued by gauge anomalies. However, one of the features of six-dimensional QFTs is the presence of tensor multiplets, which can be involved in a Green-Schwarz-West-Sagnotti

mechanism [54–56] curing any such anomalies, and leading to a well-defined theory. We come back to this point in more detail in Sec. III.

From the geometric point of view, the fusion procedure corresponds to identifying the two noncompact curves associated with the flavor symmetries and make the resulting curve compact. In the quiver language, these particular curves are called *nodes*, and their self-intersection numbers are fixed by demanding consistency of the F-theory geometry. The particular numerology depends on the ADE algebra, and are given in Table I.¹⁰

For instance, in the case $\mathfrak{g} = \mathfrak{e}_6$ encountered in Eq. (2.7), the fusion process applied to two minimal conformal matter theories leads to the presence of a (-6) -curve with a type-IV* fiber associated with an \mathfrak{e}_6 gauge interaction

$$[\mathfrak{e}_6]1 \overset{\mathfrak{su}_3}{3} 1[\mathfrak{e}_6] \oplus [\mathfrak{e}_6]1 \overset{\mathfrak{su}_3}{3} 1[\mathfrak{e}_6] = [\mathfrak{e}_6]1 \overset{\mathfrak{su}_3}{3} 1(\overset{\mathfrak{e}_6}{6})1 \overset{\mathfrak{su}_3}{3} 1[\mathfrak{e}_6]. \quad (2.9)$$

Heuristically, we obtain something very similar to quiver theories, namely links of (conformal) matter and nodes associated with gauging. However, in our case the links correspond to conformal matter rather than the usual bifundamental hypermultiplets familiar from 4d $\mathcal{N} = 2$ gauge theories, while the nodes necessitate the presence of tensor multiplets to mediate a Green-Schwarz-West-Sagnotti mechanism and ensure that the resulting theory is free of any gauge anomalies. The fusion process can then be concisely summarized utilizing the notation introduced in Eq. (2.8) as:

$$[\mathfrak{g}] - [\mathfrak{g}] \oplus [\mathfrak{g}] - [\mathfrak{g}] = [\mathfrak{g}] - \mathfrak{g} - [\mathfrak{g}], \quad (2.10)$$

where we used the symbol \oplus to denote fusion. The absence of brackets for the middle algebra indicates that the flavor symmetry has been gauged, and that there is an additional compact curve corresponding to a tensor. This notation for fusion of minimal conformal matter completely determines the quiver, the links and nodes being those given in Table I.

This process can of course be repeated *ad nauseam* to obtain patterns of minimal conformal matter joined by vector and tensor multiplets. When N minimal conformal matter of the same type undergo the fusion process, one obtains *rank N conformal matter*, $A_{N-1}^{\mathfrak{g}}$. In M-theory, this theory is realized as a stack of N M5-branes probing a \mathbb{C}^2/Γ singularity, where Γ is the McKay-dual discrete group of \mathfrak{g} .

We will refer to the SCFTs that are part of the infinite series described in the introduction as *long quivers*. Such

¹⁰Note that for minimal conformal matter of type $\mathfrak{so}(2K)$, the flavor symmetry enhances, $\mathfrak{so}(2K) \oplus \mathfrak{so}(2K) \rightarrow \mathfrak{so}(4K)$, and when $\mathfrak{g} = \mathfrak{so}(8)$, we have an undecorated (-1) -curve associated with the E-string theory endowed with \mathfrak{e}_8 flavor. However, when two of them are fused together, only a $\mathfrak{so}(2K) \oplus \mathfrak{so}(2K)$ flavor symmetry remains. As we are only discussing long quivers in this work, we will not encounter such enhancements.

long quivers can be constructed by fusing additional building blocks on each ends of higher-rank conformal matter. Furthermore, all long quivers can be understood as deformations of three families of *parent* or ultraviolet theories [20,22]:

- (1) (Fractional) higher-rank conformal matter, $\mathcal{A}_{N-1;f_L,f_R}^{\mathfrak{g}}$.
- (2) Theories whose bases are generalized type-D orbifolds, $\mathcal{D}_{N;f}^{\mathfrak{g}}$, existing only for a few specific choice of algebras.
- (3) Orbi-instantons, $\mathcal{O}_{N;f}^{\mathfrak{g}}$, a class of SCFTs with an \mathfrak{e}_8 flavor symmetry on one end.

Given a 6D SCFT with a flavor symmetry, one can give a vacuum expectation value to the associated moment map—the scalar operator inside the same supermultiplet as the flavor current—triggering a renormalization group flow. In the infrared, one obtains a new conformal fixed point. In the F-theory picture, these Higgs branch flows correspond to complex-structure deformations of the Calabi-Yau three-fold. For long quivers, the deformations are labelled by nilpotent orbits of the flavor symmetries, or by embeddings of an ADE discrete group into E_8 in the case of orbi-instanton. In the remainder of this section, we will review how to construct each of the classes of parent theories, and then turn to their deformations.

Before doing so however, we further introduce the concept of the *partial tensor branch* (PTB), which provides an alternative bookkeeping device for the parent theories. Given the generalized quiver depicting the tensor branch of a 6D SCFT, one can successively blow down all (-1) -curves, reaching the so-called endpoint of the base. Ignoring the fiber data, there are only a handful of possible partial tensor branches, which follow an ADE classification:

$$\begin{array}{ccc} n_1 n_2 \dots n_{N-2} n_{N-1}, & 2n_3 n_4 \dots n_{N-1} n_N, & \\ \overset{2}{2222}, & \overset{2}{222222}, & \overset{2}{2222222}. \end{array} \quad (2.11)$$

These partial tensor branches were used in the original classification [14] to find the possible bases, see Eq. (1.1), and one can read of the type of generalized orbifold from the intersection pattern. Generically, partial tensor branches of a quiver have nonminimal singularities supported over the intersection points of the curves in the base. The original quivers on the generic point of the tensor branch is then recovered through a series of blow-ups, reversing the process.¹¹

This special point of the tensor branch has an interpretation in the M-theory language: it is the point where all fractional M5-branes recombine into the maximal number

¹¹Technically, orbi-instantons are associated with the trivial orbifold and have in principle an empty partial tensor branch as we blow down successively all (-1) -curves. However, one generally defines their partial tensor branch to be nontrivial and reproduce the M-theory picture, see Sec. II C.

of full M5-branes. This description is particularly useful, as it makes the fusion processes, as well as Higgs branch deformations, clearer. Moreover, when discussing the anomalies of the associated 6D SCFTs, once the anomaly polynomial of minimal conformal matter is known, the partial tensor branch intersection pattern is—up to a few additional input data—enough to compute that of any long quiver.

A. (Fractional) conformal matter

The simplest class of parent theories with long quivers is the set of rank N $(\mathfrak{g}, \mathfrak{g})$ conformal matter theories: $\mathcal{A}_{(N,N-1)}^{\mathfrak{g}} = A_{N-1}^{\mathfrak{g}}$. In M-theory, they are realized as the world volume theory of a stack of N M5-brane probing a \mathbb{C}^2/Γ orbifold, where $\Gamma \subset SU(2)$ is the McKay-dual discrete group of \mathfrak{g} [19]. In the F-theory picture, one engineers them by compactification on an elliptically fibered Calabi-Yau three-fold with a base $B = \mathbb{C}^2/\mathbb{Z}_N$ and fibers of type \mathfrak{g} .¹² The partial tensor branch of these theories is given by a collection of (-2) -curves with \mathfrak{g} fibers intersecting like an A_{N-1} Dynkin diagram:

$$\underbrace{\overset{\mathfrak{g}}{2} \cdots \overset{\mathfrak{g}}{2}}_{N-1} \quad (2.12)$$

Except in cases where $\mathfrak{g} = \mathfrak{su}(K)$, these geometries have nonminimal singularities over the intersection points of the (-2) -curves; thus, we need to perform a series of blow-ups to move to the generic point of the tensor branch. As an example, let us consider the case where $\mathfrak{g} = e_6$. After blowing-up, one finds a repeating pattern of minimal conformal matter

$$A_{N-1}^{e_6} : \underbrace{\overset{e_6}{2} \cdots \overset{e_6}{2}}_{N-1} \longrightarrow [e_6] \overset{\mathfrak{su}_3}{1} \overset{e_6}{3} \overset{\mathfrak{su}_3}{16} \overset{e_6}{1} \overset{\mathfrak{su}_3}{3} \overset{e_6}{16} \cdots \overset{e_6}{61} \overset{\mathfrak{su}_3}{3} \overset{e_6}{16} \overset{\mathfrak{su}_3}{1} [e_6]. \quad (2.13)$$

The sequence $1 \overset{\mathfrak{su}_3}{3} 1$ occurs N times, and there are $N-1$ nodes $\overset{e_6}{6}$. For the other cases, one can go through a similar procedure and find a long spine of N minimal conformal matter $A_0^{\mathfrak{g}}$ that underwent the fusion process. We can therefore use the notation of links $[\mathfrak{g}]$ — $[\mathfrak{g}]$ to denote the resulting curve configurations as

$$A_{N-1}^{\mathfrak{g}} : \underbrace{\overset{\mathfrak{g}}{2} \cdots \overset{\mathfrak{g}}{2}}_{N-1} \longrightarrow [\mathfrak{g}] \underbrace{\mathfrak{g} \cdots \mathfrak{g}}_N [\mathfrak{g}], \quad (2.14)$$

¹²Note that, while similar in form, the two orbifolds appearing in either descriptions are different. In M-theory, the quotient Γ is related to the flavor algebra \mathfrak{g} , while in F-theory, it is associated with the intersection pattern A_{N-1} of the curves.

where the links and nodes are summarized in Table I. In all cases, there is a flavor symmetry associated with either outermost curves fixed by the choice of \mathfrak{g} , and the total flavor symmetry of higher-rank conformal matter $A_{N-1}^{\mathfrak{g}}$ is

$$\mathfrak{f} = \mathfrak{g} \oplus \mathfrak{g}, \quad (2.15)$$

which we will often refer to as the “left” and “right” factors, respectively.

1. Fractional conformal matter

We have seen that there are additional SCFTs with long quivers that are associated with generalized A-type orbifolds $\mathcal{A}_{(p,q)}$. Moreover, for a large-enough number of curves and given an ADE algebra, there are only a few possibilities. The associated long quivers are again made out of conformal matter as in Eq. (2.14), but either ends of the spine are now truncated versions of conformal matter, where one or more curves have been removed. As mentioned in the Introduction, when discussing long quivers the choices of (p, q) and \mathfrak{g} is quite constrained, and it is more convenient to use the fractions (f_L, f_R) introduced around Eq. (1.7). We denote the base of the elliptic fibration as $\mathcal{A}_{N-1;f_L,f_R}$. The triplet (f_L, f_R, \mathfrak{g}) then constrains the form of the quiver for the theory $\mathcal{A}_{N-1;f_L,f_R}^{\mathfrak{g}}$ uniquely.

To illustrate this, let us come back to the case where $\mathfrak{g} = e_6$. All possible A-type long quivers for this choice of algebra take the form:

$$\mathcal{A}_{N-1;f_L,f_R}^{\mathfrak{g}} : \mathcal{L}_{f_L} \underbrace{\overset{\mathfrak{su}_3}{1} \overset{e_6}{3} \overset{e_6}{16} \cdots \overset{e_6}{61} \overset{\mathfrak{su}_3}{3}}_{N-2} \mathcal{L}_{f_R}, \quad (2.16)$$

where there are $N-2$ minimal conformal matter in the center, and \mathcal{L}_L and \mathcal{L}_R denote an extra link that can be attached at each ends of the spine, and which can be chosen among the following possibilities:

$$\begin{aligned} \mathcal{L}_1 &= \overset{e_6}{61} \overset{\mathfrak{su}_3}{3} 1[e_6], & \mathcal{L}_2 &= \overset{e_6}{61} \overset{\mathfrak{su}_3}{3}, \\ \mathcal{L}_{\frac{1}{2}} &= \overset{e_6}{61} [\mathfrak{su}_3], & \mathcal{L}_{\frac{1}{3}} &= \overset{e_6}{6}. \end{aligned} \quad (2.17)$$

Note that for \mathcal{L}_{f_L} , the curve configuration is understood as being read in such a way that the node $\overset{e_6}{6}$ is connected to the rest of the spine. We can see that $f_{L,R} = 1$ gives a complete conformal matter, and smaller fraction corresponds to removing some of the curves.

Similar patterns occur for all other ADE algebras. The possible fractions f depends on the algebra \mathfrak{g} , and are of the form:

$$f = \frac{2k}{n_{\mathfrak{g}}}, \quad k = 1, 2, \dots, \frac{n_{\mathfrak{g}}}{2}, \quad (2.18)$$

TABLE II. Data for fractional conformal matter, $\mathcal{A}_{N-1;f_L,f_R}^g$. For ease of visualization, the building blocks for minimal conformal matter includes the node. The partial tensor branch (PTB) gives the curve configuration obtained after successively blowing down all (-1) -curves.

\mathfrak{g}	f	$[\mathfrak{g}_f] - \mathfrak{g}$	\mathfrak{g}_f	PTB	d_f	e
\mathfrak{so}_{2K}	$\frac{1}{2}$	\mathfrak{so}_{2K} 4	\mathfrak{sp}_{K-4}	\mathfrak{so}_{2K} 3 ...	2	0
	1	\mathfrak{sp}_{K-4} \mathfrak{so}_{2K} 1 4	\mathfrak{so}_{2K}	\mathfrak{so}_{2K} 2 ...	1	0
e_6	$\frac{1}{3}$	e_6 6	\emptyset	e_6 4 ...	3	-4
	$\frac{1}{2}$	e_6 16	\mathfrak{su}_3	e_6 3 ...	2	0
	$\frac{2}{3}$	\mathfrak{su}_3 e_6 3 16	\emptyset	\mathfrak{su}_3 e_6 2 3 ...	3	4
	1	\mathfrak{su}_3 e_6 1 3 16	e_6	e_6 2 ...	1	0
e_7	$\frac{1}{4}$	e_7 8	\emptyset	e_7 5 ...	4	-9
	$\frac{1}{3}$	e_7 18	\mathfrak{su}_2	e_7 4 ...	3	-4
	$\frac{1}{2}$	\mathfrak{su}_2 e_7 2 18	\mathfrak{so}_7	e_7 3 ...	2	0
	$\frac{2}{3}$	\mathfrak{so}_7 \mathfrak{su}_2 e_7 3 2 18	\mathfrak{su}_2	\mathfrak{so}_7 e_7 2 3 ...	3	4
	$\frac{3}{4}$	\mathfrak{su}_2 \mathfrak{so}_7 \mathfrak{su}_2 e_7 2 3 2 18	\emptyset	\mathfrak{su}_2 \mathfrak{so}_7 e_7 2 2 3 ...	4	9
	1	\mathfrak{su}_2 \mathfrak{so}_7 \mathfrak{su}_2 e_7 1 2 3 2 18	e_7	e_7 2 ...	1	0
e_8	$\frac{1}{6}$	e_8 (12)	\emptyset	e_8 7 ...	6	-20
	$\frac{1}{5}$	e_8 1(12)	\emptyset	e_8 6 ...	5	$-\frac{72}{5}$
	$\frac{1}{4}$	e_8 21(12)	\mathfrak{su}_2	e_8 5 ...	4	-9
	$\frac{1}{3}$	\mathfrak{su}_2 e_8 2 21(12)	\mathfrak{g}_2	e_8 4 ...	3	-4
	$\frac{2}{5}$	\mathfrak{g}_2 \mathfrak{su}_2 e_8 3 2 21(12)	\emptyset	\mathfrak{g}_2 e_8 2 4 ...	5	0
	$\frac{1}{2}$	\mathfrak{g}_2 \mathfrak{su}_2 e_8 13 2 21(12)	\mathfrak{f}_4	e_8 3 ...	2	0
	$\frac{3}{5}$	\mathfrak{f}_4 \mathfrak{g}_2 \mathfrak{su}_2 e_8 5 13 2 21(12)	\emptyset	\mathfrak{f}_4 e_8 3 3 ...	5	0
	$\frac{2}{3}$	\mathfrak{f}_4 \mathfrak{g}_2 \mathfrak{su}_2 e_8 15 13 2 21(12)	\mathfrak{g}_2	\mathfrak{f}_4 e_8 2 3 ...	3	4
	$\frac{3}{4}$	\mathfrak{g}_2 \mathfrak{f}_4 \mathfrak{g}_2 \mathfrak{su}_2 e_8 3 15 13 2 21(12)	\mathfrak{su}_2	\mathfrak{g}_2 \mathfrak{f}_4 e_8 2 2 3 ...	4	9
	$\frac{4}{5}$	\mathfrak{su}_2 \mathfrak{g}_2 \mathfrak{f}_4 \mathfrak{g}_2 \mathfrak{su}_2 e_8 2 3 15 13 2 21(12)	\emptyset	\mathfrak{su}_2 \mathfrak{g}_2 \mathfrak{f}_4 e_8 2 2 2 3 ...	5	$\frac{72}{5}$
	$\frac{5}{6}$	\mathfrak{su}_2 \mathfrak{g}_2 \mathfrak{f}_4 \mathfrak{g}_2 \mathfrak{su}_2 e_8 2 2 3 15 13 2 21(12)	\emptyset	\mathfrak{su}_2 \mathfrak{g}_2 \mathfrak{f}_4 e_8 2 2 2 2 3 ...	6	20
1	\mathfrak{su}_2 \mathfrak{g}_2 \mathfrak{f}_4 \mathfrak{g}_2 \mathfrak{su}_2 e_8 12 2 3 15 13 2 21(12)	e_8	e_8 2 ...	1	0	

where $n_{\mathfrak{g}} = 2, 4, 6, 8, 12$ for $\mathfrak{g} = \mathfrak{su}(K), \mathfrak{so}(2K), e_6, e_7, e_8$, respectively. Note that $n_{\mathfrak{g}}$ is (minus) the self-intersection of the corresponding nodes, see Table I. In the case of $\mathfrak{g} = \mathfrak{su}(K)$, there are no new possibilities as the only allowed fraction is $f = 1$, while $\mathfrak{g} = e_8$ has the largest number of choices. As the fraction becomes smaller, we are retaining fewer and fewer curves to obtain only part of a full conformal matter theory, giving its name to this class of theories. This further means that the choice of f is also

changing the flavor symmetry of the theory to a—possibly trivial—subalgebra $\mathfrak{g}_f \subseteq \mathfrak{g}$. All combinations of fractions of a given algebra, their curve configurations, flavor symmetry \mathfrak{g}_f , and the associated data that will be useful for the computation of their anomaly polynomials are collated in Table II.

In the same way that rank N conformal matter can be built out of minimal conformal matter via the fusion process, we can define a new type of building block which is a fractional version of minimal conformal matter, $\mathcal{A}_{0,f,1}^g$. Pictorially, we will denote them as

$$\mathcal{A}_{0,f,1}^g : [\mathfrak{g}_f] - [\mathfrak{g}]. \tag{2.19}$$

This theory can be glued to an arbitrary number of complete conformal matter (that is, those with $f = 1$) through fusion to obtain the theory $\mathcal{A}_{N-1;f_L,f_R}^g$.

$$\mathcal{A}_{N-1;f_L,f_R}^g : [\mathfrak{g}_{f_L}] - \overbrace{\mathfrak{g} - \mathfrak{g} - \dots - \mathfrak{g} - \mathfrak{g}}^{N-2} - [\mathfrak{g}_{f_R}]. \tag{2.20}$$

Each link can be considered as a theory in its own right. As they are only part of a full-fledged minimal conformal matter, we refer to these theories as *fractional* conformal matter. We can therefore unambiguously define the parent theories of all long quivers associated with an A-type generalized orbifolds. Indeed, given a quiver in the notation above, the complete curve configurations can be read out from Tables I and II. Of course, when $f_L = 1 = f_R$, we recover rank N conformal matter as shown in Eq. (2.14) and we have $\mathcal{A}_{N-1,1,1}^g = \mathcal{A}_{N-1}^g$.

While the assignment of a fractional number to each of the curve configurations of fractional minimal conformal matter may at first seem somewhat *ad hoc*, it finds its origin in the M-theory construction. There, these SCFTs are realized as the world volume of M5-branes probing a (partially) frozen version of the C^2/Γ singularity [48,57–61], where there exist BPS solutions characterized by discrete three-form fluxes:

$$\int_{S^3/\Gamma} C_3 = f \pmod{1}. \tag{2.21}$$

These frozen versions of the singularity are associated with the (possibly empty) Lie algebra $\mathfrak{g}_f \subset \mathfrak{g}$, that depends on the value of f , and can now be nonsimply laced. The possible values of the fractions and the algebras arising in this way perfectly match the numerology of the F-theory picture, as expected.

The partial tensor branch of fractional conformal matter $\mathcal{A}_{N-1;f_L,f_R}^g$ is slightly different that those of higher-rank conformal matter, see Eq. (2.12). When the fraction is of the form $f = \frac{1}{d_f}$, we obtain a curve of self-intersection $-(d_f + 1)$ with an algebra \mathfrak{g} rather than -2 . When the

numerator is different than one, we may obtain different patterns, which in the M-theory picture can be understood as a recombination of the M5-branes into fractional branes [48]. For instance the theory $\mathcal{A}_{N-1; \frac{1}{3}, \frac{2}{3}}^{\mathfrak{g}}$ has a partial tensor branch of the form

$$[\mathfrak{su}_3] 1 6 1 3 1 6 1 3 1 \cdots 6 1 3 1 6 1 3 \xrightarrow{e_6 \mathfrak{su}_3 \quad e_6 \mathfrak{su}_3 \quad e_6 \mathfrak{su}_3} 3 2 2 \cdots 2 2 3 2 \quad (2.22)$$

For completeness, we have given the curve configuration of the partial tensor branch at one side of the quiver given the choice of fraction and algebra in Table II.

B. Type-D bases

Let us now move to long quivers whose F-theory bases are given by generalized type-D orbifolds that are part of the infinite series $\mathcal{D}_{(p,q)} = \mathcal{D}_{N,f}$. As with generalized A-type orbifolds, the tensor branch of these SCFTs can again be constructed through fusion of minimal conformal matter theories together, but now they exhibit the trivalent vertex typical to type-D Dynkin diagram on one end. In M-theory, they are the world volume theory of a stack of N M5-branes probing a \mathbb{C}^2/Γ singularity, but contrary to ordinary conformal matter, the stack also contains OM5-branes [52,62,63].

Focusing for a moment on theories with a D_N base, on the partial tensor branch we have a collection of (-2) -curves arranging like the associated Dynkin diagram:

$$2 \underbrace{2 \cdots 2}_{N-3} \quad (2.23)$$

Undecorated, this quiver corresponds to the type-D $(2, 0)$ theory. As in the case of conformal matter, the fibers over each curve can be tuned to obtain theories with minimal supersymmetry, which lead to more general quivers after blowing up nonminimal singularities. However, demanding that there are only minimal singularities after this procedure is very restrictive. There are indeed only a few cases for which this is possible, corresponding to a choice of algebras $\mathfrak{g} = \mathfrak{su}(3), \mathfrak{su}(2L), \mathfrak{so}(8), e_6$. We will not go into the details of the blow-up procedure, but rather enumerate all the possible theories of type $D_N^{\mathfrak{g}}$, and argue that the generalized-orbifold versions follow immediately.

The first class of D-shaped quivers is obtained by considering hypermultiplets transforming in the bifundamental representation of $\mathfrak{su}(K) \oplus \mathfrak{su}(K)$ and a collection of (-2) -curves. Anomaly cancellation then dictates that on the trivalent intersection K is even. This fixes the algebras on the spine and up to decorations on the other end, one finds

$$D_N^{\mathfrak{su}_{2L}} : 2 \overset{\mathfrak{su}_L}{2} \underbrace{2 \cdots 2}_{N-3} [\mathfrak{su}_{2L}]. \quad (2.24)$$

There is however an exception to this condition. When dealing with the low-rank algebras $\mathfrak{su}(2)$ and $\mathfrak{su}(3)$, the absence of independent quartic Casimir invariants relaxes the constraints and one finds that the following quiver leads to a well-defined theory:

$$D_N^{\mathfrak{su}_3} : 2 \overset{2}{\mathfrak{su}_2 \mathfrak{su}_3} \underbrace{2 \cdots 2}_{N-3} [\mathfrak{su}_3]. \quad (2.25)$$

Note that in both cases, there are versions of these theories with algebras of lower rank at the end of the spine. As we will explain shortly, these can be obtained as deformations of these quivers.

One may wonder why we are not considering a variation of the quivers above, but where there is a ramp of $\mathfrak{su}(K)$ algebras of ever-increasing ranks:

$$2 \overset{\mathfrak{su}_2 \mathfrak{su}_3 \mathfrak{su}_4}{2 2 \cdots} ? \quad (2.26)$$

Naively, it appears that the $\mathfrak{su}(3)$ gauge algebra has the correct number of fundamental hypermultiplets (i.e., six) to cancel the gauge anomaly induced by the vector multiplet. However, due to the trivalent pattern, the matter arising

from the intersection of two curves $2 \overset{\mathfrak{su}_2 \mathfrak{su}_3}{2}$ transforms in the representation $(\mathbf{2} \oplus \mathbf{1}, \mathbf{3})$ rather than the usual bifundamental of $\mathfrak{su}(2) \oplus \mathfrak{su}(3)$ [64]. An $\mathfrak{su}(4)$ algebra is therefore not allowed, and quivers with such a ramp do not lead to consistent theories.

A similar phenomenon occurs for algebra of type $\mathfrak{so}(2K)$. There, the only allowed parent theory is given by $(\mathfrak{so}(8), \mathfrak{so}(8))$ conformal matter attached to one of the non-Higgsable clusters given in Eq. (2.3) to obtain the type-D shape

$$D_N^{\mathfrak{so}_8} : 2 \overset{\mathfrak{su}_2}{2} \overset{\mathfrak{so}_7}{3} 1 4 1 4 \cdots 4 1 [\mathfrak{so}_8]. \quad (2.27)$$

One could once again imagine a ramp of increasing rank, but an analysis of the associated geometry reveals that having anything but an $\mathfrak{so}(8)$ algebra on the left-most (-4) -curve does not lead to a consistent F-theory model [65].

Finally, if one consider exceptional algebras, there is a single case for which a trivalent intersection can be obtained using the gluing procedure of non-Higgsable clusters discussed around Eq. (2.6), and involves the algebra $\mathfrak{g} = e_6$

$$D_N^{e_6} : \overset{\mathfrak{su}_3}{3} \overset{1}{e_6 \mathfrak{su}_3} \underbrace{e_6 \mathfrak{su}_3 \cdots e_6 \mathfrak{su}_3}_{N-3} 1 [e_6]. \quad (2.28)$$

This quiver can be understood as fusing a rank $(N - 2)$ conformal matter theory, $A_{N-3}^{e_6}$, with two $\frac{1}{3}$ -fractional theories $\mathcal{A}_{0;1;\frac{1}{3}}^{e_6}$.

TABLE III. Quiver description of the trivalent attachments used 6D (1, 0) SCFTs of type $\mathcal{D}_{N,f}^{\mathfrak{g}}$.

\mathfrak{g}	$\mathfrak{g}_1-\mathfrak{g}_2-\mathfrak{g}$
\mathfrak{su}_{2K}	$\begin{matrix} \mathfrak{su}_L & \mathfrak{su}_{2L} & \mathfrak{su}_{2L} \\ 2 & 2 & 2 \end{matrix}$
\mathfrak{su}_3	$\begin{matrix} \mathfrak{su}_2 & \mathfrak{su}_3 \\ 2 & 2 \end{matrix}$
\mathfrak{so}_8	$\begin{matrix} \mathfrak{su}_2 & \mathfrak{so}_7 & \mathfrak{so}_8 \\ 2 & 3 & 14 \end{matrix}$
e_6	$\begin{matrix} \mathfrak{su}_3 & e_6 & \mathfrak{su}_3 & e_6 \\ 3 & 161 & 3 & 16 \end{matrix}$

In fact, all type-D families can be constructed in a similar way: the trivalent node is obtained by fusing a higher-rank conformal matter with two fractional (possibly deformed) minimal ones. To respect the symmetry of the type-D Dynkin diagram, the latter two are the same. We are also of course free to choose the other end to be associated with fractional conformal matter. Using fusion, we then easily find the fractional version associated with generalized type-D orbifolds

$$\mathcal{D}_{N,f}^{\mathfrak{g}} = D_p^{\mathfrak{g}} \oplus \mathcal{A}_{N-p-1;1,f}^{\mathfrak{g}}. \quad (2.29)$$

In the pictorial description we have used, any theory with a type-D endpoint can therefore be summarized as

$$\mathcal{D}_{N,f}^{\mathfrak{g}} : \mathfrak{g}_1-\mathfrak{g}_1-\mathfrak{g}-\overbrace{\mathfrak{g}-\mathfrak{g}-\dots-\mathfrak{g}}^{N-4}-[\mathfrak{g}_f] \quad (2.30)$$

The allowed combinations $\mathfrak{g}_1-\mathfrak{g}_2$ are summarized in Table III, while the fractional conformal matter at the other end can be found in Table II. As expected, a choice of algebra \mathfrak{g} and a fractional number f (or equivalently the parameters (p, q) of the orbifold) completely defines the quiver.

C. Orbi-instantons

The last class of long quivers corresponds to orbi-instanton theories, $\mathcal{O}_{N,f}^{\mathfrak{g}}$. In the M-theory picture, they

arise as the world volume theories on a stack of N M5-branes probing a \mathbb{C}^2/Γ orbifold, and inside an end-of-the-world M9-brane. When there are no frozen singularities, they are realized in F-theory by an elliptically fibered Calabi-Yau with a trivial base $B = \mathbb{C}^2$. On the partial tensor branch, their quivers take the following form [19]:

$$[\mathfrak{e}_8] \underbrace{1 \overset{\mathfrak{g}}{2} \overset{\mathfrak{g}}{2} \dots \overset{\mathfrak{g}}{2} \overset{\mathfrak{g}}{2}}_{N-1} [\mathfrak{g}]. \quad (2.31)$$

On a generic point of the tensor branch, we once again recover a long spine of fused minimal $(\mathfrak{g}, \mathfrak{g})$ conformal matter, but demanding the e_8 symmetry associated with the M9-brane at one end gives a more involved curve configuration. For instance, when $\mathfrak{g} = \mathfrak{su}(K)$, we obtain a single undecorated (-1) -curve followed by a long ramp of \mathfrak{su}_p curves where the rank increases until it reaches $p = K$

$$\mathcal{O}_N^{\mathfrak{su}_K} : 1 \overset{\mathfrak{su}_2}{2} \overset{\mathfrak{su}_3}{2} \dots \overset{\mathfrak{su}_K}{2} \underbrace{\overset{\mathfrak{su}_K}{2} \dots \overset{\mathfrak{su}_K}{2}}_{N-1}. \quad (2.32)$$

This pattern extends to any of the ADE algebras: a rank N $(\mathfrak{g}, \mathfrak{g})$ conformal matter is attached to the *minimal orbi-instanton*, another building block we depict by $[\mathfrak{e}_8] \rightsquigarrow [\mathfrak{g}]$ and whose curve configuration is given in Table IV for any algebra \mathfrak{g} . If there are frozen singularities in the M-theory realization of these theories, in F-theory the base of the elliptic Calabi-Yau will not be trivial, but rather a generalized type-A orbifold of low order associated with the presence of the fractional conformal matter. The fusion point of view is again very useful, as the curve configuration of any orbi-instanton can be uniquely depicted as

$$\mathcal{O}_{N,f}^{\mathfrak{g}} : [\mathfrak{e}_8] \rightsquigarrow \underbrace{\mathfrak{g} - \dots - \mathfrak{g}}_{N-2} - [\mathfrak{g}_f]. \quad (2.33)$$

The links and nodes can then be read off from Tables I, II, and IV. The non-Abelian flavor symmetry

TABLE IV. Quiver for the minimal orbi-instantons, used as a building block for 6D (1, 0) SCFTs of type $\mathcal{O}_{N,f}^{\mathfrak{g}}$. The numbers f_{OI} and α_0 are coefficients appearing in their anomaly polynomial.

\mathfrak{g}	$[\mathfrak{e}_8] \rightsquigarrow [\mathfrak{g}]$	f_{OI}	α_0
\mathfrak{su}_K	$\begin{matrix} \mathfrak{su}_2 & \mathfrak{su}_3 & \mathfrak{su}_{K-1} & \mathfrak{su}_K \\ 12 & 2 & 2 & 2 \end{matrix}$	$K + 1$	$\frac{2K(K^2-1)}{15} (3K^2 - 32)$
\mathfrak{so}_{2K}	$\begin{matrix} \mathfrak{su}_2 & \mathfrak{so}_9 & \mathfrak{so}_{11} & \mathfrak{so}_{13} & \mathfrak{so}_{15} & \mathfrak{so}_{17} & \mathfrak{so}_{19} & \mathfrak{so}_{21} & \mathfrak{so}_{23} & \mathfrak{so}_{25} \\ 12 & 2 & 3 & 1 & 4 & 1 & 4 & 1 & 4 & 1 \end{matrix}$	$K + 1$	$\frac{8K(K-1)}{15} (82 - 203K + 27K^2 + 12K^3)$
e_6	$\begin{matrix} \mathfrak{su}_2 & \mathfrak{g}_2 & \mathfrak{f}_4 & \mathfrak{su}_3 & e_6 & \mathfrak{su}_3 \\ 12 & 2 & 3 & 151 & 3 & 161 & 3 & 1 \end{matrix}$	6	93120
e_7	$\begin{matrix} \mathfrak{su}_2 & \mathfrak{g}_2 & \mathfrak{f}_4 & \mathfrak{g}_2 & \mathfrak{su}_2 & e_7 & \mathfrak{su}_2 & \mathfrak{so}_7 & \mathfrak{su}_2 \\ 12 & 2 & 3 & 1513 & 2 & 181 & 2 & 3 & 2 & 1 \end{matrix}$	6	575232
e_8	$\begin{matrix} \mathfrak{su}_2 & \mathfrak{g}_2 & \mathfrak{f}_4 & \mathfrak{g}_2 & \mathfrak{su}_2 & e_8 & \mathfrak{su}_2 & \mathfrak{g}_2 & \mathfrak{f}_4 & \mathfrak{g}_2 & \mathfrak{su}_2 \\ 12 & 2 & 3 & 1513 & 2 & 21(12) & 12 & 2 & 3 & 1513 & 2 & 21 \end{matrix}$	6	5204096

of these theories is generically given by

$$\mathfrak{f} = \mathfrak{e}_8 \oplus \mathfrak{g}_f. \quad (2.34)$$

D. Nilpotent orbits and deformations

So far, we have seen that there are three classes of long quivers associated with generalized ADE orbifolds: higher-rank (fractional) conformal matter $\mathcal{A}_{N-1;f_L,f_R}^{\mathfrak{g}}$, orbi-instanton theories $\mathcal{O}_{N;f}^{\mathfrak{g}}$, and SCFTs with generalized type-D bases, $\mathcal{D}_{N;f}^{\mathfrak{g}}$, for which only a handful of algebras are allowed. In the pictorial notation we have utilized throughout this section, the parent theories can all be summarized as

$$\begin{aligned} \mathcal{A}_{N-1;f_L,f_R}^{\mathfrak{g}} : & \quad [\mathfrak{g}_{f_L}] - \mathfrak{g} - \mathfrak{g} - \dots - \mathfrak{g} - \mathfrak{g} - [\mathfrak{g}_{f_R}], \\ \mathcal{D}_{N;f}^{\mathfrak{g}} : & \quad \begin{array}{c} \mathfrak{g}_1 \\ | \\ \mathfrak{g}_1 - \mathfrak{g}_2 - \mathfrak{g} - \mathfrak{g} - \dots - \mathfrak{g} - [\mathfrak{g}_f] \end{array}, \\ \mathcal{O}_{N;f}^{\mathfrak{g}} : & \quad [\mathfrak{e}_8] \rightsquigarrow \mathfrak{g} - \dots - \mathfrak{g} - [\mathfrak{g}_f]. \end{aligned} \quad (2.35)$$

The curve configuration of these quivers can be inferred from Tables I–IV collated throughout this section without any ambiguity, as a choice of base and algebra fixes it uniquely if N is large.

Given a parent theory, one can perform a complex-structure deformation of the associated elliptically fibered Calabi-Yau threefold, and reach a curve configuration corresponding to the tensor branch description of a new 6D (1, 0) SCFT [14,15]. In the field theory, these are equivalent to Higgs branch renormalization group flow. Starting from the parent theory in the ultraviolet, and giving a particular nontrivial vacuum expectation value to a gauge-invariant operator, we are led to a new interacting 6D SCFT in the deep infrared.

For instance, starting with the quiver of the theory $\mathcal{T}^{\text{UV}} = \mathcal{A}_{N-1}^{\mathfrak{e}_6}$, we can consider the complex-structure deformation of the geometry at the superconformal fixed point in such a way that in passing to the tensor branch geometry it was no longer necessary to perform the blow-up creating the final (−1)-curve on the left. Thus, we obtain a new quiver for the tensor branch of an SCFT \mathcal{T}^{IR} satisfying all the required properties

$$\mathcal{T}^{\text{UV}} : [\mathfrak{e}_6] \overset{\mathfrak{su}_3}{1} \overset{\mathfrak{e}_6}{3} \overset{\mathfrak{su}_3}{16} \overset{\mathfrak{su}_3}{3} 1 \dots \longrightarrow \mathcal{T}^{\text{IR}} : [\mathfrak{su}_6] \overset{\mathfrak{su}_3}{2} \overset{\mathfrak{e}_6}{16} \overset{\mathfrak{su}_3}{3} 1 \dots. \quad (2.36)$$

In the IR theory, there are six hypermultiplets arising from the left-most curve, which are rotated by a new flavor symmetry $\mathfrak{su}(6) \subset \mathfrak{e}_6$. This is in fact a generic feature of deformed theories: if the generalized quiver is long enough, the remnant flavor symmetry is always a subalgebra of that of its parent. Indeed, a property of the parent theories \mathcal{T}^{UV} is that each family has a (possibly trivial) flavor symmetry

\mathfrak{f}^{UV} arising at each end of the quiver. Then, if one deforms it to a new theory \mathcal{T}^{IR} its flavor satisfies

$$\mathfrak{f}^{\text{IR}} \subseteq \mathfrak{f}^{\text{UV}}. \quad (2.37)$$

Moreover, if one end of the quiver of a parent theory has no flavor, either because it corresponds to the trivalent end of a type-D theory, or there is a fraction with a trivial flavor, there exists no deformation preserving the algebra \mathfrak{g} on the spine or the rank N of the base, and there are no new SCFTs descending from that end of the quiver.

Based on these observations it has been proposed that in the field theory, the operator given a vacuum expectation value should be the moment map, the adjoint-valued scalar belonging to the same supermultiplet as a flavor conserved current [15,19]. The flavor \mathfrak{f}^{IR} is then understood as being generated by the unbroken generators. The notion of parent theory was in fact introduced precisely because any other long theories can be understood in such a fashion.

As the deformations are associated to each side of the quiver, we can distinguish two types: those related to an end of a quiver whose flavor come from (fractional) conformal matter, or with the \mathfrak{e}_8 symmetry of an of orbi-instanton theory $\mathcal{O}_{N;f}^{\mathfrak{g}}$. For the latter, it has been argued from M-theory that since the \mathfrak{e}_8 flavor symmetry arises from an end-of-the-world M9-brane, deformations should correspond to choices of boundary condition on the S^3/Γ boundary of the \mathbb{C}^2/Γ orbifold, amounting to embeddings of Γ into E_8 [15,19]. The quiver description of the resulting theory can then be mapped from the choice of embedding [29,49].

On the other hand, when a deformation is performed on the side of the quiver associated with fractional conformal matter with flavor \mathfrak{g}_f , the resulting theories can be labeled by nilpotent orbits of \mathfrak{g}_f . As we review in more detail in Sec. III B, nilpotent orbits O of a simple Lie algebra \mathfrak{g}_f are equivalent to embeddings $\rho_O : \mathfrak{su}(2) \rightarrow \mathfrak{g}_f$. It was then shown that the centralizer \mathfrak{f} of the embedding precisely matches the flavor symmetry of the deformed theories [20].

We can therefore denote all possible SCFTs obtained by deforming one of the three parent families by either a nilpotent orbit of the corresponding flavor symmetry, or in the case of orbi-instantons a choice of embedding of the corresponding discrete group into E_8

$$\mathcal{A}_{N-1;f_L,f_R}^{\mathfrak{g}}(O_L, O_R), \quad \mathcal{D}_{N;f}^{\mathfrak{g}}(O), \quad \mathcal{O}_{N;f}^{\mathfrak{g}}(\sigma, O), \quad (2.38)$$

where

$$\sigma \in \text{Hom}(\Gamma, E_8), \quad O \Leftrightarrow \rho_O \in \text{Hom}(\mathfrak{su}_2, \mathfrak{g}_f). \quad (2.39)$$

The discrete group Γ is the McKay-dual of the simple algebra \mathfrak{g} defining the parent theory. When the choice of embedding is trivial, which we denote $\sigma = \emptyset$, $O = \emptyset$,

corresponding to the undeformed theory, we write simply e.g. $\mathcal{O}_{N,f}^g(\emptyset, \emptyset) = \mathcal{O}_{N,f}^g$ and similarly for the other two families.

In this work, we will only focus on theories associated with a nilpotent orbit of the corresponding possible flavor, and will refer to them as obtained through *nilpotent deformations*, or *nilpotent RG flows* when discussing the corresponding field theory description. Moreover, a possible deformation might propagate through the spine of the parent theory. We will therefore only consider cases where the parameter N of the orbifold base is taken to be large enough such that a deformation on one end does not affect the other. We will refer to the quivers defined through Eq. (2.38) satisfying this property as *long quivers*. In this work, we will focus on the anomaly polynomial of long quivers and their nilpotent deformations. We leave a more detailed analysis of short quivers and orbi-instantons associated with nontrivial choices $\sigma \in \text{Hom}(\Gamma, E_8)$ for future work.

What is more, nilpotent orbits are equipped with a partial ordering given by the Zariski closure operation. One says that for two nilpotent orbits $O, O' \subset \mathfrak{g}$ of a given simple algebra, then $O \leq O'$ if $\overline{O} \subseteq \overline{O'}$, see, e.g., [66,67] and references therein for a detailed exposition. This partial ordering then enables one to arrange the corresponding 6D (1, 0) SCFTs into a Hasse diagram, establishing a hierarchy of the possible complex-structure deformations/nilpotent RG flows [20–22]. These Hasse diagrams refine the above classification as it tells us that, starting with, e.g., a theory $A_{N-1}^g(\emptyset, O_R)$, we can reach the SCFT $A_{N-1}^g(\emptyset, O'_R)$ by further deformations only if $O_R \leq O'_R$. In Appendix C, we give the Hasse diagrams of all the simple algebras appearing in conformal matter theories of exceptional types and their fractions.

Coming back to (e_6, e_6) conformal matter, in Fig. 1 we show all possible deformations, and how they fit in the Hasse diagram of e_6 . One can see that as one goes deeper in the diagram, there are fewer and fewer curves at the generic point of the tensor branch, and more than one minimal conformal matter is ultimately removed from the quiver. This occurs in the vast majority of cases, as nilpotent deformations will usually propagate throughout a portion of the spine, and justifies our focus on long quivers.

The notation for the SCFT defined in Eq. (2.38) is sufficient to (essentially) fully determine the curve configuration of any long quiver.¹³ The dictionary between the choice of orbit and the quiver describing

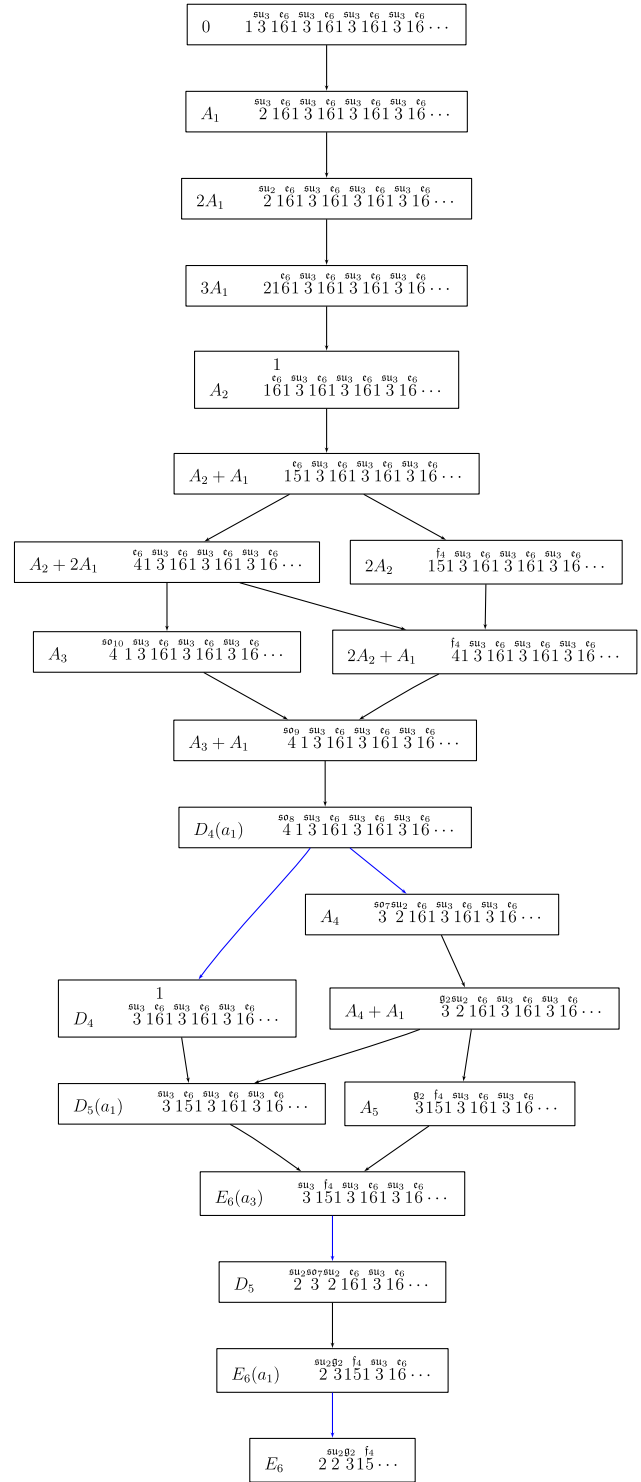


FIG. 1. Hasse diagram for the nilpotent orbits of e_6 and the associated quivers. Each SCFT arising from a nilpotent deformation of the theory $A_{N-1}^{e_6}$ can be associated with a nilpotent orbit, and each arrow can be understood as a possible RG flow. Blue arrows indicate that a new minimal conformal matter is affected with respect to the previous quiver.

¹³In the special case of $\mathfrak{g} = \mathfrak{so}_{2K}$, very-even partitions lead to the same quiver, but are in fact different theories. This can be shown by computing the Schur index of their T^2 compactification [68,69].

the tensor branch of the SCFT depends on the type of algebra—and the fraction, when applicable. For classical flavor algebras, nilpotent orbits are labelled by integer partitions, from which the quiver can be found straightforwardly. In the exceptional cases, we will use Bala-Carter labels [70,71]; there are only a finite number of possibilities, which we have tabulated in Appendix D, where we also give the procedure to obtain the quivers from integer partitions.

We close this section by noting that nilpotent deformations of parent theories and those associated with embeddings of discrete groups into E_8 do not exhaust all possibilities. While SCFTs with the same choice of base \mathbb{C}^2/Λ are on the same Higgs branch, there exists more types of deformations of the geometry or, equivalently, Higgs branch RG flows. Indeed, as mentioned above, there also exist Higgs flows between deformed theories, which are described by transverse Slowdoway slices in the associated Higgs branch moduli space. For completeness, we have labelled each of these transitions using the notation introduced by Kraft and Procesi [72,73] in the Hasse diagrams given in Appendix C. Furthermore, there also exists so-called semisimple deformations [22], which, while keeping the same choice of base in the geometry, changes the algebra, e.g., $A_{N-1}^{\mathfrak{g}} \rightarrow A_{N-1}^{\mathfrak{g}'}$ with $\mathfrak{g}' \subset \mathfrak{g}$. We will focus here only on nilpotent deformations of parent theories, as we will show that the anomaly polynomial of these theories is encoded uniquely in the notation given in Eq. (2.38).

III. ANOMALY POLYNOMIAL OF LONG 6D SCFTS

Having reviewed the possible 6D (1,0) SCFTs associated with long quivers that can be realized via F-theory engineering, we can now study part of their conformal data. We will focus on the anomaly polynomial, which encodes several features of its protected sector, such as the central charges. In six dimensions, the anomaly polynomial of a (1, 0) quantum field theory takes the general form

$$\begin{aligned}
 I_8 = & \frac{\alpha}{24} c_2(R)^2 + \frac{\beta}{24} c_2(R) p_1(T) + \frac{\gamma}{24} p_1(T)^2 + \frac{\delta}{24} p_2(T) \\
 & + \sum_a \text{Tr} F_a^2 \left(\kappa_a p_1(T) + \nu_a c_2(R) + \sum_b \rho_{ab} \text{Tr} F_b^2 \right) \\
 & + \sum_a \mu_a \text{Tr} F_a^4, \tag{3.1}
 \end{aligned}$$

where $c_2(R)$ is the second Chern class of the background R-symmetry bundle, while $p_{1,2}(T)$ are the Pontryagin classes of the spacetime tangent bundle. The index a runs over all simple non-Abelian flavor symmetry factors with background field strength F_a and the traces $\text{Tr} F_a^n$ are chosen to be one-instanton normalized by convention.

The coefficients appearing in the anomaly polynomial of a 6D theory at the SCFT point can be determined from the tensor branch theory using a variation of 't Hooft anomaly matching [37,42]. Indeed, moving onto the tensor branch does not break supersymmetry, nor the possible flavor symmetries. The anomaly polynomial, being a topological quantity, is preserved under this type of deformations and we can therefore reach a point where a gauge theory description in terms of weakly coupled supermultiplets is available. There, the procedure to compute the anomaly polynomial is purely algorithmic, and was described concisely in [43] where it was applied to a large number of theories, closing potential loopholes of the original derivation in the presence of flavor symmetries. Let us now summarize the salient points of the algorithm needed to find Eq. (3.1) for any 6D SCFT.

First, one distinguishes between two different terms, a “one-loop” part, and a Green-Schwarz (GS) contribution:

$$I_8 = I_8^{1\text{-loop}} + I_8^{\text{GS}}. \tag{3.2}$$

The first contains the individual contributions of fermionic and tensor fields inside (1, 0) supermultiplets, and can be understood in terms of four-point correlators of particular protected operators. On the tensor branch where a weakly coupled description is available, these can be computed as one-loop-exact square Feynman diagrams involving the energy-momentum tensor or conserved currents—hence its name. The result of such a computation shows that it is equivalent to study the index of the appropriate differential operator [74]. Indeed, for left-handed chiral fermions transforming in the complex representation \mathbf{R} of a symmetry algebra, it is well known that the formal eight-form related to the Dirac operator is given by¹⁴:

$$I_8^{\text{fermion}} = \frac{1}{2} \hat{A}(T) \text{ch}_{\mathbf{R}}(F) \Big|_{8\text{-form}}, \quad \text{ch}_{\mathbf{R}}(F) = \text{tr}_{\mathbf{R}} e^{iF}, \tag{3.3}$$

where the A-roof genus $\hat{A}(T)$ is associated with gravitational anomalies while the Chern character $\text{ch}_{\mathbf{R}}(F)$ encodes gauge or flavor anomalies. The definitions of these characteristic classes and related quantities are collected in Appendix A.

Note that the traces appearing in the Chern character are performed over a given representation, $\text{tr}_{\mathbf{R}} F^n$, whereas the anomaly polynomial in Eq. (3.1) is defined in terms of one-instanton normalized traces $\text{Tr} F^n$. The conversion between the two is related to Casimir invariants of the symmetry algebras, and up to quartic order we have

¹⁴The result of the computation of the Dirac index takes into account both the representation and its conjugate: $\mathbf{R} \oplus \bar{\mathbf{R}}$. This explain the factor of $\frac{1}{2}$ in Eq. (3.3).

$$\mathrm{tr}_R F^2 = A_R \mathrm{Tr} F^2, \quad \mathrm{tr}_R F^4 = B_R \mathrm{Tr} F^4 + C_R (\mathrm{Tr} F^2)^2. \quad (3.4)$$

The coefficients A_R, B_R , and C_R depend on the representation R ; for representations appearing in the matter spectrum needed in the study of 6D SCFTs, these values have been tabulated in [17].¹⁵ The study of nilpotent deformations and the associated breaking patterns however involves representations that go beyond those usually encountered in the quiver description. The trace-relation coefficients of a representation can nonetheless be found in a straightforward manner knowing the weight system of the Lie algebra. This procedure is reviewed in Appendix A 1.

In addition to contributions from the standard weakly coupled hypermultiplets, the one-loop term $I_8^{\text{1-loop}}$ of a theory might also involve (2, 0) tensor multiplets and E-strings, which may arise in the presence of undecorated (−1)- and (−2)-curves, respectively. The anomaly polynomial of the former can be decomposed in terms of its (1, 0) supermultiplet content, while the contribution of an E-string can be computed via anomaly inflow [41]. The explicit expression of each individual contribution to the one-loop term can be found in, e.g., [37,41,43]. The particular cases of the tensor and vector multiplets, which are the supermultiplets most relevant in this work, are written explicitly later in this section, see Eqs. (3.13) and (3.14).

After summing the contributions of each multiplet in the matter spectrum—which can be read directly from the tensor branch quiver—the one-loop term will generically not be free of all gauge anomalies. However, due to the presence of tensor multiplets in the spectrum, these can be cured via a six-dimensional Green-Schwarz-West-Sagnotti mechanism [54–56], leading to a well-defined theory. This term is a generalized version of the

¹⁵A word of caution to the reader: while most of the recent literature on the anomaly polynomial of 6D SCFTs follow the same conventions as in this work, there has been a myriad of different choices, which sometimes make comparisons arduous. To wit, our normalizations for the traces are:

$$\mathrm{tr}_{\mathrm{adj}} F^2 = h^\vee \mathrm{Tr} F^2, \quad \mathrm{tr}_{\mathcal{F}} F^4 = 1 \cdot \mathrm{Tr} F^4, \quad (3.5)$$

where \mathcal{F} refers to the defining representation of classical algebras. For exceptional cases, $B_R = 0$ due to the absence of an independent order-four Casimir invariant, and the normalization $A_{\mathrm{adj}} = h^\vee$ fixes that of C_R . Additionally, the case of \mathfrak{so}_8 needs special attention as it has two independent quartic Casimir invariants. More details can be found in Appendix A and references therein.

Moreover, since there is no uniform normalization of the trace-relation coefficients, their names also vary greatly across different fields of both mathematics and physics. In the review of 6D SCFTs [17], which tabulates them in Appendix F for representations appearing in generalized quivers, they are defined as: $h_R = A_R$, $x_R = B_R$, and $y_R = C_R$.

celebrated Green-Schwarz mechanism in ten dimensions, and is therefore commonly referred to simply as the Green-Schwarz or “GS” term.

The contribution I_8^{GS} is found at a nongeneric point of the tensor branch reached by successively blowing down all undecorated (−1)-curves. At that point the quiver is described by an adjacency matrix \tilde{A}^{ij} , and the GS term is given by

$$I_8^{\mathrm{GS}} = -\frac{1}{2} \tilde{A}_{ij} I^i I^j, \\ I^i = -\tilde{A}^{ij} c_2(F_j) - B^{ia} c_2(F_a) - (2 + \tilde{A}^{ii}) p_1(T) + y^i c_2(R), \quad (3.6)$$

where $\tilde{A}_{ij} = (\tilde{A}^{-1})_{ij}$, and $c_2(F) = \frac{1}{4} \mathrm{Tr} F^2$ denotes the second Chern class of the gauge and flavor bundles. Note that we will always define them in terms of one-instanton normalized traces, see Eq. (3.4). The four-form I^i is furthermore related to the Bianchi identity for the three-form field strength of the tensor multiplet H_i on the i th curve:

$$dH^i = I^i. \quad (3.7)$$

At the generic point of the tensor branch, the coefficients y^i are given by the dual Coxeter number $h_{\mathfrak{g}_i}^\vee$ of the algebra on the curve, and their changes must be tracked when blowing down (−1)-curves. Finally, the matrix B^{ia} encodes the intersection of noncompact flavor curves with those associated with gauge algebras and is often either zero or one, although special care must be taken when the flavor involves E-strings or (pseudo)-real representations. We defer to the algorithm described in [43] for a detailed explanation of how to obtain the GS contribution.

Once both the one-loop and Green-Schwarz-West-Sagnotti terms have been determined, one obtains a final expression free of any gauge anomaly. While it may seem very cumbersome to track the various coefficients associated to the potentially quite large number of curves for either terms given a quiver, under the classification scheme described in Sec. II, it turns out that the resulting anomaly polynomial always takes a relatively simple form depending only on the parent theory and the nilpotent orbit describing the Higgs mechanism applied to the moment map.

A. Anomaly polynomial of conformal matter

To emphasize the simplicity of the resulting expressions, let us first consider the case of $A_{N-1}^{\mathfrak{g}}$, the rank N ($\mathfrak{g}, \mathfrak{g}$) conformal matter theory, see Sec. II A. Going through the algorithm summarized above, one finds expressions that depend solely on quantities related to \mathfrak{g} [37]

$$\begin{aligned}
 I_8(A_{N-1}^{\mathfrak{g}}) &= \frac{\alpha_{\text{CM}}}{24} c_2(R)^2 + \frac{\beta_{\text{CM}}}{24} c_2(R) p_1(T) + \frac{\gamma_{\text{CM}}}{24} p_1(T)^2 + \frac{\delta_{\text{CM}}}{24} p_2(T) + \frac{B_{\text{adj}}}{48} (\text{Tr} F_L^4 + \text{Tr} F_R^4) \\
 &\quad - \left(\frac{1}{32N} - \frac{C_{\text{adj}}}{48} \right) ((\text{Tr} F_L^2)^2 + (\text{Tr} F_R^2)^2) + \frac{1}{16N} \text{Tr} F_L^2 \text{Tr} F_R^2 + \left(\frac{h_{\mathfrak{g}}^{\vee} p_1(T)}{4} - \frac{1}{8} (\Gamma N - h_{\mathfrak{g}}^{\vee}) c_2(R) \right) (\text{Tr} F_L^2 + \text{Tr} F_R^2).
 \end{aligned} \tag{3.8}$$

By abuse of notation, Γ will denote the order of the McKay-discrete group of \mathfrak{g} —that is, the ADE discrete subgroup of $SU(2)$ of the same type—when appearing in expressions related to the anomaly polynomial. Its value as well as some of the main quantities of simple Lie algebras are collated in Table V for convenience. The coefficients involving purely R-symmetry or spacetime terms are given by

$$\begin{aligned}
 \alpha_{\text{CM}} &= \Gamma^2 N^3 - 2\Gamma\chi N + (\dim(\mathfrak{g}) - 1), \\
 \beta_{\text{CM}} &= -\frac{1}{2}(\Gamma\chi - 1)N + \frac{1}{2}(\dim(\mathfrak{g}) - 1), \\
 \gamma_{\text{CM}} &= \frac{N}{8} + \frac{7 \dim(\mathfrak{g}) - 23}{240}, \\
 \delta_{\text{CM}} &= -\frac{N}{2} - \frac{\dim(\mathfrak{g}) - 29}{60}.
 \end{aligned} \tag{3.9}$$

The form of the tensor branch description of conformal matter depends on the choice of \mathfrak{g} , see Table I, and the gauge spectrum entails various representations of the involved algebras, in particular for exceptional algebras. However, note that the above expressions only depend on standard group-theoretical quantities associated with \mathfrak{g} and its adjoint representation, rather than the details of the quiver. In particular, χ is a combination of the rank of the

TABLE V. Group-theoretic quantities associated with simple Lie algebras relevant in this work. Note that the order of the McKay-dual discrete group, Γ , is defined only for ADE algebra $\mathfrak{su}_n, \mathfrak{so}_{2k}, \mathfrak{e}_{6,7,8}$. Furthermore, exceptional algebras, including $\mathfrak{su}_2, \mathfrak{su}_3$ do not have quartic Casimir invariant, while \mathfrak{so}_8 has two. This changes the values of B_{adj} and C_{adj} for these algebras as a result, see Appendix A for additional details.

\mathfrak{g}	$r_{\mathfrak{g}}$	$\dim(\mathfrak{g})$	$h_{\mathfrak{g}}^{\vee}$	Γ	B_{adj}	C_{adj}
\mathfrak{su}_2	1	3	2	2	0	2
\mathfrak{su}_3	2	8	3	3	0	$\frac{9}{4}$
$\mathfrak{su}_{n \geq 4}$	$n-1$	n^2-1	n	n	$2n$	$\frac{3}{2}$
\mathfrak{so}_8	4	28	6	8	6	3
$\mathfrak{so}_{p \neq 8}$	$\lfloor \frac{p}{2} \rfloor$	$\frac{1}{2}p(p-1)$	$p-2$	$2p-8$	$p-8$	3
\mathfrak{sp}_k	k	$k(2k+1)$	$k+1$	\dots	$2k+8$	$\frac{3}{4}$
\mathfrak{g}_2	2	14	4	\dots	0	$\frac{5}{2}$
\mathfrak{f}_4	4	52	9	\dots	0	$\frac{15}{4}$
\mathfrak{e}_6	6	78	12	24	0	$\frac{9}{2}$
\mathfrak{e}_7	7	133	18	48	0	$\frac{6}{2}$
\mathfrak{e}_8	8	248	30	120	0	$\frac{9}{2}$

algebra and the order of the associated discrete group, and is defined as

$$\chi = r_{\mathfrak{g}} + 1 - \frac{1}{\Gamma}. \tag{3.10}$$

This is our first hint that the moment map—falling in the same multiplet as the flavor current—plays a special role in the anomaly polynomial of conformal matter and its deformations.

The expression given in Eq. (3.8) was first obtained from the tensor branch description in [37], where the result of the algorithm was also cross-checked with an anomaly inflow computation from the M-theory realization, namely as the world volume theory of a stack N M5-branes probing a \mathbb{C}^2/Γ singularity. Through this method, one obtains a more elegant and compact expression for the anomaly polynomial

$$\begin{aligned}
 I_8(A_{N-1}^{\mathfrak{g}}) &= \frac{N^3}{24} (c_2(R)\Gamma)^2 - \frac{N}{2} (c_2(R)\Gamma)(J(F_L) + J(F_R)) \\
 &\quad - \frac{1}{2N} (J(F_L) - J(F_R))^2 + NI_{\text{sing}} - I_8^{\text{tensor}} \\
 &\quad - \frac{1}{2} (I_8^{\text{vec}}(F_L) - I_8^{\text{vec}}(F_R)),
 \end{aligned} \tag{3.11}$$

where we defined the following quantities:

$$\begin{aligned}
 I_{\text{sing}} &= \frac{1}{24} \left(\frac{1}{2} p_1(T) c_2(R) + \frac{1}{8} p_1(T)^2 - \frac{1}{2} p_2(T) \right), \\
 J(F) &= \frac{\chi}{48} (4c_2(R) + p_1(T)) + c_2(F),
 \end{aligned} \tag{3.12}$$

which find their origin in the reduction of the M-theory Chern-Simons terms, and lead to contributions from degrees of freedom localized at the orbifold singularity.¹⁶ In the M-theory realization, one must also remove contributions from the center-of-mass tensor multiplet and those associated with boundary conditions for directions normal to the M5-branes. These are proportional to the anomaly polynomial of tensor and vector multiplets, respectively. As mentioned above, the contribution of these

¹⁶The term proportional to N^{-1} is associated with center-of-mass contributions and was written in Ref. [37] simply as $-\frac{1}{8N} (\text{Tr} F_L^2 - \text{Tr} F_R^2)^2$. While *a priori* unrelated to the reduction of terms near the singularity, in Eq. (3.11) we write it in terms of $J(F)$ for later convenience.

two types of multiplet are given in terms of characteristic classes, see Appendix A

$$\begin{aligned} I_8^{\text{tensor}} &= \left(\frac{1}{2} \text{ch}_2(R) \hat{A}(T) - \frac{1}{8} L(T) \right) \Big|_{8\text{-form}} \\ &= \frac{1}{24} c_2(R)^2 + \frac{1}{48} c_2(R) p_1(T) \\ &\quad + \frac{1}{5760} (23 p_1(T)^2 - 116 p_2(T)), \end{aligned} \quad (3.13)$$

$$\begin{aligned} I_8^{\text{vec}}(F) &= -\frac{1}{2} \hat{A}(T) \text{ch}_2(R) \text{ch}_{\text{adj}}(F) \Big|_{8\text{-form}} \\ &= -\frac{1}{24} (\text{tr}_{\text{adj}} F^4 + 6 c_2(R) \text{tr}_{\text{adj}} F^2 + \dim(\mathfrak{g}) c_2(R)^2) \\ &\quad - \frac{1}{48} p_1(T) (\text{tr}_{\text{adj}} F^2 + \dim(\mathfrak{g}) c_2(R)) \\ &\quad - \frac{\dim(\mathfrak{g})}{5760} (7 p_1(T)^2 - 4 p_2(T)). \end{aligned} \quad (3.14)$$

Equation (3.11) therefore neatly repackages every flavor contribution either in the Chern character of the adjoint representation, or quantities scaling with N , and encoded in $J(F)$. The only remaining explicit dependence on \mathfrak{g} appears through the order of the McKay dual discrete group Γ .

Beyond its elegant form, the usefulness of this expression for the anomaly polynomial is its behavior under fusion, as it makes clear that the resulting theory will be free of any gauge anomaly. Indeed, we have reviewed in the previous section that fusion allows us to “glue” quivers together by gauging common flavor symmetries. Equivalently, in the field theory we are gauging this flavor, and using the tensor multiplet to mediate a Green-Schwarz-West-Sagnotti mechanism so as to ensure a gauge-anomaly-free result. Therefore, the form of the anomaly polynomial in Eq. (3.11) teaches us that we can in fact use it as if it was a one-loop contribution.

To illustrate this, let us consider two minimal, i.e., rank one, $(\mathfrak{g}, \mathfrak{g})$ conformal matter theories, $A_0^{\mathfrak{g}}$. If we fuse them together by gauging one of the common flavor factors, we obtain rank two conformal matter, $A_1^{\mathfrak{g}}$

$$[\mathfrak{g}_L] - [\mathfrak{g}_1] \oplus [\mathfrak{g}_1] - [\mathfrak{g}_R] = [\mathfrak{g}_L] - \mathfrak{g}_1 - [\mathfrak{g}_R], \quad (3.15)$$

where we differentiated the different factors of the same algebra \mathfrak{g} by their respective subscript. By gauging the common the flavor factor \mathfrak{g}_1 , we introduce a vector multiplet in the spectrum, as well as a tensor multiplet to mediate the Green-Schwarz-West-Sagnotti mechanism. The effective one-loop term of the new theory is then given by

$$I_8^{1\text{-loop}} = I_8(A_0^{\mathfrak{g}}; F_L, F_1) + I_8(A_0^{\mathfrak{g}}; F_1, F_R) + I_8^{\text{vec}}(F_1) + I_8^{\text{tensor}}, \quad (3.16)$$

where for clarity, we have shown each of the field strengths explicitly. The form of the anomaly polynomial for $A_{N-1}^{\mathfrak{g}}$, given in Eq. (3.11), makes it clear that the one-loop contribution cannot depend on quartic traces of the gauge algebra, $\text{Tr} F_1^4$, as all contributions $I_8^{\text{vec}}(F_1)$ cancel, and only potentially dangerous terms involving the second Chern class $c_2(F_1)$ remain. These can however be canceled via Green-Schwarz-West-Sagnotti mechanism, using a term of the form

$$\begin{aligned} I_8^{\text{GS}} &= -\frac{1}{2} (\tilde{A}^{11})^{-1} (I^1)^2, \\ I^1 &= -\tilde{A}^{11} J(F_1) - B^{1L} J(F_L) - B^{1R} J(F_R) + \chi e^1 c_2(R). \end{aligned} \quad (3.17)$$

A short inspection of the involved terms reveals that we must choose $\tilde{A}^{11} = -2$, $B^{1L} = B^{1R} = e^1 = 1$. This is precisely what we expect from the partial tensor branch description. In the F-theory construction, when fusing two conformal matter links together we must introduce a compact curve of self-intersection (-2) , possibly leading to nonminimal fibers, see the discussion around Eq. (2.12). We therefore find the base corresponding to the algebra A_1 . Moreover, B^{1L} and B^{1R} can also be understood as the intersection numbers between this (-2) -curve and the noncompact curves supporting the flavor symmetries.

Adding the two contributions from Eqs. (3.16) and (3.17) together, we obtain an expression free of gauge anomalies:

$$\begin{aligned} I_8(A_1^{\mathfrak{g}}) &= I_8(A_0^{\mathfrak{g}}; F_L, F_1) + I_8(A_0^{\mathfrak{g}}; F_1, F_R) + I_8^{\text{vec}}(F_1) \\ &\quad + I_8^{\text{tensor}} + I_8^{\text{GS}}. \end{aligned} \quad (3.18)$$

Comparing this result with Eq. (3.11), one can check that this exactly reproduces the anomaly polynomial of rank two conformal matter, $A_1^{\mathfrak{g}}$. By recursion, this is true also for higher-rank conformal matter; we simply need to fuse N of them together as if they were simple hypermultiplets. The one-loop term is

$$\begin{aligned} I_8^{1\text{-loop}} &= I_8(A_0^{\mathfrak{g}}; F_L, F_1) + I_8(A_0^{\mathfrak{g}}; F_{N-1}, F_R) + (N-1) I_8^{\text{tensor}} \\ &\quad + \sum_{i=1}^{N-1} \left(I_8(A_0^{\mathfrak{g}}; F_i, F_{i+1}) + I_8^{\text{vec}}(F_i) \right), \end{aligned} \quad (3.19)$$

and the remaining gauge terms are cancelled by a similar Green-Schwarz-West-Sagnotti mechanism:

$$\begin{aligned} I_8^{\text{GS}} &= -\frac{1}{2} \tilde{A}_{ij} I^i I^j, \\ I_i &= -\tilde{A}^{ik} J(F_k) - B^{ia} J(F_a) + \chi e^i c_2(R), \end{aligned} \quad (3.20)$$

where $e^i = 1 \forall i$, $\tilde{A}_{ij} = (\tilde{A}^{ij})^{-1}$, and $B^{ia} = \delta_{i-a=1}$. It is easy to see the adjacency matrix \tilde{A}^{ij} must be exactly

(minus) the Cartan matrix of the algebra A_{N-1} associated with the base. The quantity $J(F)$ is then interpreted as a contribution to the Bianchi identity related to the associated tensionless string:

$$dH \sim J(F), \quad (3.21)$$

where H is the field strength of the associated tensor field. This should not be too surprising, as in the anomaly inflow computation in M-theory, the quantity J is by construction associated with a solution for the four-flux form in eleven dimensions: $G_4 \sim J$ [37]. In Eq. (3.11), we can therefore think of the second line as a “one-loop” contribution, essentially depending simply on characteristic classes, while the first originates from the GS term.

This simple argument teaches us that while ’t Hooft anomaly matching enables us to find the anomaly polynomial via the full tensor branch description, once we know the contribution of a single elementary building block at the singular point, namely minimal conformal matter $\mathcal{A}_0^{\mathfrak{g}}$, the rest follows as if we were in a weakly coupled regime. It is in spirit much the same as the case of E-strings: these theories are themselves nonperturbative objects, but once their contribution to the anomaly polynomial has been determined [41], when they are coupled to other weakly coupled supermultiplets to form a more complicated theory, they follow the same rules as if they were regular supermultiplets.

One might think that the case of conformal matter is quite special, and this line of thought should not generalize to more complicated theories. However, since long quivers are made up by fusing minimal conformal matter together up to decorations at each ends, we will now see that a similar reasoning can be applied not only to any parent theory of long quivers, but their nilpotent breakings as well.

Let us first consider the case of fractional conformal matter $\mathcal{A}_{N-1;f_L,f_R}^{\mathfrak{g}}$. Since the fractions are only allowed for algebras \mathfrak{g} of type DE and their number limited, it is straightforward to apply the algorithm and compute the anomaly polynomial of the long quivers in each case. When $f_L = f_R$, this analysis was already performed in [48] by fusing together multiple copies of fractional theories.¹⁷ Based on their results, we have obtained an expression that also applies in cases where $f_L \neq f_R$. As we have seen in the previous section, fractional conformal matter can be depicted as

¹⁷We note that we use different conventions than in [48] to label the theories. There, a long quiver is obtained by fusing different types of quiver than the one we have defined in Table II. For instance, the theory we defined as $\mathcal{A}_{N-1;\frac{1}{3},\frac{1}{3}}^{\mathfrak{e}_6}$ is obtained by fusing the N times the quiver 161 with $N-1$ “nodes” 3 . This notation unfortunately obscures the possibility of having different fractions at each end, and makes breaking patterns harder to track.

$$\mathcal{A}_{N-1;f_L,f_R}^{\mathfrak{g}} : [\mathfrak{g}_{f_L}] - \overbrace{\mathfrak{g} - \mathfrak{g} - \dots - \mathfrak{g} - \mathfrak{g}}^{N-2} - [\mathfrak{g}_{f_R}], \quad (3.22)$$

and we can see that there are $N-2$ “full” minimal conformal matter forming the long spine, and two $\mathcal{A}_{0;1,f_{L,R}}^{\mathfrak{g}}$ theories with a fraction at each end. Defining the “effective” total number of conformal matter as

$$N_{\text{eff}} = (N-2) + f_L + f_R, \quad (3.23)$$

the anomaly polynomial of $\mathcal{A}_{N;f_L,f_R}^{\mathfrak{g}}$ takes a form that, barring the use of N_{eff} rather than N , closely resembles that of its nonfractional cousin—see Eq. (3.11)

$$\begin{aligned} I_8(\mathcal{A}_{N-1;f_L,f_R}^{\mathfrak{g}}) &= \frac{N_{\text{eff}}^3}{24} (c_2(R)\Gamma)^2 \\ &\quad - \frac{N_{\text{eff}}}{2} (c_2(R)\Gamma)(J_{\text{fr}}(F_L) + J_{\text{fr}}(F_R)) \\ &\quad - \frac{1}{2N_{\text{eff}}} (J_{\text{fr}}(F_L) - J_{\text{fr}}(F_R))^2 + N_{\text{eff}} I_{\text{sing}} \\ &\quad - I_8^{\text{tensor}} - \frac{1}{2} (I_8^{\text{vec}}(F_L) + I_8^{\text{vec}}(F_R)) \\ &\quad - (e_L + e_R) I_{\text{fr}}, \end{aligned} \quad (3.24)$$

where the coefficients $e_{L,R}$ are collated in Table II and I_{fr} is defined in Eq. (3.26) below. The main difference between this case and the original anomaly polynomial of conformal matter is that the contribution of the vector multiplets are now taken with respect to the algebras associated with the fractions, \mathfrak{g}_{f_L} and \mathfrak{g}_{f_R} , see Table II, and the four-form related to the Bianchi identity at the fixed point needs to be slightly modified

$$\begin{aligned} J_{\text{fr}}(F) &= \frac{\chi_{\text{fr}}}{48} (4c_2(R) + p_1(T)) + \frac{1}{d_f} c_2(F), \\ \chi_{\text{fr}} &= \chi + 12 \left(1 - \frac{1}{d_f} \right), \quad d_f = \text{denom}(f). \end{aligned} \quad (3.25)$$

In Eq. (3.24), we stress that $r_{\mathfrak{g}}, \Gamma$ are those associated with the “full” algebra \mathfrak{g} , rather than $\mathfrak{g}_{f_{L,R}} \subseteq \mathfrak{g}$, and $J_{\text{fr}}(F_{L,R})$ is defined with respect to the left, respectively right, fraction. In addition, there is also an extra contribution whose prefactor depends on the fractions

$$I_{\text{fr}} = \frac{1}{24} \left(c_2(R)^2 + \frac{1}{6} c_2(R) p_1(T) - \frac{1}{48} (p_1(T)^2 - 4p_2(T)) \right), \quad (3.26)$$

This terms can be understood as coming from the frozen singularity, or equivalently as descending from the contribution of the full, nonfractional, vector multiplet $I_8^{\text{vec}}(F_{\mathfrak{g}})$, which is now decomposed into the fractional

part of the remnant flavor symmetry and I_{fr} . The particular values of the coefficients $e_{L,R}$ are given in Table II. While we have not found a closed-form expression in terms of the fraction numbers and characters such as the A-roof genus \hat{A} , we observe that they do not depend on the full algebra \mathfrak{g} but rather on the fractional number itself, and have a reflection symmetry around $f = \frac{1}{2}$.

As a sanity check, we can see that when $f_L = 1 = f_R$, we recover the result for conformal matter: $J_{\text{fr}}(F) = J(F)$ and $e = 0$ in that case, and the above expression is identical to that of Eq. (3.11).

The anomaly polynomial of higher-rank fractional conformal matter $\mathcal{A}_{N-1;f_L,f_R}^{\mathfrak{g}}$ given in Eq. (3.24) once again enables us to understand this theory as coming from quantities computed directly at the partial tensor branch by fusing rank one building blocks

$$\begin{aligned} I_8(\mathcal{A}_{N-1;f_L,f_R}^{\mathfrak{g}}) &= I_8(\mathcal{A}_{0;f_L,1}^{\mathfrak{g}}; F_L, F_1) \\ &+ \sum_{i=1}^{N-2} (I_8(\mathcal{A}_0^{\mathfrak{g}}; F_i, F_{i+1}) + I_8^{\text{vec}}(F_i)) \\ &+ I_8(\mathcal{A}_{0;1,f_R}^{\mathfrak{g}}; F_{N-1}, F_R) + (N-1)I_8^{\text{tensor}} \\ &+ I_8^{\text{GS}}. \end{aligned} \quad (3.27)$$

The GS terms takes the same form as in Eq. (3.20) with the replacement $J(F) \rightarrow J_{\text{fr}}(O)$ for the contribution at each end, and the pairing matrix \tilde{A}^{ij} must be slightly modified with respect to that of conformal matter. Taking the fractions with unit numerators, $f_{L,R} = \frac{1}{d_{L,R}}$, the presence of incomplete minimal conformal matter at either sides will change the charge of the strings associated with the gauge algebras at both ends of the quiver, and a short computation shows that the pairing matrix is that of the quiver

$$(1 + d_L) \underbrace{\frac{\mathfrak{g}}{2} \dots \frac{\mathfrak{g}}{2}}_{N-2} (1 + d_R). \quad (3.28)$$

This is again exactly what one would expect for the geometry, as it is the partial tensor branch quiver obtained after successively shrinking all (-1) -curves, see Table II.

When the numerators of the fractions are not one, this interpretation gets slightly obscured and the form of the partial tensor branch in Eq. (3.28) needs to be modified. Indeed, as we have discussed in Sec. II, the bases in those cases involve more curves than for the complete conformal matter theories of the same rank. These can however be understood as being realized by fusing further rank one fractional theories to the main spine until the correct fractional number has been achieved. The self-intersection of the additional branes is then understood as above: coming from the Green-Schwarz-West-Sagnotti mechanism the singular point. In the M-theory picture, this phenomenon can also be understood as the recombination

of fractional M5-branes into larger fractional—or even full—M5-branes [48].

Beyond conformal matter, other long quivers with type-D bases $\mathcal{D}_{N;f}^{\mathfrak{g}}$ and orbi-instantons $\mathcal{O}_{N;f}^{\mathfrak{g}}$ can be understood in a similar fashion. We come back to those cases in Sec. III C.

B. Nilpotent Higgs branch flows in six dimensions

The interpretation of the anomaly polynomial of conformal matter as obtained by fusing minimal conformal matter theories together to obtain arbitrary large quivers is quite suggestive, and we will now show that there are similar expressions when a parent theory is deformed to another with deformations associated to nilpotent orbits of the flavor symmetries.

For a given F-theory base, $\mathcal{A}_{N-1;f_L,f_R}$, $\mathcal{D}_{N;f}$ and $\mathcal{O}_{N;f}$, there can be multiple 6D (1, 0) SCFTs, which from the geometric point of view are reached through complex-structure deformations. As alluded to above, in the case of long quivers—that is for large-enough values of N —it has been proposed that a partial classification scheme is given by nilpotent orbits O of simple components of the flavor symmetry [20,47].

Field theoretically, these are interpreted as renormalization group flows. More precisely, the presence of flavor implies the existence of a conserved flavor current, which is part of a $\mathcal{D}[2]$ superconformal multiplet in the nomenclature of [5,6]. Its superconformal primary, called the moment map, is a scalar operator ϕ of conformal dimension $\Delta = 4$, transforming in the adjoint representation of the flavor symmetry, as well as a doublet of the $SU(2)$ R-symmetry. Through the usual arguments, giving a vacuum expectation value to the moment map will trigger an RG flow, ultimately reaching another conformal fixed point in the infrared. The flows of interest are then associated with those where the vacuum expectation values of ϕ is chosen to be a representative of the nilpotent orbit

$$\langle \phi \rangle = X \in O. \quad (3.29)$$

We will refer to such deformations as nilpotent RG flows. Note that in the case of orbi-instantons, nilpotent RG flows are not sufficient to classify all long quivers, and must be supplemented by a choice of embedding of a discrete group $\Gamma \subset SU(2)$ into E_8 . The associated flows are more involved than those coming from nilpotent orbits, and will not be considered here—see however [14,15,29,75,76]. We leave a systematic analysis of their anomaly polynomial for future work.

The case of (fractional) conformal matter corresponds to an unbroken $\mathfrak{g}_L \oplus \mathfrak{g}_R$ flavor symmetry, and therefore the trivial nilpotent orbits $O_{L,R} = \emptyset$ are used: $\mathcal{A}_{N-1;f_L,f_R}^{\mathfrak{g}} = \mathcal{A}_{N-1;f_L,f_R}^{\mathfrak{g}}(\emptyset, \emptyset)$. As we have discussed above, at the level of the anomaly polynomial, these theories can be understood without referring to the details of the F-theory

geometry. One may therefore ask whether the proposed classification scheme from nilpotent orbits can also be understood fully in terms of the gauge-invariant conformal data.

This is indeed the case, and as we will now show, knowing the anomaly polynomial of a parent theory, that of an SCFT reached via an RG flow described by a nilpotent orbit can be obtained directly from simple group-theoretic data, without going through the tensor branch description and the associated algorithm invoking 't Hooft anomaly-matching arguments.

Before describing the prescription to obtain the IR anomaly polynomial, let us first summarize some of the relevant properties of nilpotent orbits of a simple algebra \mathfrak{g} . For an in-depth treatment of the topic, we refer to [67]. Given a nilpotent orbit O , by the Jacobson-Morozov theorem one can construct a triplet (X, Y, H) of generators of \mathfrak{g} satisfying the standard \mathfrak{su}_2 commutation relations, with $X \in O$ and H in the Cartan subalgebra of \mathfrak{g} . A nilpotent orbit therefore defines a homomorphism $\rho_O: \mathfrak{su}(2) \hookrightarrow \mathfrak{g}$.

It follows that for any generator E_i of \mathfrak{g} associated with a simple root, H -eigenvalues of these generators can only take values 0, 1, and 2 (up to conjugacy). They can then be arranged into a *weighted Dynkin diagram* labeling uniquely the nilpotent orbit O ¹⁸:

$$O: [w_1, \dots, w_{r_{\mathfrak{g}}}], \quad [H, E_i] = w_i E_i, \quad w_i = 0, 1, 2. \quad (3.30)$$

While this labeling exists for any type of simple Lie algebra, it is sometimes useful to use an algebra-specific scheme. For instance, nilpotent orbits of \mathfrak{su}_K are in one-to-one correspondence with partitions of K , while those of \mathfrak{so}_{2K} are associated with *even* partitions of K . For exceptional algebras, there are no classification in terms of partitions, and it is common to use so-called Bala-Carter labels [70,71]—see [67] for a discussion of the different ways to label nilpotent orbits. While there is a procedure to find the quiver from a partition for classical algebras, we are not aware of a simple connection between the weighted Dynkin diagram of a nilpotent orbit or its Bala-Carter labels and its curve configuration. We recall that the procedure for partitions and the tables giving the mapping between Bala-Carter labels of exceptional algebras and the associated quivers are given in Appendix D.

As the triplet (X, Y, H) defines the embedding ρ_O , it also induces a branching rule for the adjoint (or any other) representation:

$$\begin{aligned} \rho_O: \mathfrak{g} &\longrightarrow \mathfrak{su}(2)_X \oplus \mathfrak{f}, \\ \mathbf{adj} &\longrightarrow \bigoplus_{\ell} (\mathbf{d}_{\ell}, \mathbf{R}_{\ell}), \end{aligned} \quad (3.31)$$

¹⁸The converse is not true, not all weighted Dynkin diagrams with $w_i = 0, 1, 2$ are associated with a nilpotent orbit.

where $\mathfrak{su}(2)_X$ is written so to emphasize that it is related to the nilpotent element X , rather than the R-symmetry, and \mathfrak{f} is its centralizer in \mathfrak{g} . When X is interpreted as the vacuum expectation value of the moment map, \mathfrak{f} is the (possibly semisimple, or even trivial) remnant flavor symmetry of the infrared theory. For nilpotent deformations of 6D (1, 0) SCFT, they perfectly match the ones that can be read off the tensor branch quivers described in the previous section [20–22].

In the mathematics literature, the branching rule defined in Eq. (3.31) is known as the Jacobson-Morozov decomposition. While the weighted Dynkin diagrams defined in Eq. (3.30) are in principle enough to obtain the branching rule of the adjoint representation of \mathfrak{g} , we have tabulated them in Appendix B for all exceptional algebras. For the classical series, the Jacobson-Morozov decomposition of the defining representation can be read off directly from partitions, and that of the adjoint can then be found using tensor products. This procedure is explained in detail in the same Appendix.

We will now show that the Jacobson-Morozov decomposition is not only enough to find the flavor of a given 6D (1, 0) theory, but the complete anomaly polynomial as well. We will focus first on conformal matter theories with only a single nilpotent orbit turned on, that is the class of SCFT given by $\mathcal{A}_{N-1;1,1}^{\mathfrak{g}}(O, \emptyset)$. If N is large, the breaking on the left will not affect the right-hand side of the quiver.

The anomaly polynomial of the parent theory—that is when O is trivial—in the form given in Eq. (3.11), in addition to its compact form and making it easier to implement the fusion process, has the property that the flavor dependence appears only through $J(F)$ and I_8^{vec} . These two quantities have the advantage that by construction, they behave nicely under branching rules, and will be the basis for our prescription to obtain the anomaly polynomial of the IR theory. It is therefore easy to implement the branching rule given in Eq. (3.31) and rewrite the anomaly polynomial of the parent theory in terms of the flavor data of the IR description. Of course, along the RG flows, there are modes that will decouple, and the IR anomaly polynomial must take this into account. As we will see shortly, once we have found the prescription for conformal matter, we may argue that in the same way that other long quivers are obtained through fusion of lower-rank conformal matter, the prescription also applies to any theory with large-enough N .

To illustrate how the Jacobson-Morozov decomposition encodes data in the IR theory, let us first focus on the anomaly coefficient δ . As the Green-Schwarz-West-Sagnotti mechanism described above does not involve terms proportional to $p_2(T)$, this ensures that from the tensor branch point of view, δ can only arise from one-loop contributions. In [47], it was observed that in the case of conformal matter, the difference in this coefficient between the UV parent theory and the IR SCFT obtained by turning

on a nilpotent orbit O was given by

$$\delta^{\text{UV}} - \delta^{\text{IR}} = -\frac{1}{120} \dim(O). \quad (3.32)$$

Through the tensor branch description, it can be understood as decoupling the various vector and hypermultiplets getting massive after performing a complex-structure deformation. In fact, this coefficient is related to the dimension of the Higgs branch of the SCFTs [47,60,61]

$$\dim(\text{HB}^{\text{UV}}) - \dim(\text{HB}^{\text{IR}}) = -60(\delta^{\text{UV}} - \delta^{\text{IR}}), \quad (3.33)$$

and it is therefore natural to expect that it decreases as we go to the IR fixed point. Note that the complex dimension of a nilpotent orbit is always even, and thus that the change in the quaternionic dimension of the Higgs branch is an integer.

One can however interpret Eq. (3.32) from a slightly different, but ultimately equivalent, point of view that does not involve fields charged under a gauge symmetry and is agnostic about the details of the parent theory: the appearance of the dimension of the orbit is a consequence of Goldstone's theorem. In the UV theory, the moment map transforms in the adjoint representation of the flavor symmetry and there are therefore $\dim(\mathfrak{g})$ degrees of freedom. After turning on a nilpotent vacuum expectation value $\langle \phi \rangle = X$, there is a massless field associated with each of the unbroken generators. That is, they are part of the commutant of the image of ρ_O

$$\mathcal{C}(O) = \{Z \in \mathfrak{adj} \mid [X, Z] = 0\}. \quad (3.34)$$

Using that $\dim(\mathfrak{g}) = \dim(O) + \dim(\mathcal{C}(O))$, there are therefore $\dim(O)$ degrees of freedom that become massive, and whose contributions must be removed from the anomaly polynomial.

More generally, given a representation $(\mathbf{d}_\ell, \mathbf{R}_\ell)$ appearing in the Jacobson-Morozov decomposition of O , there are $\dim(\mathbf{R}_\ell)$ elements commuting with X : by definition, given an irreducible representations of \mathfrak{su}_2 , only the highest-weight state commutes with X . In the infrared the coefficient δ is therefore given by

$$\begin{aligned} \delta^{\text{UV}} - \delta^{\text{IR}} &= -\frac{1}{120} \left(\dim(\mathfrak{g}) - \sum_{\ell} \dim(\mathbf{R}_\ell) \right) \\ &= -\frac{1}{120} \dim(O). \end{aligned} \quad (3.35)$$

Note that while the original argument [47,60,61] used the tensor branch description to argue the validity of Eq. (3.32), here we reinterpret this result by invoking solely the Jacobson-Morozov decomposition of the nilpotent orbit, and in terms of gauge-invariant data of the SCFTs. The number of unbroken generators in the adjoint representation are thus explained as a consequence of Goldstone's

theorem applied to the moment-map superconformal multiplet.

Since we are giving a nilpotent vacuum expectation to the moment map, it is therefore not surprising that all complex-structure deformations of conformal matter arrange themselves into Hasse diagrams of the relevant nilpotent orbits. We however need to argue that the remaining coefficients of the anomaly polynomial can be explained in a similar fashion. A key point to obtain such a result is that the modification of the coefficient δ can be traced back to the contribution proportional to $I_8^{\text{vec}}(F_L)$ in Eq. (3.11).

“One-loop” contributions of vector multiplets depend on the Chern character of the flavor bundle, see Eq. (3.14). As summarized in Appendix A the Chern character has, by construction, particularly nice properties under branching rules. In the parent UV theory, we can therefore decompose quantities involving the background field strength of the flavor symmetry $F_{\mathfrak{g}}$ into those appearing in the Jacobson-Morozov decomposition given in Eq. (3.31)

$$\text{ch}_{\mathfrak{adj}}(F_{\mathfrak{g}}) = \sum_{\ell} \text{ch}_{\mathbf{d}_\ell}(F_X) \text{ch}_{\mathbf{R}_\ell}(F_{\mathfrak{f}}), \quad (3.36)$$

where we have used the notation F_X to emphasize that this \mathfrak{su}_2 background field strength is associated with the element $X \in O$, rather than a possible remnant flavor symmetry.

Note that at this point, the above decomposition simply amounts to a relabeling of the various roots of the adjoint representation of \mathfrak{g} in the yet-unbroken parent theory. Now, when one does turn on a vacuum expectation value for the momentum map, the symmetry associated with F_X is broken, and only the highest-weight states remain massless. Moreover, as ϕ also transforms as a doublet of the R-symmetry, supersymmetry is also broken away from the fixed point. However, in the IR a new R-symmetry emerges as the unbroken diagonal subgroup of $\mathfrak{su}(2)_{R^{\text{UV}}} \oplus \mathfrak{su}(2)_X$ [77,78]

$$c_2(R^{\text{IR}}) = c_2(R^{\text{UV}}) + c_2(F_X), \quad (3.37)$$

in the obvious notation. The second Chern classes are given in terms of one-instanton normalized traces, that is $c_2(F) = \frac{1}{4} \text{Tr} F^2$.

While the result for δ , see Eq. (3.35), suggests to sum over all multiplets in the commutant of X , from the discussion above we must take the new R-symmetry into account. The Chern characters appearing in the definition of $I_8^{\text{vec}}(F_{\mathfrak{g}})$ after taking into account the Jacobson-Morozov decomposition, need to be rewritten in terms of the one-instanton normalized second Chern class, $c_2(R^{\text{IR}})$, and only take into account unbroken modes. We find that the correct combination is given by

$$\begin{aligned} \text{ch}_2(R^{\text{UV}})\text{ch}_d(F_X) \xrightarrow{\text{IR}} \widetilde{\text{ch}}_d(R^{\text{IR}}) &= 2 - (dc_2(R^{\text{IR}})) \\ &+ \frac{1}{12}(dc_2(R^{\text{IR}}))^2 + \dots \end{aligned} \quad (3.38)$$

Comparing the right-hand side of Eq. (3.38) with the usual definition of the Chern character, see, e.g., Eq. (A4), we see that $\widetilde{\text{ch}}_d(R)$ can be understood as a “twisted” version that selects only the highest-weight state of the \mathfrak{su}_2 representation with Cartan eigenvalue d . This quantity is enough to completely account for the one-loop part of the anomaly polynomial after the nilpotent Higgs branch renormalization flow. Indeed, as the contribution from the vector multiplet is the only source of the broken flavor symmetry in second line of Eq. (3.11), which we have interpreted as the one-loop part of the anomaly polynomial, we must simply replace

$$I_8^{\text{vec}}(F_{\mathfrak{g}}, R^{\text{UV}}) \xrightarrow{\text{IR}} I_8^{\text{vec}}(O) = -\frac{1}{2}\hat{A}(T) \sum_{\ell} \widetilde{\text{ch}}_{d_{\ell}}(R^{\text{IR}})\text{ch}_{R_{\ell}}(F_{\mathfrak{f}}), \quad (3.39)$$

where by abuse of language $I_8^{\text{vec}}(O)$ denotes the contribution in the infrared after the decoupling of the massive modes, and is written in terms of the IR R-symmetry. Note that the terms involving the remnant flavor symmetry must once again be converted to one-instanton normalized traces. Generically, they will now involve representations beyond the usual singlet, defining, and adjoint representations. The procedure to find the trace-relation coefficients for arbitrary representation can be obtained from the associated weight system, and is reviewed in Appendix A.

Having given a prescription on how to find the one-loop contributions of the IR theory, let us now turn our attention to the Green-Schwarz-West-Sagnotti mechanism. There, the flavor only appears via its second Chern class $c_2(F_{\mathfrak{g}})$. To rewrite it in terms of the IR data, we can simply use the branching-rules properties of the Chern character shown in Eq. (3.36)

$$c_2(F_{\mathfrak{g}}) = \frac{1}{4}\text{Tr}F_{\mathfrak{g}}^2 = \frac{1}{4h_{\mathfrak{g}}^{\vee}}\text{tr}_{\text{adj}}F_{\mathfrak{g}}^2 = \frac{1}{2h_{\mathfrak{g}}^{\vee}}\text{ch}_{\text{adj}}(F_{\mathfrak{g}}) \Big|_{4\text{-form}}. \quad (3.40)$$

It is then straightforward to see that the decomposition of the second Chern class depends only on the second-order embedding indices

$$c_2(F_{\mathfrak{g}}) = I_{\mathfrak{su}_2 \hookrightarrow \mathfrak{g}} c_2(F_X) + \sum_a I_{\mathfrak{f}_a \hookrightarrow \mathfrak{g}} c_2(F_{\mathfrak{f}_a}), \quad (3.41)$$

where we have allowed for the remnant flavor symmetry to have semisimple components: $\mathfrak{f} = \bigoplus_a \mathfrak{f}_a$. The embedding index of a subalgebra \mathfrak{g}' into \mathfrak{g} can be computed from the

branching rule of a representation as

$$I_{\mathfrak{g}' \hookrightarrow \mathfrak{g}} = \frac{1}{A_{\mathbf{R}}} \sum_{\ell} m_{\ell} A_{\mathbf{R}_{\ell}}, \quad \mathbf{R} \rightarrow \bigoplus_{\ell} m_{\ell} \mathbf{R}_{\ell}, \quad (3.42)$$

where m_{ℓ} is the multiplicity of \mathbf{R}_{ℓ} and $A_{\mathbf{R}_{\ell}}$ its Dynkin index, see Eq. (3.4) as well as Appendix A for details. It is furthermore possible to show that the embedding index does not depend on the representation, only the choice of embedding.¹⁹ Moreover, if \mathfrak{g}' is semisimple, it is computed independently for each simple factor, and we sum over each component as in Eq. (3.41).

For the particular case of nilpotent orbits, the embedding index can be computed directly from the orbit data. As reviewed earlier in this section, every nilpotent orbit can be uniquely labelled by a weighted Dynkin diagram w , seen as a vector in the weight lattice of \mathfrak{g} . It satisfies the property

$$I_X = I_{\mathfrak{su}_2 \hookrightarrow \mathfrak{g}} = \frac{1}{2} \langle w, w \rangle, \quad (3.43)$$

where $\langle \cdot, \cdot \rangle$ is the pairing on the root lattice. For simply laced algebras, it is given via the Cartan matrix; using the conventions defined in Table VIII, we have $\langle \alpha, \beta \rangle = \alpha^T \cdot C^{-1} \cdot \beta$. In practical applications, such as when studying the central charges of the SCFT, it is often enough to compute terms of the anomaly polynomial involving only $c_2(R)$, $p_i(T)$, and Eq. (3.43) can therefore give a way of directly finding them without going through the Jacobson-Morozov decomposition. For the reader's convenience, the embedding indices I_X and $I_{\mathfrak{f}_a \hookrightarrow \mathfrak{g}}$ are tabulated in Appendix B.

The GS contribution to the anomaly polynomial, namely the first line in Eq. (3.11), therefore simply needs to be rewritten in term of the IR R-symmetry, which corresponds to the replacement

$$c_2(F_{\mathfrak{g}}) \xrightarrow{\text{IR}} I_X c_2(R^{\text{IR}}) + I_{\mathfrak{g} \rightarrow \mathfrak{f}} c_2(F). \quad (3.44)$$

As the second Chern class of the flavor symmetry appears through $J(F)$ in the anomaly polynomial of conformal matter given in Eq. (3.11), we can define an IR version

$$J(O) = \frac{\chi}{48} (4c_2(R) + p_1(T)) + I_X c_2(R) + \sum_a I_{\mathfrak{f}_a \hookrightarrow \mathfrak{g}} c_2(F_{\mathfrak{f}_a}), \quad (3.45)$$

where we have again allowed for the possible presence of semisimple factors, $\mathfrak{f} = \bigoplus_a \mathfrak{f}_a$ in the remnant symmetry.

We have now found an IR prescription for every contribution involving the flavor symmetry after a nilpotent

¹⁹For a recent review in the physics literature of Dynkin indices, Dynkin embedding indices, and their relevant properties, see [79].

Higgs branch flow. Moreover, since in the GS term we only need to replace $c_2(R^{\text{UV}}) \rightarrow c_2(R^{\text{IR}})$, see the discussion around Eq. (3.37), we conclude that the anomaly polynomial of a theory obtained by a nilpotent deformation of conformal matter is given by

$$I_8(A_{N-1}^{\mathfrak{g}}(O_L, \emptyset)) = I_8(A_{N-1}^{\mathfrak{g}})|_{J(F_L) \rightarrow J(O), I_8^{\text{vec}}(F_L) \rightarrow I_8^{\text{vec}}(O_L)}, \quad (3.46)$$

where on the right-hand side, everything is understood to be in terms of the IR R-symmetry.

While we have so far argued for this prescription only for long conformal matter theories where only one of the flavor is broken, nothing prevents us to consider a nilpotent breaking on each end. By assumption, the quiver is long enough so that a deformation on one end cannot affect the other. We can therefore repeat our argument applied to both sides independently. As can be seen from Eq. (3.11), the anomaly polynomial is symmetric under exchange of the left and right flavor, and the generalization of Eq. (3.46) is straightforward. We need only consider the fusion of two different conformal matter theories with only one deformation

$$A_{N-1}^{\mathfrak{g}}(O_L, O_R) = A_{N-p-1}^{\mathfrak{g}}(O_L, \emptyset) \oplus A_p^{\mathfrak{g}}(\emptyset, O_R). \quad (3.47)$$

We then obtain the same prescription as in Eq. (3.46), but doing the replacement for nilpotent orbits on both sides. Moreover, the approach described above is unaffected by the presence of fractional conformal matter. The anomaly polynomial has only minimal changes: as long as the fraction does not imply the absence of a flavor symmetry, there is still a moment map for which a nilpotent vacuum expectation can be turned on, and our prescription remains valid. The only difference is the presence of the term I_{fr} , and the four-form $J(O)$ is changed to

$$J_{\text{fr}}(O) = \frac{\chi_{\text{fr}}}{48}(4c_2(R) + p_1(T)) + \frac{I_X}{d_f}c_2(R) + \frac{1}{d_f} \sum_a I_{\mathfrak{f}_a \hookrightarrow \mathfrak{g}_f} c_2(F_{\mathfrak{f}_a}), \quad (3.48)$$

where we recall that d_f is the denominator of the associated fraction f , and O is a nilpotent orbit of the flavor symmetry associated with the fraction, \mathfrak{g}_f .

In summary, given a parent theory $\mathcal{A}_{N-1;f_L,f_R}^{\mathfrak{g}}$ for which we turn on (possibly trivial) vacuum expectation values for the moment maps associated with nilpotent orbits O_L, O_R , the anomaly polynomial of the resulting theory $\mathcal{A}_{N-1;f_L,f_R}^{\mathfrak{g}}(O_L, O_R)$ is given by

$$\begin{aligned} & I_8(\mathcal{A}_{N-1;f_L,f_R}^{\mathfrak{g}}(O_L, O_R)) \\ &= \frac{N_{\text{eff}}^3}{24}(c_2(R)\Gamma)^2 - \frac{N_{\text{eff}}}{2}(c_2(R)\Gamma)(J_{\text{fr}}(O_L) + J_{\text{fr}}(O_R)) \\ &\quad - \frac{1}{2N_{\text{eff}}}(J(O_L) - J(O_R))^2 + N_{\text{eff}}I_{\text{sing}} - I_8^{\text{tensor}} \\ &\quad - \frac{1}{2}(I_8^{\text{vec}}(O_L) + I_8^{\text{vec}}(O_R)) - (e_L + e_R)I_{\text{fr}}. \end{aligned} \quad (3.49)$$

The R-symmetry is understood to be that of the IR theory, and the decomposition of the quantities $I_8^{\text{vec}}(O_L)$ and $J_{\text{fr}}(O_R)$ are given in Eqs. (3.39) and (3.48), respectively. The other contributions have been defined around Eq. (3.24). In all cases, only the Jacobson-Morozov decomposition of the adjoint representation is required. For all relevant cases, these branching rules are summarized in Appendix B.

Note that $I_8^{\text{vec}}(O_L)$ is associated with the ‘‘one-loop’’ contribution of the surviving moment map modes after the nilpotent flow. While the definition of $\text{ch}_{d_e}(R)$ in Eq. (3.38) taking into account the IR R-symmetry might seem *ad hoc*, in Sec. IV we will show that it is justified and equivalent to removing the contributions of the Nambu-Goldstone modes decoupling from the parent theory. We have indeed checked using the tensor branch description that Eq. (3.49) is correct. In the case of exceptional algebras, the proof is done by exhaustion as the number of possible cases is finite, and we give a derivation of the validity of this formula for type-A algebras in the next section. While we have not performed a similar proof for type-D algebras—this is left as an exercise for the diligent reader—we have checked it exhaustively for $r_{\mathfrak{g}} \leq 20$ and $f_{L,R} = \frac{1}{2}, 1$, with some additional sporadic crosschecks at $r_{\mathfrak{g}} = \mathcal{O}(100)$.

We stress once again that while the tensor branch description can be used to confirm the validity of the formula given in Eq. (3.49), the details of the underlying geometric description does not matter: for long quivers, the complete data needed is encoded into the notation $\mathcal{A}_{N-1;f_L,f_R}^{\mathfrak{g}}(O_L, O_R)$, up to the Jacobson-Morozov decompositions that can be easily computed or read off from tables. The gauge spectrum and the curve-intersection patterns specific to a given algebra \mathfrak{g} is completely irrelevant, and the anomaly polynomial is only given in terms of gauge-invariant data.

C. Other long quivers

So far, we have focused solely on (possibly fractional) conformal matter theories and their deformations. We have however seen that there are three families of long quivers

$$\mathcal{A}_{N-1;f_L,f_R}^{\mathfrak{g}}(O_L, O_R), \quad \mathcal{D}_{N;f}^{\mathfrak{g}}(O), \quad \mathcal{O}_{N;f}^{\mathfrak{g}}(\rho, O). \quad (3.50)$$

Except for orbi-instanton theories, which also have deformations parameterized by embedding of ADE discrete

groups into E_8 , all other possible deformations of the parents theories are nilpotent. As such, the same kind of arguments that allowed us to find the anomaly polynomial of $\mathcal{A}_{N-1;f_L,f_R}^{\mathfrak{g}}(O_L, O_R)$ from that of $\mathcal{A}_{N-1;1,f_R}^{\mathfrak{g}}(\emptyset, O_R)$, can be repeated for the other types of long quivers. Indeed, as we have described in Sec. II, we can use the fusion point of view to obtain them from their undeformed counterparts fused with deformed conformal matter

$$\begin{aligned} \mathcal{D}_{N,f}^{\mathfrak{g}}(O) &= D_{N-\rho}^{\mathfrak{g}}(\emptyset) \oplus \mathcal{A}_{p-1;1,f}(\emptyset, O), \\ \mathcal{O}_{N,f}^{\mathfrak{g}}(\emptyset, O) &= \mathcal{O}_{N-\rho}^{\mathfrak{g}}(\emptyset, \emptyset) \oplus \mathcal{A}_{p-1;1,f}(\emptyset, O), \end{aligned} \quad (3.51)$$

where we used \oplus to indicate fusion of the unbroken common \mathfrak{g} factors. This means that if we can find the anomaly polynomial of orbi-instantons or type-D SCFTs at low rank, which is achieved easily through the tensor branch algorithm, that of the broken theory can be found for an arbitrary quiver length N by recurrence, and the prescription for its anomaly polynomial is the same sort of replacements showed in Eq. (3.46).

For type D, the result turns out to be quite simple. We however must distinguish between $\mathfrak{g} = \mathfrak{su}(2K)$ and the three sporadic series $\mathfrak{g} = \mathfrak{su}(3), \mathfrak{so}(8), e_6$. For the former, there cannot be fractions, i.e., $f = 1$, and we find

$$\begin{aligned} I_8(D_N^{\mathfrak{su}_{2K}}(O)) &= \frac{N_{\text{eff}}^3}{6} (c_2(R)\Gamma)^2 - N_{\text{eff}}(c_2(R)\Gamma)J(O) \\ &\quad + N_{\text{eff}}I_{\text{sing}} - \frac{1}{2}I_8^{\text{vec}}(O) + I_8^{\text{tensor}} + \frac{3}{2}I_8^{\text{free}}, \end{aligned} \quad (3.52)$$

with $N_{\text{eff}} = N - 1$, and I_8^{free} is the contribution of a free fermion transforming in the doublet of the R-symmetry, see Eq. (A6). For the latter three cases, the expression is slightly different, and of course may depend on the fractions

$$\begin{aligned} I_8(\mathcal{D}_{\mathfrak{g};N;f}(O)) &= \frac{N_{\text{eff}}^3}{6} (c_2(R)\Gamma)^2 - N_{\text{eff}}(c_2(R)\Gamma)J_{\text{fr}}(O) \\ &\quad + N_{\text{eff}}I_{\text{sing}} - \frac{1}{2}I_8^{\text{vec}}(O) - I_8^{\text{tensor}} \\ &\quad - (e + 15)I_{\text{fr}} + I_8^{\mathcal{D},\mathfrak{g}}. \end{aligned} \quad (3.53)$$

In this case, the parameter N_{eff} must be slightly modified

$$N_{\text{eff}} = (N - 3) + f + \frac{1}{2} \quad (3.54)$$

This trivalent pattern also gives rise to an extra term depending only on the $c_2(R)$ and $p_1(T)$ but whose coefficients depend on the choice of algebra \mathfrak{g} ; they are given in Table VI. The quantities depending explicitly on the nilpotent orbit O are the ones appearing in the anomaly polynomial of conformal matter, see Eqs. (3.38) and (3.45).

TABLE VI. Term appearing in the anomaly polynomial of type-D quiver, originating from the trivalent intersection.

\mathfrak{g}	$I_8^{\mathcal{D},\mathfrak{g}}$
\mathfrak{su}_3	$c_2(R)\left(\frac{23}{16}c_2(R) + \frac{25}{96}p_1(T)\right)$
\mathfrak{so}_8	$c_2(R)\left(\frac{5}{2}c_2(R) + \frac{7}{24}p_1(T)\right)$
e_6	$c_2(R)\left(\frac{5}{2}c_2(R) + \frac{7}{24}p_1(T)\right)$

Orbi-instantons theories are dealt with in a similar fashion. We note however that turning on a deformation for the e_8 flavor associated with an end-of-the-world brane in the M-theory description substantially complicates the analysis. When $\mathfrak{g} = \mathfrak{su}(K)$, corresponding to $\Gamma = \mathbb{Z}_K$, the anomaly polynomial of theories with nontrivial ρ —but trivial nilpotent orbits of \mathfrak{su}_K —were studied in [49]. Here, we will conversely allow for any choice of \mathfrak{g} and its nilpotent orbits, but keep ρ trivial.

While slightly more involved than previous cases, we find a closed-form expression for the anomaly polynomial that depends once again only group-theoretical quantities related to \mathfrak{g}

$$\begin{aligned} I_8(\mathcal{O}_{N;f}^{\mathfrak{g}}(\emptyset, O)) &= \frac{N_{\text{eff}}^3}{6} (c_2(R)\Gamma)^2 - \frac{N_{\text{eff}}^2}{2} (c_2(R)\Gamma)\tilde{J}(F_{e_8}) + N_{\text{eff}}I_{\text{sing}} \\ &\quad + N_{\text{eff}}\left(\frac{1}{2}\tilde{J}(F_{e_8})^2 - (\Gamma c_2(R))J_{\text{fr}}(O)\right) \\ &\quad + \tilde{J}(F_{e_8})\left(J_{\text{fr}}(O) - \frac{\chi_{\text{fr}}}{48}(4c_2(R) + p_1(T))\right) \\ &\quad - \frac{\alpha_0}{24}c_2(R)^2 + \frac{r_{\mathfrak{g}}}{2}I_{\text{free}} - \frac{\dim(\mathfrak{g})h_{\mathfrak{g}}^{\vee}}{6}c_2(R) \\ &\quad \times \left(\frac{1}{6}p_1(T) + c_2(F_{e_8})\right) - \frac{1}{2}I_8^{\text{vec}}(O) - eI_{\text{fr}}. \end{aligned} \quad (3.55)$$

The possible values of e given a fraction f are shown in Table II, and quantities depending on the nilpotent orbit are given in Eqs. (3.39) and (3.48). The contribution of a free fermion in a doublet of the R-symmetry I_{free} is given in Eq. (A6), and we have defined

$$N_{\text{eff}} = (N - 2) + f_{\text{OI}} + f, \quad (3.56)$$

$$\tilde{J}(F_{e_8}) = \frac{1}{2}(\Gamma\chi - 1)c_2(R) + \frac{1}{4}p_1(T) + c_2(F_{e_8}). \quad (3.57)$$

The quantity $\tilde{J}(F_{e_8})$ can be understood in the same way as $J(F_{\mathfrak{g}})$, namely as a contribution to the Green-Schwarz term appearing in the Bianchi identity for the tensor multiplet dual to the tensionless strings at the fixed point, see the discussion around Eq. (3.20). Contrary to other long quivers, the “effective” number of conformal matter theories N_{eff} now depends on the choice of algebra \mathfrak{g} , and in

the anomaly polynomial is encoded in the parameter f_{OI} . Additionally, there is a contribution to the $c_2(R)^2$ term, α_0 , for which we did not find a simple expression in terms of the data of \mathfrak{g} . We show the values for both these quantities in Table IV.

D. Examples

To illustrate the simplicity of the formula given in Eq. (3.49), we now turn to two examples. For ease of exposition we will only consider conformal matter with $f_{L,R} = 1$, and a single deformation.

The minimal orbit of e_6 : we first consider the theory obtained by breaking the left flavor of higher-rank (e_6, e_6) conformal with the A_1 nilpotent orbit of e_6 in the Bala-Carter notation. It is therefore the $A_{N-1}^{e_6}(A_1, 0)$ theory, described at a generic point of the tensor branch by the following quiver:

$$A_{N-1}^{e_6}(A_1, 0): [\mathfrak{su}_6] \overset{\mathfrak{su}_3}{2} \overset{e_6}{161} \overset{\mathfrak{su}_3}{3} \overset{e_6}{1} \cdots \overset{e_6}{61} \overset{\mathfrak{su}_3}{3} \overset{e_6}{161} \overset{\mathfrak{su}_3}{3} 1[e_6]. \quad (3.58)$$

This nilpotent orbit is minimal, in the sense that it is smallest with respect to the partial ordering of nilpotent orbits, i.e., the first nontrivial level in the corresponding Hasse diagram. In the geometric description, this is reflected by the fact that the simplest deformation is obtained by blowing down the left-most (-1) -curve of

the conformal matter quiver. Furthermore, its weighted Dynkin diagram is given by $w = [0, 0, 0, 0, 0, 1]$, and Jacobson-Morozov decomposition for the adjoint representation yields

$$\begin{aligned} \rho_{A_1}: e_6 &\longrightarrow \mathfrak{su}(2)_X \oplus \mathfrak{su}(6) \\ \mathbf{78} &\longrightarrow (\mathbf{1}, \mathbf{35}) \oplus (\mathbf{2}, \mathbf{20}) \oplus (\mathbf{3}, \mathbf{1}). \end{aligned} \quad (3.59)$$

This branching rule is simple, and as can be checked from the tables collated in Appendix B, or using Eq. (3.42), the embedding indices are both equal to one. The second Chern class decomposes as

$$c_2(F_{e_6}) = c_2(F_X) + c_2(F_{\mathfrak{su}_6}). \quad (3.60)$$

Using that after the nilpotent breaking we must replace $c_2(R^{\text{UV}}) = c_2(R) = c_2(F_X)$, we have

$$J(A_1) = \frac{455}{288} c_2(R) + \frac{167}{1152} p_1(T) + c_2(F_{\mathfrak{su}_6}). \quad (3.61)$$

To use the decomposition of $I_8^{\text{vec}}(A_1)$ defined in Eq. (3.39), we need to convert the traces over the representations $\mathbf{20}$ and $\mathbf{35}$ of \mathfrak{su}_6 into one-instanton normalized traces. Using the techniques explained above and in Appendix A, one finds

$$\text{ch}_{\mathbf{20}}(F_{\mathfrak{su}_6}) = 20 - \frac{1}{2} (3\text{Tr}F_{\mathfrak{su}_6}^2) + \frac{1}{4!} \left(-6\text{Tr}F_{\mathfrak{su}_6}^4 + \frac{3}{2} (\text{Tr}F_{\mathfrak{su}_6}^2)^2 \right) + \dots, \quad (3.62)$$

$$\text{ch}_{\mathbf{35}}(F_{\mathfrak{su}_6}) = 35 - \frac{1}{2} (6\text{Tr}F_{\mathfrak{su}_6}^2) + \frac{1}{4!} \left(12\text{Tr}F_{\mathfrak{su}_6}^4 + \frac{3}{2} (\text{Tr}F_{\mathfrak{su}_6}^2)^2 \right) + \dots. \quad (3.63)$$

Taking into account the ‘‘twisted’’ character for the R-symmetry in the deformed theory, we have

$$I_8^{\text{vec}}(A_1) = -\frac{1}{2} \hat{A}(T) (\tilde{\text{ch}}_1(R) \text{ch}_{\mathbf{35}}(F_{\mathfrak{su}_6}) + \tilde{\text{ch}}_2(R) \text{ch}_{\mathbf{20}}(F_{\mathfrak{su}_6}) + \tilde{\text{ch}}_3(R)) \quad (3.64)$$

$$= -\frac{109}{6} c_2(R)^2 - \frac{31}{12} c_2(R) p_1(T) - \frac{56}{5760} (7p_1(T)^2 - 4p_2(T)) \quad (3.65)$$

$$- \frac{9}{2} c_2(R) \text{Tr}(F_{\mathfrak{su}_6}^2) - \frac{3}{16} p_1(T) \text{Tr}F_{\mathfrak{su}_6}^2 - \frac{1}{8} (\text{Tr}F_{\mathfrak{su}_6})^2 - \frac{1}{4} \text{Tr}F_{\mathfrak{su}_6}^4. \quad (3.66)$$

Note that the coefficient of $p_2(T)$ is proportional to the dimension of the commutant of the nilpotent orbit $\dim(e_6) - \dim(A_1) = 56$, as expected. Putting everything together as in Eq. (3.49), the complete anomaly polynomial of the theory after breaking is given by

$$\begin{aligned} I_8(A_{N-1}^{e_6}(A_1, 0)) &= \frac{288N^4 - 311N^2 + 128N - 6}{12N} c_2(R)^2 - \frac{83N - 50}{24} p_1(T) c_2(R) + \frac{15N + 223}{2880} p_1(T)^2 - \frac{15N + 19}{720} p_2(T) \\ &+ p_1(T) \left(\frac{1}{8} \text{Tr}F_{e_6}^2 + \frac{3}{32} \text{Tr}F_{\mathfrak{su}_6}^2 \right) - c_2(R) \left(\frac{12N^2 - 6N - 1}{4N} \text{Tr}F_{e_6}^2 + \frac{12N^2 - 9N + 1}{4N} \text{Tr}F_{\mathfrak{su}_6}^2 \right) \\ &+ \frac{3N - 1}{32N} (\text{Tr}F_{e_6}^2)^2 + \frac{1}{16N} \text{Tr}F_{e_6}^2 \text{Tr}F_{\mathfrak{su}_6}^2 + \frac{2N - 1}{32N} (\text{Tr}F_{\mathfrak{su}_6}^2)^2 + \frac{1}{8} \text{Tr}F_{\mathfrak{su}_6}^4. \end{aligned} \quad (3.67)$$

This result can then be compared against the computation on the tensor branch description, and one can check that the two results agree.

Partitions of \mathfrak{su}_8 : when the flavor algebra is of type \mathfrak{su}_K , conformal matter takes a particularly simple form, and the nilpotent deformations are described by partitions of K . We now specialize to $\mathfrak{g} = \mathfrak{su}(8)$, where conformal matter has been deformed by the nilpotent orbit associated with the partition $[2^4]$ on the left, while the right flavor is left untouched—or equivalently described by the trivial partition $[1^8]$

$$A_{N-1}^{\mathfrak{su}_8}([2^4], [1^8]): [\mathfrak{su}_4] \underbrace{2 \ 2 \ 2 \ \cdots \ 2 \ 2}_{N-1} [\mathfrak{su}_8]. \quad (3.68)$$

The relations between the partitions and the tensor branch quivers are discussed in Appendix D. As discussed there, the remnant flavor is found from the multiplicities of each partition, and we therefore have total non-Abelian flavor $\mathfrak{f} = \mathfrak{su}_4 \oplus \mathfrak{su}_8$ in the IR theory.

We once again need to use the Jacobson-Morozov decomposition to find the anomaly polynomial. For the fundamental representation, it can be read off directly from the partition, from which that of the adjoint is easily computed, as $\mathbf{K} \otimes \bar{\mathbf{K}} = \mathbf{adj} \oplus \mathbf{1}$ for type-A algebras

$$\begin{aligned} \rho_{[2^4]}: \mathfrak{su}(8) &\rightarrow \mathfrak{su}(2)_X \oplus \mathfrak{su}(4), \\ \mathbf{8} &\rightarrow (\mathbf{2}, \mathbf{4}), \\ \mathbf{63} &\rightarrow (\mathbf{3}, \mathbf{1}) \oplus (\mathbf{1}, \mathbf{15}) \oplus (\mathbf{3}, \mathbf{15}). \end{aligned} \quad (3.69)$$

In the IR theory, using Eq. (3.44), we therefore have

$$\begin{aligned} c_2(F_L) &= 4c_2(R) + 2c_2(F_{\mathfrak{su}_4}), \\ I_8^{\text{vec}}([2^4]) &= -\frac{1}{2}\hat{A}(T)(\tilde{c}h_3(R) + (\tilde{c}h_1(R) \\ &\quad + \tilde{c}h_3(R))\text{ch}_{15}(F_{\mathfrak{su}_4})), \end{aligned} \quad (3.70)$$

where we have written everything in terms of the IR R-symmetry. For completeness, we recall that the weighted Dynkin diagram of this nilpotent orbit is given by $w = [0, 0, 0, 2, 0, 0, 0]$ [67], and one can check that the index of the \mathfrak{su}_2 embedding is indeed given by $I_X = 4$ via Eq. (3.43).

Note that this case is simpler than the minimal orbit of \mathfrak{e}_6 , as the only nontrivial representation is the adjoint, for which the trace relations are given by

$$\begin{aligned} \text{tr}_{\text{adj}} F_{\mathfrak{su}_K}^2 &= K \text{Tr} F_{\mathfrak{su}_K}, & \text{tr}_{\text{adj}} F_{\mathfrak{su}_K}^4 \\ &= 2K \text{Tr} F_{\mathfrak{su}_K}^4 + \frac{3}{2} (\text{Tr} F_{\mathfrak{su}_K}^2)^2. \end{aligned} \quad (3.71)$$

The anomaly polynomial of the theory $A_{N-1}^{\mathfrak{su}_8}([2^4], [1^8])$ is finally obtained by plugging back Eq. (3.70) into the formula given in Eq. (3.49). When the dust settles, we obtain

$$\begin{aligned} I_8(A_{N-1}^{\mathfrak{su}_8}([2^4], [1^8])) &= \frac{32N^4 - 255N^2 + 343N - 96}{12N} c_2(R)^2 - \frac{31N - 55}{24} p_1(T) c_2(R) + \frac{5N + 51}{960} p_1(T)^2 - \frac{5N + 3}{240} p_2(T) \\ &\quad + p_1(T) \left(\frac{1}{12} \text{Tr} F_{\mathfrak{su}_8}^2 + \frac{1}{12} \text{Tr} F_{\mathfrak{su}_4}^2 \right) - c_2(R) \left(\frac{N^2 - N - 1}{N} \text{Tr} F_{\mathfrak{su}_8}^2 + \frac{2N^2 - 5N + 2}{N} \text{Tr} F_{\mathfrak{su}_4}^2 \right) \\ &\quad + \frac{N - 1}{32N} (\text{Tr} F_{\mathfrak{su}_8}^2)^2 + \frac{1}{8N} \text{Tr} F_{\mathfrak{su}_8}^2 \text{Tr} F_{\mathfrak{su}_4}^2 + \frac{N - 2}{16N} (\text{Tr} F_{\mathfrak{su}_4}^2)^2 + \frac{1}{3} \text{Tr} F_{\mathfrak{su}_8}^4 + \frac{1}{3} \text{Tr} F_{\mathfrak{su}_4}^4. \end{aligned} \quad (3.72)$$

In Sec. IV, we will give the form of the anomaly polynomial for any theory of type $A_{N-1}^{\mathfrak{su}_K}(O_L, O_R)$, and one can check that the above result is correct.

IV. ANOMALIES FROM NAMBU-GOLDSTONE MODES

In the previous section, we have given closed-form expressions for the anomaly polynomials of every long 6D (1, 0) SCFT. We found them using the anomaly polynomial of conformal matter and obtained that of its

nilpotent deformations by studying which moment map modes were surviving the flow to the infrared theory. The other cases were then reached through fusion, and our results confirmed by using the generic tensor branch geometry. In this section, we will determine the putative anomaly polynomials from a bottom-up perspective without invoking the tensor branch geometry and show that they match with the closed-form expressions.

We consider here the parent theory of a long quiver, which we will refer to as the UV theory, \mathcal{T}^{UV} . To wit, these are the three classes of infinite series

$$\mathcal{A}_{N-1;f_L,f_R}^{\mathfrak{g}}, \quad \mathcal{D}_{N;f}^{\mathfrak{g}}, \quad \mathcal{O}_{N;f}^{\mathfrak{g}}. \quad (4.1)$$

We assume that N is large enough such that giving nilpotent vacuum expectation values to the moment maps lead to an interacting SCFT, and, when the parent theory is of conformal matter type, that the Higgsing of the left and right moment maps do not influence each other.²⁰ Giving a nilpotent vacuum expectation to these operators, $\langle \phi \rangle = X \in O$, where O is a nilpotent orbit, we trigger a Higgs branch renormalization group flow leading to an infrared fixed point corresponding to an interacting SCFT which we label as \mathcal{T}^{IR} .

It is natural to ask: can we determine the anomaly polynomial of the SCFT \mathcal{T}^{IR} using only the information of the anomaly polynomial of \mathcal{T}^{UV} and the information contained in the nilpotent orbit O by which we Higgs. Of course, if we allow ourselves to use the tensor branch description of \mathcal{T}^{UV} the path to determining the anomaly polynomial of \mathcal{T}^{IR} is straightforward, if circuitous: we know how the tensor branch geometry is modified by the nilpotent orbit O , and then it is direct to determine the infrared anomaly polynomial from the known tensor branch description of \mathcal{T}^{IR} . Instead, we only assume knowledge of the anomaly polynomial of \mathcal{T}^{UV} , and no additional, microscopic details of the theory.

Under a nilpotent Higgsing, the superconformal symmetry, and thus the $\mathfrak{su}(2)_R$ R-symmetry, is broken along the flow. At the interacting fixed point a new R-symmetry emerges: $\mathfrak{su}(2)_{R^{\text{IR}}}$. A nilpotent orbit of a simple flavor symmetry factor \mathfrak{f} corresponds to a homomorphism $\mathfrak{su}(2)_X \rightarrow \mathfrak{g}$, and when a nilpotent Higgsing is performed, the new infrared R-symmetry is simply the diagonal of the original $\mathfrak{su}(2)_R$ and the $\mathfrak{su}(2)_X$. See [78] for a review of nilpotent Higgsing, particularly in the context of 4d $\mathcal{N} = 2$ SCFTs. In addition to the breaking and emergence of the R-symmetry, we must take care of modes which decouple along the flow into the infrared. One class of modes which decouple belong to the moment map (and its superpartners) to which we give the VEV; we refer to these as the Nambu-Goldstone modes inside of the moment map. In particular, the moment map supermultiplet contains chiral fermions, and the decoupling of these fermions in the infrared affects the anomalies of \mathcal{T}^{IR} .

In six dimensions, a positive-chirality fermion transforming in the representation ℓ of $\mathfrak{su}(2)_{R^{\text{IR}}}$ and some representation \mathbf{R} of a flavor symmetry \mathfrak{f} contributes to the

²⁰Recall that we are not considering Higgsing by giving a nilpotent vacuum expectation value to the moment map of the e_8 flavor symmetry on the left in the parent theory $\mathcal{O}_{N;f}^{\mathfrak{g}}$.

anomaly polynomial as²¹

$$I_8^{\text{fermion}}(\ell, \mathbf{R}) = \frac{1}{2} \hat{A}(T) \text{ch}_{\ell}(R^{\text{IR}}) \text{ch}_{\mathbf{R}}(F) \Big|_{8\text{-form}}. \quad (4.2)$$

Thus, once we know the representations of $\mathfrak{su}(2)_{R^{\text{IR}}}$ and \mathfrak{f} under which the Nambu-Goldstone fermions inside of the moment map transform, we can determine the contribution to the anomaly polynomial from these modes, which must be removed in the IR. Conveniently, the representations under the global symmetries of the Nambu-Goldstone modes belonging to the moment map are known [78].²² Given the homomorphism $\mathfrak{su}(2)_X \rightarrow \mathfrak{g}$ associated to the nilpotent orbit, there is an induced branching rule

$$\begin{aligned} \mathfrak{g} &\longrightarrow \mathfrak{su}(2)_X \oplus \mathfrak{f}, \\ \mathbf{adj} &\longrightarrow \bigoplus_{\ell} (\mathbf{d}_{\ell}, \mathbf{R}_{\ell}), \end{aligned} \quad (4.3)$$

where \mathfrak{f} is the centralizer of the image of the homomorphism. The Nambu-Goldstone fermions transform in the $\mathfrak{su}(2)_{R^{\text{IR}}} \oplus \mathfrak{f}$ representations

$$\bigoplus_{\ell} (\mathbf{d}_{\ell} - \mathbf{1}, \mathbf{R}_{\ell}). \quad (4.4)$$

Thus, we can determine the contribution to the infrared anomaly polynomial that comes from the decoupled Nambu-Goldstone modes inside of the moment map.

In principle, there may be anomaly-contributing modes that decouple along the flow into the infrared that do not belong to the Nambu-Goldstone fermions inside of the moment map supermultiplet. In fact, such modes often exist when considering the nilpotent Higgsing of the flavor symmetry factor \mathfrak{g} in an arbitrary SCFT, as has been noted in both 4d $\mathcal{N} = 2$ and 6D (1, 0) contexts in [80,81]. We propose that when the parent theory is one of those in Eq. (4.1), then the only modes that decouple in the infrared and contribute nontrivially to the anomaly are those that belong to the moment map; we verify this by demonstrating that the anomaly polynomial worked out under such an assumption is identical to the anomaly polynomial worked out using the tensor branch geometry.

Putting everything together concisely, the anomaly polynomial of the interacting infrared SCFT can be determined via the following algorithm.

²¹The $1/2$ -prefactor appears in Eq. (4.2) as \mathbf{R} may be a real irreducible representation of \mathfrak{f} .

²²The analysis in [78] focused on 4d $\mathcal{N} = 2$ SCFTs, however the generalization to the structure of the Nambu-Goldstone modes inside of the moment map in 6D (1, 0) is clear.

ALGORITHM 1.

Given the anomaly polynomial, $I_8(\mathcal{T}^{\text{UV}})$, for a long quiver, \mathcal{T}^{UV} , chosen among the theories given in Eq. (4.1), and a nilpotent orbit, O , of one of the simple flavor factors, \mathfrak{g} , of \mathcal{T}^{UV} , the anomaly polynomial, $I_8(\mathcal{T}^{\text{IR}})$, of the SCFT \mathcal{T}^{IR} obtained via giving a VEV valued in O to the moment map of \mathfrak{g} is found as follows.

- (1) In $I_8(\mathcal{T}^{\text{UV}})$, rewrite the one-instanton normalized traces of the flavor symmetries in terms of the curvatures of the algebras $\mathfrak{su}(2)_X$ and \mathfrak{f} appearing in Eq. (4.3): $\text{Tr}F_X^n$ and $\text{Tr}F_{\mathfrak{f}}^n$.
- (2) Replace the second Chern class of the UV R-symmetry $c_2(R^{\text{UV}})$ and $c_2(F_X)$ by that of the IR R-symmetry

$$c_2(R^{\text{UV}}), \quad c_2(F_X) \rightarrow c_2(R^{\text{IR}}). \quad (4.5)$$

Steps 1 and 2 define the quantity $I_8(\mathcal{T}^{\text{UV}}; R^{\text{IR}})$.

- (3) The IR anomaly polynomial is then obtained by removing the Nambu-Goldstone modes

$$I_8(\mathcal{T}^{\text{IR}}) = I_8(\mathcal{T}^{\text{UV}}; R^{\text{IR}}) - \sum_{\ell} J_8^{\text{fermion}}(\mathbf{d}_{\ell} - \mathbf{1}, \mathbf{R}_{\ell}), \quad (4.6)$$

where the representations of fermions are given from the decomposition in Eq. (4.3). The contribution of each fermionic Nambu-Goldstone mode is as defined in Eq. (4.2).

If $\mathcal{T}^{\text{UV}} = \mathcal{A}_{N-1; f_L, f_R}^{\mathfrak{g}}$, there can be a nilpotent vacuum expectation value for both moment maps. Then we perform the three steps sequentially for each nilpotent deformations.

Having given the algorithm, one can show that its result is equivalent to the closed-form expression presented in Sec. III. To see this, recall that we have interpreted these anomaly polynomials as coming from both one-loop and GS contributions at the fixed point. The quantity $I_8^{\text{ec}}(O)$, defined in Eq. (3.38), was introduced as a way to sum only over the contribution of massless modes of the adjoint representation after the nilpotent breaking. It is straightforward to show that this contribution and that of the Nambu-Goldstone modes as defined above reorganize into the anomaly polynomial of a full vector multiplet written in terms of the IR data. This is expected, as $I_8^{\text{ec}}(O)$ counts $\mathfrak{su}(2)_X$ highest-weight states appearing in the Jacobson-Morozov, weighted by the IR R-symmetry through the twisted character $\widehat{\text{ch}}_{\mathfrak{d}}$, while the Nambu-Goldstone modes are by definition those that do not commute with the representative X of the nilpotent orbit. This takes care of the one-loop part of the closed-form expression, while the replacement $J_{\text{fr}}(F) \rightarrow J_{\text{fr}}(O)$ is equivalent to steps 1 and 2

of the Algorithm 1 applied to the Green-Schwarz contribution, when the R-symmetry is understood to be that of the infrared theory. This therefore justifies *a posteriori* the introduction of $\widehat{\text{ch}}_{\mathfrak{d}}$ as a quantity encoding the R-symmetry of the modes remaining massless in the IR theory.

Note that while equivalent, the results of previous section and Algorithm 1 have different advantages. Starting from a nilpotent deformation of conformal matter, we can reach a long quiver of, e.g., an orbi-instanton through fusion, and both the one-loop and Green-Schwarz terms can be easily identified with the closed-form expressions. On the other hand, using Algorithm 1 we can find the anomaly polynomial of any 6D (1, 0) SCFT reached by nilpotent RG flows without knowing the precise details of its quiver.

For completeness, and as they are usually the most relevant quantities in practical computations, we give here the shifts that the gravitational and R-symmetry anomaly coefficients undergo when (fractional) conformal matter $\mathcal{A}_{N-1; f_L, f_R}^{\mathfrak{g}}$ is Higgsed via nilpotent orbits O_L and O_R

$$\begin{aligned} \alpha^{\text{UV}} - \alpha^{\text{IR}} &= 12\Gamma N_{\text{eff}} \left(\frac{I_{X_L}}{d_{f_L}} + \frac{I_{X_R}}{d_{f_R}} \right) + \frac{12}{N_{\text{eff}}} \left(\frac{I_{X_L}}{d_{f_L}} - \frac{I_{X_R}}{d_{f_R}} \right)^2 + 4(\beta^{\text{UV}} - \beta^{\text{IR}}) - (4\varphi_3(w_L) + \varphi_0(w_L) + 4\varphi_3(w_R) + \varphi_0(w_R)), \\ \beta^{\text{UV}} - \beta^{\text{IR}} &= + \frac{6}{N_{\text{eff}}} \left(\frac{1}{d_{f_L}} - \frac{1}{d_{f_R}} \right) \left(\frac{I_{X_L}}{d_{f_L}} - \frac{I_{X_R}}{d_{f_R}} \right) - \left(\varphi_1(w_L) - \frac{1}{2}\varphi_0(w_L) + \varphi_1(w_R) - \frac{1}{2}\varphi_0(w_R) \right), \\ \gamma^{\text{UV}} - \gamma^{\text{IR}} &= + \frac{7}{240} (\dim(O_L) + \dim(O_R)), \\ \delta^{\text{UV}} - \delta^{\text{IR}} &= - \frac{1}{120} (\dim(O_L) + \dim(O_R)). \end{aligned} \quad (4.7)$$

Here, N_{eff} is as given in Eq. (3.23), d_{f_L} and d_{f_R} are the denominators of the fractions f_L and f_R , respectively, and I_{X_L}, I_{X_R} are the embedding indices for the $\mathfrak{su}(2)_X$ under the branching of the respective nilpotent orbits. The quantity $\varphi_n(w)$ can be obtained directly from the weighted Dynkin diagram associated with O , and the set of positive roots Λ^+ of \mathfrak{g}_f

$$\varphi_n(w) = \sum_{\alpha \in \Lambda^+} \langle \alpha, w \rangle^n, \quad (4.8)$$

with the weighted Dynkin diagram understood as an element of the weight lattice, and the scalar product is the pairing on that lattice. We remind the reader that in our convention, for simply laced algebras, it is given by $\langle \alpha, \beta \rangle = \alpha^T \cdot C^{-1} \cdot \beta$, where C is the associated Cartan matrix, see Table VIII. Note that $\varphi_0(w)$ is understood as counting the number of positive roots α for which $\langle \alpha, w \rangle \neq 0$. The quantities defined in Eq. (4.7) are therefore easy to compute from the tables in Appendix B for any theory without needing to know the complete Jacobson-Morozov decomposition, but only the weighted Dynkin diagrams of the nilpotent orbits.

In Sec. IVA, we provide a proof that Algorithm 1 as applied to nilpotent RG flows of rank N ($\mathfrak{su}_K, \mathfrak{su}_K$) conformal matter leads to the same anomaly polynomial that is obtained from an analysis of the tensor branch effective field theory, following [37,42,43]. In essence, we can consider this as a proof that when a nilpotent vacuum expectation value is given to the moment map of the flavor symmetry of these theories, the only modes to decouple along the flow are the Nambu-Goldstone modes arising from the moment map itself. General proofs that Algorithm 1 reproduces the known anomaly polynomials (as determined from the tensor branch geometry) for the theories

$$\mathcal{A}_{N-1;f_L,f_R}^{\mathfrak{g}}(O_L, O_R), \quad \mathcal{D}_{N;f}^{\mathfrak{g}}(O), \quad \mathcal{O}_{N;f}^{\mathfrak{g}}(\emptyset, O), \quad (4.9)$$

where \mathfrak{g} is any allowed simply laced classical Lie algebra can be shown in a similar manner; it is tedious to be explicit. When \mathfrak{g} is an allowed exceptional Lie algebra, then the number of nilpotent orbits is finite, and the proof of the matching between Algorithm 1 and the tensor branch analysis can be shown by exhaustion; in Sec. IV B, we provide an explicit example: $A_{N-1}^{\mathfrak{e}_6}(0, A_1)$. In particular, this requires the knowledge of the branching rules of the adjoint representation for the nilpotent orbits of the exceptional simple Lie algebras, which we collate for convenience in Appendix B.

A. General proof for $A_{N-1}^{\mathfrak{su}_K}(O_L, O_R)$

In this section, we provide a general proof that Algorithm 1 determines the correct anomaly polynomial for arbitrary nilpotent deformations of rank N ($\mathfrak{su}(K)$, $\mathfrak{su}(K)$) conformal matter. We apply the algorithm to

$A_{N-1}^{\mathfrak{su}_K}(O_L, O_R)$ generically, and we show that this produces the same anomaly polynomial as can be read off from the known tensor branch geometry. For ease of notation, we assume that $K \geq 4$.

1. From the algorithm

The first step in Algorithm 1 is to determine the decompositions of the traces under the decomposition of the $\mathfrak{su}(K)$ algebra induced by the choice of nilpotent orbits. We begin by writing the one-instanton normalized traces in terms of traces over the fundamental representation

$$\text{Tr}F^2 = 2\text{tr}_{\text{fund}}F^2, \quad \text{Tr}F^4 = \text{tr}_{\text{fund}}F^4. \quad (4.10)$$

Let O be a nilpotent orbit of $\mathfrak{su}(K)$ represented by the integer partition

$$P_O = [1^{m_1}, 2^{m_2}, \dots, K^{m_K}] \quad \text{such that} \quad \sum_{i=1}^K im_i = K. \quad (4.11)$$

The decomposition of Lie algebras associated to this nilpotent orbit is

$$\mathfrak{su}(K) \rightarrow \mathfrak{su}(2)_X \oplus \bigoplus_{i=1}^K \mathfrak{su}(m_i), \quad (4.12)$$

where we have ignored Abelian factors.²³ Under this decomposition, the branching rule of the fundamental representation is

$$K \rightarrow \bigoplus_{i=1}^K (\mathbf{i}, \mathbf{m}_i), \quad (4.13)$$

where \mathbf{i} is the i -dimensional irreducible representation of $\mathfrak{su}(2)_X$ and \mathbf{m}_i is the fundamental representation of $\mathfrak{su}(m_i)$.²⁴ Recalling the following simple identities regarding the traces

$$\begin{aligned} \text{tr}_{A \oplus B} F^k &= \text{tr}_A F^k + \text{tr}_B F^k, \\ \text{tr}_{A \otimes B} F^2 &= \dim(B)\text{tr}_A F^2 + \dim(A)\text{tr}_B F^2, \\ \text{tr}_{A \otimes B} F^4 &= \dim(B)\text{tr}_A F^4 + \dim(A)\text{tr}_B F^4 + 6\text{tr}_A F^2 \text{tr}_B F^2, \end{aligned} \quad (4.14)$$

it is then straightforward to determine the decompositions of the traces. In particular, let F_X denote the curvature of the

²³We also assume that the Higgsing is not the trivial Higgsing, i.e., $O \neq [1^K]$.

²⁴More precisely, \mathbf{m}_i is the representation of $\bigoplus_{j=1}^K \mathfrak{su}(m_j)$ obtained by taking the tensor product of the fundamental representation of $\mathfrak{su}(m_i)$ with the trivial representation of all $\mathfrak{su}(m_{j \neq i})$ factors.

$\mathfrak{su}(2)_X$ bundle and F_i the curvature of the $\mathfrak{su}(m_i)$ bundle, then

$$\mathrm{Tr}F^2 \rightarrow \sum_{i=1}^K \left(i\mathrm{Tr}F_i^2 + \frac{m_i i(i^2 - 1)}{6} \mathrm{Tr}F_X^2 \right), \quad (4.15)$$

where we have used that

$$\mathrm{tr}_d F^2 = \frac{d(d^2 - 1)}{12} \mathrm{Tr}F^2, \quad (4.16)$$

for an arbitrary irreducible representation d of $\mathfrak{su}(2)$. We can now utilize a similar procedure to work out the decomposition of $\mathrm{Tr}F^4$. We find

$$\mathrm{Tr}F^4 \rightarrow \sum_{i=1}^K (i\mathrm{tr}_{m_i} F_i^4 + m_i \mathrm{tr}_i F_X^4 + 6\mathrm{tr}_{m_i} F_i^2 \mathrm{tr}_i F_X^2). \quad (4.17)$$

To convert all the traces to one-instanton normalized traces, we need to know several identities. First, for an arbitrary d -dimensional irreducible representation of $\mathfrak{su}(2)$, we have

$$\mathrm{tr}_d F^4 = \frac{d(3d^4 - 10d^2 + 7)}{240} (\mathrm{Tr}F^2)^2. \quad (4.18)$$

For the $\mathrm{tr}_{m_i} F_i^4$, the trace converts differently depending on whether $m_i = 2, 3$ or $m_i \geq 4$. We have

$$\mathrm{tr}_{m_i} F_i^4 = \begin{cases} \mathrm{Tr}F_i^4 & \text{if } m_i \geq 4, \\ \frac{1}{8} (\mathrm{Tr}F_i^2)^2 & \text{if } m_i = 2, 3. \end{cases} \quad (4.19)$$

Thus, we have completed the first step of decomposing the traces.

Next, we need to determine the anomaly polynomial of the Nambu-Goldstone modes arising from the moment map. Under the algebras after the decomposition in Eq. (4.12), where we recall that $\mathfrak{su}(2)_X$ is replaced with $\mathfrak{su}(2)_{R^{\mathrm{IR}}}$, the Nambu-Goldstone modes transform in the following reducible representation:

$$\begin{aligned} \mathbf{R} = & \bigoplus_{\substack{i,j=1 \\ j \neq i}}^K \bigoplus_{k=1}^{\min(i,j)} (i+j-2k, m_i, \bar{m}_j) \\ & \bigoplus_{i=1}^K \bigoplus_{k=1}^i (2i-2k, \mathbf{adj}_i \oplus \mathbf{1}), \end{aligned} \quad (4.20)$$

where \mathbf{adj}_i is the adjoint representation of $\mathfrak{su}(m_i)$. The anomaly contribution from the Nambu-Goldstone modes is simply

$$I_8^{\mathrm{NG}} = \frac{1}{2} \mathrm{ch}_{\mathbf{R}}(\{R^{\mathrm{IR}}, F_i\}) \hat{A}(T), \quad (4.21)$$

where we use $\{R^{\mathrm{IR}}, F_i\}$ to collectively denote the curvatures of the $\mathfrak{su}(2)_{R^{\mathrm{IR}}}$ bundles and all the $\mathfrak{su}(m_i)$ bundles.

Recalling that the Chern character can be written in terms of the traces as

$$ch_{\rho}(F) = \mathrm{tr}_{\rho} F^0 - \frac{1}{2} \mathrm{tr}_{\rho} F^2 + \frac{1}{24} \mathrm{tr}_{\rho} F^4 + \dots, \quad (4.22)$$

where we have ignored the terms of odd form-degree, it is straightforward to expand the anomaly polynomial in Eq. (4.21) in terms of the irreducible components of the representation in Eq. (4.20). As we will see, certain expressions appear regularly in the expansions of the traces; for convenience we define the following matrices

$$\begin{aligned} X_{i,j} &= ij - \min(i,j), \\ Y_{i,j} &= (ij - \min(i,j))(i^2 + j^2 - 2(i+j - \min(i,j)) - 1), \\ Z_{i,j} &= \frac{1}{15} \sum_{k=1}^{\min(i,j)} (i+j-2k+1)(i+j-2k) \\ &\quad \times (i+j-2k-1)(3(i+j-2k)^2 - 7). \end{aligned} \quad (4.23)$$

Now we consider the traces appearing in the expansion of the Nambu-Goldstone anomaly polynomial. We begin with

$$\mathrm{tr}_{\mathbf{R}} F^0 = \sum_{i,j=1}^K m_i m_j X_{i,j} = \dim(\mathbf{R}), \quad (4.24)$$

which is simply the dimension of the representation \mathbf{R} . We now turn to the second term, which decomposes as

$$\begin{aligned} \mathrm{tr}_{\mathbf{R}} F^2 &= \sum_{i,j=1}^K \frac{1}{2} X_{i,j} (m_i \mathrm{Tr}F_j^2 + m_j \mathrm{Tr}F_i^2) \\ &\quad + \sum_{i,j=1}^K \frac{1}{3} m_i m_j Y_{i,j} c_2(R^{\mathrm{IR}}). \end{aligned} \quad (4.25)$$

Here we have used that

$$c_2(R^{\mathrm{IR}}) = \frac{1}{4} \mathrm{Tr}F_{R^{\mathrm{IR}}}^2. \quad (4.26)$$

The quartic trace is the most tedious term to decompose, however, after a little algebra, one finds the following:

$$\begin{aligned} \mathrm{tr}_{\mathbf{R}} F^4 &= \sum_{i,j=1}^K m_i m_j Z_{i,j} c_2(R^{\mathrm{IR}})^2 + X_{i,j} (m_i \mathrm{tr}_{m_j} F_j^4 + m_j \mathrm{tr}_{m_i} F_i^4) \\ &\quad + Y_{i,j} (m_i \mathrm{Tr}F_j^2 + m_j \mathrm{Tr}F_i^2) c_2(R^{\mathrm{IR}}) + \frac{3}{2} X_{i,j} \mathrm{Tr}F_i^2 \mathrm{Tr}F_j^2. \end{aligned} \quad (4.27)$$

Now that we have determined the appropriate decompositions of the traces and the anomaly contribution for the

Nambu-Goldstone modes, we are ready to apply Algorithm 1 to determine the anomaly polynomial of $A_{N-1}^{\mathfrak{su}(K)}(O_L, O_R)$. Let the integer partitions of K associated to the nilpotent orbits O_L and O_R be

$$P_{O_L} = [1^{m_1}, 2^{m_2}, \dots, K^{m_K}], \quad P_{O_R} = [1^{m'_1}, 2^{m'_2}, \dots, K^{m'_K}]. \quad (4.28)$$

To aid in the comparison with the tensor branch 't Hooft anomaly matching approach to determining the anomaly polynomial, we will be extremely explicit here, and go coefficient-by-coefficient.

First, the contributions to the coefficients γ^{IR} and δ^{IR} come only from the Nambu-Goldstone modes

$$\begin{aligned} \gamma^{\text{IR}} &= \gamma^{\text{UV}} - \frac{7}{480} \sum_{i,j=1}^K (m_i m_j + m'_i m'_j) X_{i,j} \\ &= \gamma^{\text{UV}} - \frac{7}{480} (\dim(O_L) + \dim(O_R)), \\ \delta^{\text{IR}} &= \delta^{\text{UV}} + \frac{1}{120} \sum_{i,j=1}^K (m_i m_j + m'_i m'_j) X_{i,j} \\ &= \delta^{\text{UV}} + \frac{1}{120} (\dim(O_L) + \dim(O_R)). \end{aligned} \quad (4.29)$$

The relation between the partition data and the dimension of the orbit can be found in, e.g., [47,67], and this result is therefore consistent with Eq. (4.7).

Next, we turn to β^{IR} ; there are three contributions to the infrared anomaly from the ultraviolet anomaly polynomial, coming from the terms

$$c_2(R)p_1(T), \quad p_1(T)\text{Tr}F_L^2, \quad \text{and} \quad p_1(T)\text{Tr}F_R^2, \quad (4.30)$$

together with the Nambu-Goldstone contribution. To succinctly write how these UV terms enter in the infrared anomaly coefficients, we define the embedding index for the $\mathfrak{su}(2)_X$ factor associated to the nilpotent orbit O_L , following Eq. (3.43), as

$$I_{X_L} = \sum_{i=1}^K m_i \frac{i(i^2 - 1)}{6}, \quad (4.31)$$

and similarly we define I_{X_R} . Putting all four contributions together, we find

$$\begin{aligned} \beta^{\text{IR}} &= \beta^{\text{UV}} + 96(I_{X_L} \kappa_L^{\text{UV}} + I_{X_R} \kappa_R^{\text{UV}}) \\ &\quad - \frac{1}{12} \sum_{i,j=1}^K (m_i m_j + m'_i m'_j) Y_{i,j}. \end{aligned} \quad (4.32)$$

Finally, we turn to the $c_2(R^{\text{IR}})^2$ anomaly coefficient α^{IR} . In addition to the Nambu-Goldstone modes, there exist eight

terms in the UV anomaly polynomial that contribute to this IR coefficient; these are

$$\begin{aligned} c_2(R)^2, \quad c_2(R)\text{Tr}F_L^2, \quad c_2(R)\text{Tr}F_R^2, \quad \text{Tr}F_L^4, \quad \text{Tr}F_R^4, \\ \text{Tr}F_L^2\text{Tr}F_L^2, \quad \text{Tr}F_L^2\text{Tr}F_R^2, \quad \text{Tr}F_R^2\text{Tr}F_R^2. \end{aligned} \quad (4.33)$$

For ease of notation, we define the following quantity:

$$I_{O_L^2} = \sum_{i=1}^K m_i \frac{i(3i^4 - 10i^2 + 7)}{240}, \quad (4.34)$$

and again analogously for $I_{O_R^2}$. Then

$$\begin{aligned} \alpha^{\text{IR}} &= \alpha^{\text{UV}} + 96(I_{X_L} \nu_L^{\text{UV}} + I_{X_R} \nu_R^{\text{UV}}) \\ &\quad + 384(I_{O_L^2} \mu_L^{\text{UV}} + I_{O_R^2} \mu_R^{\text{UV}}) \\ &\quad + 384(I_{X_L}^2 \rho_{LL}^{\text{UV}} + I_{X_L} I_{X_R} \rho_{LR}^{\text{UV}} + I_{X_R}^2 \rho_{RR}^{\text{UV}}) \\ &\quad - \frac{1}{2} \sum_{i,j=1}^K (m_i m_j + m'_i m'_j) Z_{i,j}. \end{aligned} \quad (4.35)$$

The anomalies involving the infrared non-Abelian flavor symmetries are our next port of call. We begin with the mixed flavor-gravitational anomalies. We find

$$\kappa_{L,i}^{\text{IR}} = i\kappa_L^{\text{UV}} - \frac{1}{96} \sum_{j=1}^K m_j X_{i,j}, \quad \kappa_{R,i}^{\text{IR}} = i\kappa_R^{\text{UV}} - \frac{1}{96} \sum_{j=1}^K m'_j X_{i,j}. \quad (4.36)$$

Next, we consider the quartic anomalies of the $\mathfrak{su}(m_i)$ flavor symmetries—obviously these $\text{Tr}F_i^4$ terms can only exist if the flavor algebra admits an independent quartic Casimir, i.e., $m_i > 3$. Assuming that this condition is satisfied, we find

$$\mu_{L,i}^{\text{IR}} = i\mu_L^{\text{UV}} - \frac{1}{24} \sum_{j=1}^K m_j X_{i,j}, \quad \mu_{R,i}^{\text{IR}} = i\mu_R^{\text{UV}} - \frac{1}{24} \sum_{j=1}^K m'_j X_{i,j}. \quad (4.37)$$

Let us now consider the mixed R-flavor anomalies. In addition to the Nambu-Goldstone modes which must be subtracted, these anomalies have contributions from three distinct UV anomalies. We have

$$\nu_{L,i}^{\text{IR}} = i\nu_L^{\text{UV}} + 8iI_{X_L} \rho_{LL}^{\text{UV}} + i(i^2 - 1)\mu_L^{\text{UV}} - \frac{1}{24} \sum_{j=1}^K m_j Y_{i,j}, \quad (4.38)$$

and analogously for $\nu_{R,i}^{\text{IR}}$. Finally, we consider the mixed flavor-flavor anomalies. We begin with the anomalies from

the infrared flavor algebras that come from either the left or the right UV flavor algebra. We have

$$\rho_{LL,ij}^{\text{IR}} = ij\rho_{LL}^{\text{UV}} - \frac{1}{32}X_{i,j}. \quad (4.39)$$

If i is such that $m_i = 2, 3$, then there are two extra contributions to the $j = i$ anomaly coefficient

$$\rho_{LL,ii}^{\text{IR}} = i^2\rho_{LL}^{\text{UV}} + \frac{i}{8}\mu_L^{\text{UV}} - \frac{1}{32}X_{i,i} - \frac{1}{192}\sum_{j=1}^K X_{i,j}m_j. \quad (4.40)$$

The obvious modifications hold for the anomaly coefficients $\rho_{RR,ij}$. We also consider the flavor-flavor anomalies that mix the flavor symmetry factors localized on the left and the right; such anomalies lack a Nambu-Goldstone contribution. We find

$$\rho_{LR,ij}^{\text{IR}} = ij\rho_{LR}^{\text{UV}}. \quad (4.41)$$

We have now used Algorithm 1 to determine the generic form of the anomaly polynomial $A_{N-1}^{\mathfrak{su}_K}(O_L, O_R)$ written in terms of the partitions in Eq. (4.28) defining the nilpotent orbits O_L and O_R . While we have focused on the cases where $K > 3$, the special cases of $K = 2, 3$ are governed by identical formulas, except that one needs to formally set $\mu_L^{\text{UV}} = \mu_R^{\text{UV}} = 0$, to account for the absence of an independent quartic Casimir for $\mathfrak{su}(2)$ and $\mathfrak{su}(3)$.

2. From the tensor branch

We now determine the anomaly polynomial of $A_{N-1}^{\mathfrak{su}_K}(O_L, O_R)$ from the geometric description of the effective field theory at the generic point of the tensor branch. The tensor branch configuration takes the form

$$A_{N-1}^{\mathfrak{su}_K}(O_L, O_R): \begin{array}{ccccccc} \mathfrak{su}_{k_1} & \mathfrak{su}_{k_2} & & \mathfrak{su}_{k_K} & \mathfrak{su}_{k_K} & \mathfrak{su}_{k'_K} & \mathfrak{su}_{k'_K} \\ 2 & 2 & \cdots & 2 & \cdots & 2 & 2 \\ [m_1] & [m_2] & \cdots & [m_K] & \underbrace{\cdots}_{N-2K-1} & [m'_K] & [m'_1] \end{array}, \quad (4.42)$$

as described in Appendix D. We will assume that neither O_L nor O_R are the nilpotent orbits associated to the $[K]$ partition; these special cases can be handled individually. The anomaly polynomial can be written as

$$I_8 = I_8^{\text{1-loop}} + I_8^{\text{GS}}, \quad (4.43)$$

where the one-loop contribution is the sum of the contributions of the vector, tensor and hypermultiplets. We refer in particular to [43], where the algorithm to determine the anomaly polynomial from the tensor branch geometry is given explicitly, and for the anomaly contributions from each multiplet. The Green-Schwarz contribution is

$$I_8^{\text{GS}} = -\frac{1}{2}\tilde{A}_{i,j}I^iI^j, \quad I^i = -\frac{1}{4}B^{ia}\text{Tr}F_a^2 + h_i^\vee c_2(R). \quad (4.44)$$

Here i, j index the (-2) -curves, left-to-right. We have not written the gauge field strengths in I^i as they all cancel in the final result, a runs over the simple non-Abelian flavor factors of the SCFT, and h_i^\vee is the dual Coxeter number of the algebra supported over the i th curve. Finally, the matrix \tilde{A} is the inverse of the (negative-definite) Cartan matrix of A_{N-1} ; it has entries

$$\tilde{A}_{i,j} = \frac{ij}{N} - \min(i, j). \quad (4.45)$$

To compare to the anomalies as determined by Algorithm 1, we need to know the UV anomaly coefficients for conformal matter; these appear in Eq. (3.8). We study the 't Hooft anomalies associated to the flavor symmetries first, as they are the simplest. Consider $\kappa_{L,i}$; the only contribution is from the bifundamental hypermultiplet charged under $\mathfrak{su}(m_i)$. We find that

$$\begin{aligned} \kappa_{L,i} &= \frac{1}{96}k_i = \frac{1}{96}\left(K - \sum_{j=1}^{K-i} jm_{i+j}\right) \\ &= i\left(\frac{K}{96}\right) - \frac{1}{96}\sum_{j=1}^K m_j X_{i,j}. \end{aligned} \quad (4.46)$$

Here we have used the elementary fact about integer partitions of K that

$$K - \sum_{j=1}^{K-i} jm_{i+j} = iK - \sum_{j=1}^K m_j(ij - \min(i, j)). \quad (4.47)$$

We have thus verified Eq. (4.36). Contributions of $\mu_{L,i}$ similarly arise only from the bifundamental hypermultiplet between $\mathfrak{su}(m_i)$ and $\mathfrak{su}(k_i)$, and thus almost identical manipulations reveal that the tensor branch calculation reproduces Eq. (4.37). Consider now the $\rho_{LR,ij}$ coefficient; the only contribution is the Green-Schwarz term and we find

$$\begin{aligned} \rho_{LR,ij} &= -\frac{1}{16}\tilde{A}_{i,N-j} = \frac{1}{16}\left(\min(i, N-j) - \frac{i(N-j)}{N}\right) \\ &= \frac{1}{16}ij\left(1 - \frac{N-1}{N}\right) = ij\left(-\frac{\tilde{A}_{1,N-1}}{16}\right). \end{aligned} \quad (4.48)$$

This verifies Eq. (4.41). Henceforth, we silently use the fact that

$$\tilde{A}_{i,N-j} = ij\tilde{A}_{1,N-1}. \quad (4.49)$$

Next, we consider $\rho_{LL,ij}$; we first assume that $i \neq j$ or $m_i > 3$. The only contribution is from the Green-Schwarz term and we find

$$\begin{aligned}\rho_{LL,ij} &= -\frac{1}{16}\tilde{A}_{i,j} = \frac{1}{32}\left(\min(i,j) - \frac{ij}{N}\right) \\ &= ij\left(\frac{N-1}{32N}\right) - \frac{1}{32}(ij - \min(i,j)).\end{aligned}\quad (4.50)$$

When $i = j$ and $m_i = 2, 3$ then there is an additional contribution from the bifundamental hypermultiplet charged under $\mathfrak{su}(m_i)$. This contributes in the same way as the bifundamental hypermultiplet for the $\kappa_{L,i}$ and $\mu_{L,i}$, and thus we find

$$\begin{aligned}\rho_{LL,ii} &= i^2\left(\frac{N-1}{32N}\right) - \frac{1}{32}i(i-1) + \frac{i}{8}\left(\frac{K}{24}\right) \\ &\quad - \frac{1}{192}\sum_{j=1}^K X_{i,j}m_j.\end{aligned}\quad (4.51)$$

Thus, we have shown that Eqs. (4.39) and (4.40) from the algorithm agree with the geometric calculation. Next, we turn to $\nu_{L,i}$. Only Green-Schwarz terms can contribute to this anomaly coefficient. We find

$$\begin{aligned}\nu_{L,i} &= \frac{1}{4}\sum_{j=1}^{N-1} k_i\tilde{A}_{j,i} = \frac{i}{4N} + (N-1)I_{X_L} + \frac{K}{24}i(i^2 + 2) \\ &\quad - \frac{iKN}{8} - \frac{1}{24}\sum_{j=1}^K m_j Y_{i,j},\end{aligned}\quad (4.52)$$

where we have rewritten the sum over the whole quiver in terms of the partition data, therefore recovering Eq. (4.38).

We now move on to the terms that do not involve the flavor symmetry. Closed-form expression in terms of the gauge group ranks k_i and the pairing matrix are straightforward to determine, see, e.g., [47]. We must therefore convert them into the partition data to compare them with the expressions found in the previous subsection.

The coefficients γ and δ have contributions from all three types of multiplets, but not from the Green-Schwarz term. For the former, one finds that

$$\begin{aligned}\delta &= -\frac{N-1}{2} - \frac{1}{120}\sum_{i=1}^{N-1} k_i m_i = -\frac{N}{2} - \frac{(K^2-1) - 29}{60} \\ &\quad + \frac{1}{120}\sum_{i,j=1}^K (m_i m_j + m'_i m'_j) X_{i,j},\end{aligned}\quad (4.53)$$

where we have used the relation between the value of k_i for the gauge algebra and the partition data, see Appendix (D5), as well as Eq. (4.47) to simplify the result and put it in the same form the value of δ given in Eq. (4.29). Up to small difference in the numerology of the constant factors, one can verify that the same is also true for γ .

For β , the only contributions are from the tensor and vector multiplets in the one-loop anomaly polynomial. We find

$$\beta = -\frac{1}{2}\left(\sum_{i=1}^K (k_i^2 + k_i'^2) - 2K^3 - K^2 + 2 + N(K^2 - 2)\right),\quad (4.54)$$

where we written the Green-Schwarz contribution in terms of the k_i on the left and the right. These can then be converted to the partition data using the relation

$$\sum_{i=1}^K k_i^2 = K^3 - 2I_X K + \frac{1}{6}\sum_{i=1}^K m_i m_j Y_{i,j},\quad (4.55)$$

and we therefore recover what we have found for in the previous subsection, see Eq. (4.32). Finally, the $c_2(R)^2$ term arise from contributions of both tensor and vector multiplets, as well as the Green-Schwarz term

$$\alpha = -12\sum_{i,j=1}^{N-1} k_i k_j \tilde{A}_{i,j} + 2\beta.\quad (4.56)$$

Decomposing the first term into the partition orders m_i and m'_i is tedious, but straightforward. When the dust settles, one finds

$$\begin{aligned}\sum_{i,j=1}^{N-1} k_i k_j \tilde{A}_{i,j} &= -\frac{N(N^2-1)}{12} + \frac{1}{N}(I_{X_L} + I_{X_R}) - (I_{X_L}^2 + I_{X_R}^2) \\ &\quad + \frac{6N-5}{6}K(I_{X_L} + I_{X_R}) - \frac{4}{3}(I_{O_L^2} + I_{O_R^2}) \\ &\quad + \frac{1}{24}\sum_{i,j=1}^K (m_i m_j + m'_i m'_j) \left(Z_{i,j} - \frac{1}{3}Y_{i,j}\right),\end{aligned}\quad (4.57)$$

from which we once obtain the same expression as in Eq. (4.35), as expected.

Thus, we have proven that the anomaly polynomial of Higgsed rank N ($\mathfrak{su}(K)$, $\mathfrak{su}(K)$) as determined from the geometric description of the tensor branch is identical to the anomaly polynomial obtained by following Algorithm 1.

B. An exceptional example: $A_{N-1}^{\mathfrak{e}_6}(A_1, \mathbf{0})$

For the parent theories in Eq. (4.1) where \mathfrak{g} is an exceptional Lie group, there are only a finite number of nilpotent orbits, and thus one can verify that Algorithm 1 produces the same result as the geometry, exhaustively. While we have carried out this exhaustive process, we present here only one example: $A_{N-1}^{\mathfrak{e}_6}(0, A_1)$. This example also appeared in Sec. III D.

First, we consider the anomalies of the ultraviolet theory: $A_{N-1}^{e_6}$. These can be determined directly from the geometry, and we find

$$\begin{aligned}\alpha^{\text{UV}} &= 576N^3 - 334N + 77, & \beta^{\text{UV}} &= \frac{77 - 166N}{2}, \\ \gamma^{\text{UV}} &= \frac{30N + 523}{240}, & \delta^{\text{UV}} &= \frac{-30N - 49}{60}, & \kappa_{L,R}^{\text{UV}} &= \frac{1}{8}, \\ \nu_{L,R}^{\text{UV}} &= \frac{3 - 6N}{2}, & \mu_{L,R}^{\text{UV}} &= 0, & \rho_{LL,RR}^{\text{UV}} &= \frac{3N - 1}{32N}, & \rho_{LR,RL}^{\text{UV}} &= \frac{1}{16N},\end{aligned}\quad (4.58)$$

where the subscripts L and R refer to the ‘‘left’’ and ‘‘right’’ e_6 flavor symmetry factors, respectively. Similarly, we can determine the anomalies of the infrared theory, $A_{N-1}^{e_6}(0, A_1)$, from the geometry. In this case, the effective field theory on the tensor branch is

$$\underbrace{1 \ 3 \ 16 \ \cdots \ 1 \ 3 \ 16 \ 1 \ 2}_{N-1}, \quad (4.59)$$

and thus we find that the anomaly coefficients are

$$\begin{aligned}\alpha^{\text{IR}} &= 576N^3 - 622N + 256 - \frac{12}{N}, & \beta^{\text{IR}} &= \frac{100 - 166N}{2}, \\ \gamma^{\text{IR}} &= \frac{30N + 446}{240}, & \delta^{\text{IR}} &= \frac{-30N - 38}{60}, & \kappa_L^{\text{IR}} &= \frac{1}{8}, & \kappa_R^{\text{IR}} &= \frac{3}{32}, \\ \nu_L^{\text{IR}} &= \frac{3 - 6N}{2} + \frac{1}{4N}, & \nu_R^{\text{IR}} &= \frac{3 - 6N}{2} + \frac{3N - 1}{4N}, & \mu_L^{\text{IR}} &= 0, & \mu_R^{\text{IR}} &= \frac{1}{8}, \\ \rho_{LL}^{\text{IR}} &= \frac{3N - 1}{32N}, & \rho_{RR}^{\text{IR}} &= \frac{2N - 1}{32N}, & \rho_{LR,RL}^{\text{IR}} &= \frac{1}{16N},\end{aligned}\quad (4.60)$$

where the subscript L denotes the unbroken e_6 flavor symmetry, and R is for the $\mathfrak{su}(6)$ flavor that right e_6 is broken to by the Higgsing.

We would now like to reproduce these infrared anomalies from the Nambu-Goldstone analysis of Algorithm 1. The nilpotent orbit A_1 of e_6 is associated to the decomposition

$$e_6 \rightarrow \mathfrak{su}(2)_X \oplus \mathfrak{su}(6), \quad (4.61)$$

where both factors in the decomposition have embedding index one; this can be seen easily from the adjoint branching, which is

$$78 \rightarrow (3, 1) \oplus (1, 35) \oplus (2, 20). \quad (4.62)$$

Thus, we can see that we must decompose the curvature of the right e_6 flavor bundle as

$$\text{Tr}F_R^2 \rightarrow \text{Tr}F_X^2 + \text{Tr}F_R^2, \quad (4.63)$$

where we have abused notation and used F_R on the left to refer to the curvature of the UV e_6 bundle, and on the right to refer to the curvature of the IR $\mathfrak{su}(6)$ bundle. We do not

need to discuss the decomposition of the $\text{Tr}F_R^4$ as e_6 does not possess a quartic Casimir.

From the decomposition of the adjoint representation in Eq. (4.62), the Nambu-Goldstone fermions transform in the following representations of the $\mathfrak{su}(2)_{R^{\text{IR}}} \oplus \mathfrak{su}(6)$ infrared global symmetry

$$(2, 1), \quad (1, 20). \quad (4.64)$$

Thus, the contribution to the anomaly polynomial from the Nambu-Goldstone modes is

$$I_8^{\text{NG}} = \frac{1}{2} ch_2(R^{\text{IR}}) \hat{A}(T) + \frac{1}{2} ch_{20}(F_R) \hat{A}(T) \Big|_{8\text{-form}}, \quad (4.65)$$

where we have just written R^{IR} for the curvature of the $\mathfrak{su}(2)_{R^{\text{IR}}}$ bundle. To expand this, we must convert traces in the 20 representation of $\mathfrak{su}(6)$ to one-instanton normalized traces

$$\begin{aligned}ch_{20}(F_R) &= 20 - \frac{3}{2} \text{Tr}F_R^2 + \frac{1}{24} \left(-6 \text{Tr}F_R^4 + \frac{3}{2} (\text{Tr}F_R^2)^2 \right) \\ &+ \cdots.\end{aligned}\quad (4.66)$$

Altogether, then, we find that the Nambu-Goldstone modes contribute to the infrared anomaly in the following explicit way

$$I_8^{\text{NG}} = 11 \times \frac{1}{5760} (7p_1(T)^2 - 4p_2(T)) + \left(-\frac{3}{4} \text{Tr} F_R^2 - \frac{1}{2} c_2(R^{\text{IR}}) \right) \times \left(-\frac{1}{24} p_1(T) \right) + \frac{1}{24} c_2(R^{\text{IR}})^2 + \frac{1}{32} (\text{Tr} F_R^2)^2 - \frac{1}{8} \text{Tr} F_R^4. \quad (4.67)$$

Now that we have determined I_8^{NG} , we can combine it with the UV anomaly coefficients as in Eq. (4.58), following Algorithm 1, and we see that the infrared anomalies that were given via the geometry in Eq. (4.60) appear directly. It is straightforward to apply this simple procedure to any exceptional parent theory by utilizing the nilpotent orbit data collated in Appendix B.

V. DISCUSSION

The main results of our work are the closed-form expressions for the anomaly polynomials of any long quivers, or equivalently Algorithm 1, giving a prescription to find the complete anomaly polynomial of a 6D (1, 0) SCFT obtained through nilpotent renormalization group flows of the parent theories. Beyond their usefulness as tools to efficiently obtain the numerical values of its coefficients, they also enable us to study the deformed theories purely in terms of gauge-invariant quantities computed directly at the conformal fixed point, without invoking the effective field theory on the generic point of the tensor branch. That is, we can understand the complete anomaly polynomial of an SCFT in terms of its conformal spectrum rather than its geometric description.

As we have already alluded to, a particularly important set of quantities of a 6D conformal field theory are its central charges. These are part of the conformal data, and are in principle defined independently of any gauge description or geometric engineering. For instance, the central charges C_T and C_J are obtained by computing the two-point correlators of the energy-momentum tensor $T_{\mu\nu}$ and flavor currents J_a^μ , respectively [82,83]

$$\langle T^{\mu\nu}(x) T^{\rho\sigma}(0) \rangle = \frac{C_T}{\text{Vol}(\mathcal{S}^5)^2} \frac{P^{\mu\nu\rho\sigma}}{x^{12}},$$

$$\langle J_a^\mu(x) J_b^\nu(0) \rangle = \frac{C_{J,a}}{\text{Vol}(\mathcal{S}^5)^2} \frac{\delta^{ab} P^{\mu\nu}}{x^{10}}, \quad (5.1)$$

where $P^{\mu\nu\rho\sigma}$ and $P^{\mu\nu}$ are the spin-two and spin-one projectors, respectively. It is also well-known that in the presence of a background metric, there is a Weyl anomaly and the tracelessness condition of the energy-momentum tensor is broken [84,85]

$$\langle T_\mu^\mu \rangle = \frac{a}{(4\pi)^3} E_6 + \dots, \quad (5.2)$$

where E_6 is the six-dimensional Euler density, while the \dots encode both Weyl-invariant and scheme-dependent terms. In unitary theories, the central charges and the coefficient a must be positive. They are in particular also related to OPE coefficients, which makes them particularly relevant in the modern incarnation—numerical or analytical—of the conformal bootstrap [86,87]. These quantities are furthermore related to particular combinations of the coefficients appearing in the anomaly polynomial of a given (1, 0) SCFT [2,83]

$$C_T = 168(2\alpha - 3\beta + 4\gamma + \delta), \quad (5.3)$$

$$C_{J,a} = 240(\kappa_a - \nu_a), \quad (5.4)$$

$$a = \frac{16}{7} \left(\alpha - \beta + \gamma + \frac{3}{8} \delta \right). \quad (5.5)$$

Our results therefore make it particularly easy to find them directly without going through geometric engineering.

In Sec. VA, we discuss how the anomaly polynomial of theories described by short quivers can be understood as limits of long quivers, and how one can define additional minimal building blocks encoding the nilpotent breakings that are well behaved under fusion, despite possibly having negative central charges. In Sec. VB, we come back to the Weyl anomaly coefficient a defined in Eq. (5.2), and give a proof of the a -theorem for nilpotent RG flows using only the group theory related to nilpotent orbits. We close by discussing possible future directions in Sec. VC.

A. Building blocks and analytic continuation

As we go along the Higgs branch RG flows, there are fewer and fewer curves in the tensor branch description, and we have assumed throughout that the quiver is long enough so that either of its ends cannot influence the other. On the other hand, even when one of its tails is kept undeformed, if the quiver is short enough, as we go through nilpotent RG flows we could ultimately have no curves left even though the end of the Hasse diagram of the associated flavor symmetry has not been reached.

It is however possible to “analytically continue” the anomaly polynomial of long quivers [22,48] and consider values of N that are smaller than the number of minimal conformal matter affected by the nilpotent orbits. When $\mathfrak{g} = \mathfrak{su}_K$ for instance, a nilpotent orbit can affect the gauge symmetry of up to K curves, but we can in principle set $N < K$ in the anomaly polynomial. This enables us to formally define a deformed version of minimal conformal matter

$$\mathcal{A}_{0;1,f}^{\mathfrak{g}}(\emptyset, O): [\mathfrak{g}] - [O], \quad (5.6)$$

which we have depicted in a pictorial way as before. These putative theories, along with the other types of building blocks we have encountered, allow us to construct any long quiver, even when the nilpotent orbit corresponds to a curve configuration where one or more conformal matter links are “eaten” by a nilpotent deformation, and the building block therefore does not have an associated quiver. In fact, in many cases, when the nilpotent orbit O is located too deep in the Hasse diagram, the central charges, C_T or $C_{J,a}$, of $\mathcal{A}_{0;1,f}^{\mathfrak{g}}(\emptyset, O)$ are negative, in apparent violation of unitarity.

In Sec. III A, we have however seen that we can compute the anomaly polynomial directly at the conformal fixed point, and consider minimal conformal matter as a one-loop contribution. Even though $\mathcal{A}_{0;1,f}^{\mathfrak{g}}(\emptyset, O)$ might have a seemingly inconsistent anomaly polynomial, when it is fused with more minimal conformal matter theories, we obtain an anomaly polynomial that matches exactly that of the tensor branch computation. This is shown in the same way we have done around Eq. (3.20) for higher-rank conformal matter, but now using $\mathcal{A}_{0;1,f}^{\mathfrak{g}}(\emptyset, O)$ at both ends of the quiver. This further has the advantage of completely bypassing the possible propagation of the breaking throughout the quiver.

Furthermore, the fact that the minimal building blocks defined in Eq. (5.6) do not have a quiver that can be read out from a table or a partition does not mean that they do not correspond to well-defined theories. In fact, a number of theories with short bases—that is, those with a small number of curves on the tensor branch—can be understood as an analytical continuation of a long quiver [22,48]. For instance, one can find that the following non-Higgsable cluster

$$\mathcal{T}: \overset{\mathfrak{su}_2}{2} \overset{\mathfrak{g}_2}{3}, \quad (5.7)$$

has the same anomaly polynomial as a fractional $(\mathfrak{e}_6, \mathfrak{e}_6)$ conformal matter deformed with a nilpotent orbit $O = A_4 + A_1$ when $N \rightarrow 2$

$$\begin{aligned} I_8(\mathcal{T}) &= I_8\left(\mathcal{A}_{1;1,\frac{2}{3}}^{\mathfrak{e}_6}(A_4 + A_1, \emptyset)\right), \\ \mathcal{T} &\simeq [A_4 + A_1] - \mathfrak{g} - [\mathfrak{g}_{\frac{2}{3}} = \emptyset]. \end{aligned} \quad (5.8)$$

These two theories have *a priori* nothing in common. No \mathfrak{e}_6 node appears in the quiver of \mathcal{T} , and as can be seen from Table XV, a complete minimal conformal matter has been “eaten” in the quiver of $\mathcal{A}_{N-1;1,\frac{2}{3}}^{\mathfrak{e}_6}(A_4 + A_1, \emptyset)$. Nonetheless, it is straightforward to check that both anomaly polynomials precisely match. This can be extended to all non-Higgsable clusters [22]. In this sense, as our results do not involve the tensor branch description and we can work directly at the conformal fixed point; we can not only deal

with long quivers by fusing the building blocks defined in Eq. (5.6) to other conformal matter, but they can describe short quivers as well.

In [22], it was also shown that in some cases, short quivers obtained by analytic continuation exhibit flavor enhancement. It would therefore be interesting to see if more general types of short quivers can be obtained using these deformed building blocks, and whether the enhancement can be understood from the Jacobson-Morozov decomposition.

On the other hand, we stress the fact that using analytical continuation gives rise to negative central charges does not necessarily mean that giving a vacuum expectation value to the moment map with the corresponding nilpotent orbit is forbidden. At the field theory level, there is *a priori* nothing preventing one to do so, and the apparent violation of unitarity should be thought of more as a failure of Algorithm 1 rather than an obstruction to the corresponding deformation. Indeed we have assumed the quiver to be long enough precisely to avoid these kinds of edge cases. It might well be that there are additional modes decoupling, or that our prescription to find the IR R-symmetry is not correct. Since the relations between the central charges and the anomaly polynomial all involve R-symmetry terms, it might be that a modification of the prescription in the case of short bases cures this apparent problem. Note that in three dimensions something similar happens for “ugly” theories, where a naive IR R-symmetry assignment for certain BPS monopoles lead to similar “violations” of unitarity [88]. We leave a systematic analysis of short quivers, including the question of these types of breaking and analytic continuation for future work.

B. The a -theorem for nilpotent deformations

The a -anomaly has a preeminent role in the study of RG flows. In two [89] and four [90] dimensions, an a -theorem has been shown: along an RG flow between two (*a priori* nonsupersymmetric) CFTs, the coefficient a decreases

$$a^{UV} - a^{IR} > 0. \quad (5.9)$$

This can be understood as a statement on the irreversibility of RG flows, as a is a measure of the number of degrees of freedom of the CFT. In six dimensions, the question has been tackled using a background dilaton [91–94], but the fate of a general a -theorem remains uncertain in even dimensions higher than four. For 6D (1, 0) SCFTs, the a -theorem has been shown for tensor branch flows, as well as for large classes of Higgs branch flows [2,47,95,96].

Following the spirit of [47,95], we can use our results to establish the a -theorem for nilpotent flows in a short and concise way. Since the anomaly polynomial depends only on group-theoretical quantities, we need only describe how the coefficients change as we go from one theory to another. We will focus on conformal matter with a nilpotent

deformation on one side $A_{N-1}^{\mathfrak{g}}(O, \emptyset)$ for ease of exposition, but the argument extends to all other theories. From Eq. (4.7), the shifts in the relevant coefficients are given by

$$\begin{aligned}\alpha^{\text{UV}} - \alpha^{\text{IR}} &= 12\Gamma N I_X + \frac{12}{N} I_X^2 + 4(\beta^{\text{UV}} - \beta^{\text{IR}}) \\ &\quad - (4\varphi_3(w) + \varphi_0(w)), \\ \beta^{\text{UV}} - \beta^{\text{IR}} &= -\varphi_1(w) + \frac{1}{2}\varphi_0(w), \\ \gamma^{\text{UV}} - \gamma^{\text{IR}} &= +\frac{7}{240}\dim(O), \quad \delta^{\text{UV}} - \delta^{\text{IR}} = -\frac{1}{120}\dim(O).\end{aligned}\tag{5.10}$$

Using Eq. (5.5), the change in the quantity a between the two theories related by a nilpotent deformation is given by

$$\begin{aligned}a^{\text{UV}} - a^{\text{IR}} &= \frac{16}{7} \left((\alpha^{\text{UV}} - \alpha^{\text{IR}}) - (\beta^{\text{UV}} - \beta^{\text{IR}}) + (\gamma^{\text{UV}} - \gamma^{\text{IR}}) \right. \\ &\quad \left. + \frac{3}{8}(\delta^{\text{UV}} - \delta^{\text{IR}}) \right),\end{aligned}\tag{5.11}$$

The shifts of γ, δ depending only on the dimension of the nilpotent orbit, their combined contribution is clearly positive. To establish the a -theorem for nilpotent deformations, we therefore need only show that the shift in α is always positive, while that of β is always negative. The signs of these shifts depends on the behavior of the function $\varphi_n(w)$ defined in Eq. (4.8), which we recall here for convenience

$$\varphi_n(w) = \sum_{\alpha \in \Lambda^+} \langle \alpha, w \rangle^n, \tag{5.12}$$

As discussed around Eq. (3.30), the entries of the vector w defining the weighted Dynkin diagram labeling the nilpotent orbit correspond to the charges of the simple roots under the $\mathfrak{su}(2)_X$ Cartan element, which can only take values 0, 1, 2. One can then show that for a given nilpotent orbit with weighted Dynkin diagram w , if $m \leq n$, then $\varphi_m(w) \leq \varphi_n(w)$. The shift in β is therefore always negative. On the other hand that of α is more involved and depends on the embedding index I_X , which can also be written as a function of $\varphi_2(w)$

$$I_X = \frac{1}{2} \langle w, w \rangle = \frac{\varphi_2(w)}{2h_{\mathfrak{g}}^{\vee}}, \tag{5.13}$$

as a consequence of the definition of the Killing form. As can be seen from Appendix D, long quivers must have $N \geq r_{\mathfrak{g}}$.²⁵ From the strange formula of Freudenthal and de

²⁵For exceptional algebras, the long quiver condition is $N \geq 5$, but the bound on the embedding indices is also satisfied in that case.

Vries, one can then show that $I_X < 6r_{\mathfrak{g}}\Gamma$, and using $\varphi_3(w) \leq \varphi_2(w)^2$, it is then straightforward to see that the shift in α is always positive for long quivers. The contribution from γ and δ depending only on the dimension of the nilpotent orbits, this establishes the a -theorem for RG flows between conformal matter and the SCFT associated with the nilpotent orbit O .

We can however do better and consider flows between two theories in the Hasse diagram of the corresponding flavor algebras. Under the partial ordering of nilpotent orbits, see Sec. II D, one can check that if $O_1 < O_2$ then $\varphi_n(w_1) \geq \varphi_n(w_2)$ for $n \leq 3$. This can be understood as follows: as we go deeper in the Hasse diagram of a given algebra, more and more roots are charged under the $\mathfrak{su}(2)$ subalgebra defining the embedding ρ_O . The quantity $\varphi_n(w)$ being essentially a positive weighted sum over those charges, this explains the relation. For instance, in the case of $\varphi_0(w)$, this is immediate, and for $\varphi_2(w)$ this can be understood as a consequence of the embedding index I_X growing along the Hasse diagram.

Now, since the a -theorem is satisfied for any choice of nilpotent deformations of the parent theory, these relations imply that if $O_1 < O_2$, it is also satisfied for an RG flow between $A_{N-1}^{\mathfrak{g}}(O_1, \emptyset)$ and $A_{N-1}^{\mathfrak{g}}(O_2, \emptyset)$.

This can be extended to any type of long quiver, including possible fractions, generalizing the results previously obtained in [47]. From these simple group-theoretical arguments, we have therefore shown that a is monotonically decreasing as we go down in the Hasse diagram without needing to ever refer to the tensor branch description or the F-theory construction.

We note that there can be theories $A_{N-1}^{\mathfrak{g}}(O, \emptyset)$ for which $N < r_{\mathfrak{g}}$. From Eq. (5.10), one will sometimes find that the value of $a^{\text{UV}} - a^{\text{IR}}$ becomes negative. Those cases however correspond to analytically continued theories in the sense used in the previous subsection: the nilpotent orbit is too large and there is no associated quiver describing the tensor branch of the theory. Similar cases also occur when there is a deformation on both sides and one end of the quiver is affecting the other.

C. Beyond nilpotent orbits

Algorithm 1 heavily utilizes the properties of the Jacobson-Morozov decomposition to find the IR anomaly polynomial, as well as the fact that in the infrared, the R-symmetry is diagonal combination of the $\mathfrak{su}(2)_R$ UV R-symmetry and the $\mathfrak{su}(2)_X$ subalgebra of the flavor symmetry. A natural generalization would be to see if a similar prescription can be found in the case of deformations of orbi-instantons related to embedding of ADE discrete groups into E_8 . In the case of $\mathcal{O}_N^{\mathfrak{su}\kappa}(\sigma, \emptyset)$, closed-form expressions for the gravitational and R-symmetry coefficients resembling those appearing in Eq. (4.7) are known [49]. Indeed, in those cases the homomorphisms

$\sigma \in \text{Hom}(\mathbb{Z}_K, E_8)$ are classified by Kac labels, which can be interpreted as weighted Dynkin diagrams similar to those labeling nilpotent orbits.

When the Kac labels are equivalent to the weighted Dynkin diagrams of nilpotent orbits of e_8 , applying Algorithm 1 as if the orbi-instanton deformation was nilpotent often, but not always, leads to the correct result. However, this only occurs in a handful of cases given a choice of K , and Kac labels have no generalizations to algebras of DE type. Moreover, expressing the IR R-symmetry in terms of the UV data is more opaque in those cases, as we now deal with embeddings of discrete groups rather than $\mathfrak{su}(2)$ subalgebras into the unbroken flavor symmetry. Finding an algorithm in terms of the Nambu-Goldstone modes decoupling from the UV theory \mathcal{O}_N^g would however help us better understand the orbi-instanton theory. Indeed if there are modes beyond those associated with the moment map becoming massive along the RG flow, this would teach us about the other low-lying protected superconformal multiplets in its gauge-invariant spectrum, and how they are related to the moment map. Having closed-form expressions for the anomaly polynomials of Higgsed orbi-instanton theories is particularly interesting as these 6D (1, 0) SCFTs are *very Higgsable*, and thus their anomalies behave in a simple way under torus-compactification [49,60,61]. Such understanding would be especially useful to study torus-compactifications with nontrivial twists, such as Stiefel-Whitney twists, turned on along the torus [97–99].

Beyond superconformal theories, the techniques we have used throughout this work can also be applied to Little String Theories (LSTs). These theories, specific to six dimensions, describe strings decoupled from gravity and can be realized in F-theory in a very similar way to SCFT, and also admit a classification scheme [100], see [101] for a concise review. In the case of heterotic LSTs, the structure of the Higgs branch flows are similar to those of orbi-instantons, and has been under recent scrutiny, in particular due to their connection to fiber-base duality [102–107]. For type-II LSTs however, the flavor symmetries are severely constrained by both field- and string-theoretic arguments [108], and therefore so are their Higgs branch flows. Since some of the quantities relevant to the study of the duality are captured via anomalies [96], performing a similar analysis as in this work for LSTs could shed additional light on how gauge-invariant quantities are related under the duality from a bottom-up perspective.

ACKNOWLEDGMENTS

We thank Hamza Ahmed, António Antunes, Chris Couzens, Jacques Distler, Jonathan Heckman, Monica Jinwoo Kang, Lorenzo Mansi, Paul-Konstantin Oehlmann, Fabian Rühle, and Matteo Sacchi for discussions. This work was partially supported by the Deutsche Forschungsgemeinschaft under Germany’s Excellence

Strategy—EXC 2121 “Quantum Universe”—390833306, and the Collaborative Research Center—SFB 1624 “Higher Structures, Moduli Spaces, and Integrability”—506632645. The work of F. B. was partly supported by the Swiss National Science Foundation (SNSF), Grant No. P400P2_194341, the German Research Foundation through a German-Israeli Project Cooperation (DIP) grant “Holography and the Swampland.” The work of C. L. is supported by DESY (Hamburg, Germany), a member of the Helmholtz Association HGF.

APPENDIX A: CHARACTERISTIC CLASSES AND TRACE RELATIONS

In d dimensions, the contribution of a left-handed Weyl fermion transforming in a representation \mathbf{R} to the anomaly polynomial is given by the index of the Dirac operator [74], which can in turn be written in terms of characteristic classes of the curvatures via the Atiyah-Singer theorem

$$I_{d+2}^{\text{fermion}} = \frac{1}{2} \hat{A}(T) \text{ch}_{\mathbf{R}}(F) \Big|_{d+2}. \quad (\text{A1})$$

Note that we are using a convention giving only the contribution of the representation \mathbf{R} , justifying the presence of the one-half factor. Other conventions may not have this prefactor, as the counting includes the conjugate representation: $\mathbf{R} \oplus \bar{\mathbf{R}}$. The A-roof genus $\hat{A}(T)$ can be expanded in terms of Pontryagin classes $p_n(T)$ of the tangent bundle of spacetime. Up to eighth order, one finds

$$\hat{A}(T) = 1 - \frac{1}{24} p_1(T) + \frac{1}{5760} (7p_1(T)^2 - 4p_2(T)) + \dots, \quad (\text{A2})$$

$$L(T) = 1 + \frac{1}{3} p_1(T) - \frac{1}{45} (p_1(T)^2 - 7p_2(T)) + \dots, \quad (\text{A3})$$

where we also defined the Hirzebruch genus $L(T)$ appearing in the anomaly polynomials of anti-symmetric chiral two-forms. Similarly, the Chern character associated with the various gauge and flavor bundles can be expanded into traces of their field strength F . As in [37], we follow a convention where F is anti-Hermitian and rescaled to absorb the usual factors of (2π) , so that the Chern character of non-Abelian algebras is defined as

$$\text{ch}_{\mathbf{R}}(F) = \text{tr}_{\mathbf{R}} e^{iF} = \dim(\mathbf{R}) - \frac{1}{2} \text{tr}_{\mathbf{R}} F^2 + \frac{1}{24} \text{tr}_{\mathbf{R}} F^4 + \dots. \quad (\text{A4})$$

For the special case of the R-symmetry $\mathfrak{su}(2)_R$ bundle, we have for the d -dimensional representation

$$\begin{aligned} \text{ch}_d(\mathbf{R}) &= d - \frac{d(d^2 - 1)}{6} c_2(\mathbf{R}) + \frac{d(7 - 10d^2 + 3d^4)}{360} c_2(\mathbf{R})^2 \\ &+ \dots, \quad c_2(\mathbf{R}) = \frac{1}{4} \text{Tr}(R^2), \end{aligned} \quad (\text{A5})$$

where R is understood as the background field strength, and the traces are one-instanton normalized. The prefactors are explained by the trace-relation identities, see below. For instance, the anomaly polynomial of a free left-handed fermion in six dimensions transforming as a doublet of the $\mathfrak{su}(2)_R$ R-symmetry is given by

$$I_{\text{free}} = \frac{1}{2} \hat{A}(T) \text{ch}_2(R) \Big|_{8\text{-form}} = \frac{1}{24} c_2(R)^2 + \frac{1}{48} c_2(R) p_1(T) + \frac{1}{5760} (7p_1(T)^2 - 4p_2(T)). \quad (\text{A6})$$

One of the advantages of writing the one-loop part of the anomaly in terms of characteristic classes is that the Chern character satisfies a set of useful properties under the tensor product and direct sum of representations, which are utilized extensively in the main text

$$\begin{aligned} \text{ch}_{R \otimes R'}(F) &= \text{ch}_R(F) \text{ch}_{R'}(F), \\ \text{ch}_{R \oplus R'}(F) &= \text{ch}_R(F) + \text{ch}_{R'}(F). \end{aligned} \quad (\text{A7})$$

Indeed, using these relations we find that under a given branching rule

$$\begin{aligned} \mathfrak{g} &\longrightarrow \mathfrak{g}', \\ R &\longrightarrow \bigoplus_{\ell} m_{\ell} R_{\ell}, \end{aligned} \quad (\text{A8})$$

where the representation R_{ℓ} of \mathfrak{g}' appears with a possible nontrivial multiplicity, m_{ℓ} , the character simply decomposes as

$$\text{ch}_R(F_{\mathfrak{g}}) = \sum_{\ell} m_{\ell} \text{ch}_{R_{\ell}}(F_{\mathfrak{g}'}), \quad (\text{A9})$$

where $F_{\mathfrak{g}}, F_{\mathfrak{g}'}$ are the field strengths associated with \mathfrak{g} and \mathfrak{g}' , respectively.

1. Representation indices and trace relations

The various traces in the Chern character, as in Eq. (A4), must then be converted to one-instanton normalized traces, $\text{Tr} F^n$. We again follow the conventions of [37,60]. For the adjoint representation, we have

$$\text{tr}_{\text{adj}} F^2 = h^{\vee} \text{Tr} F^2, \quad \text{Tr} F^2 = \text{Tr}(T_a T_b) F^a \wedge F^b, \quad (\text{A10})$$

which fixes the overall normalization of the Killing form. For our purpose we will only be interested in quadratic and quartic traces, and the trace relations always take the generic form

$$\text{tr}_{\mathbf{R}} F^2 = A_{\mathbf{R}} \text{Tr} F^2, \quad \text{tr}_{\mathbf{R}} F^4 = B_{\mathbf{R}} \text{Tr} F^4 + C_{\mathbf{R}} (\text{Tr} F^2)^2. \quad (\text{A11})$$

The quadratic index, $A_{\mathbf{R}}$, was first introduced by Dynkin [109], and was generalized to higher order in [110].

For specific cases, the trace relations defined in Eq. (A11) are usually computed using algebra-specific relations or via so-called *Birdtrack* techniques [111], and the results having been tabulated for the most common representations, see, e.g., [112], as well as [17,113] for applications in six dimensions specifically. While the literature is often mostly concerned about the adjoint and fundamental representations, when discussing nilpotent orbits we are led to deal with more exotic representations. Furthermore as there are various normalizations for the trace-relation coefficients in the literature, we now review how to obtain them for arbitrary representations following the works pioneered by Okubo and Patera [114–116], enabling us to at the same time set the conventions used in this work.

Representation indices are closely related to Casimir invariants, defined as polynomial operators of a fixed degree commuting with all generators

$$C_p = g^{a_1 \dots a_p} T_{a_1} \dots T_{a_p}, \quad [C_p, T_a] = 0, \quad (\text{A12})$$

where $g_{a_1 \dots a_p}$ is an invariant symmetric tensor and indices are raised and lowered with the Killing metric, $g_{ab} = \text{Tr}(T_a T_b)$.

It is well-known that if the algebra \mathfrak{g} is simple there are exactly $r_{\mathfrak{g}}$ independent invariant tensors. It is then always possible to choose those invariants so that they satisfy orthogonality relations, e.g., $g^{ab} g^{cd} g_{abcd} = 0$. In that basis, the Casimir operators are unique up to a normalization constant, and $C_p = 0$ if there are no independent Casimir operator of order p . There is then at most one Casimir operator for a given p , except for $\mathfrak{g} = D_n$ which has two at order n . For $p = 2, 4$, the quartic and quadratic invariants form a basis of the symmetrized traces over the generator of any algebra $\mathfrak{g} \neq \mathfrak{so}(8)$ and we therefore have the decomposition

$$\text{tr}_{\mathbf{R}} F^2 = \tilde{\ell}_2(\mathbf{R}) g_{ab} F^a \wedge F^b, \quad (\text{A13})$$

$$\begin{aligned} \text{tr}_{\mathbf{R}} F^4 &= (\tilde{\ell}_4(\mathbf{R}) g_{abcd} + \tilde{\ell}_{2,2}(\mathbf{R}) g_{(ab} g_{cd)}) F^a \\ &\wedge F^b \wedge F^c \wedge F^d. \end{aligned} \quad (\text{A14})$$

The special case of $\mathfrak{g} = \mathfrak{so}(8)$ is treated below. The coefficients $\tilde{\ell}_n$ were first studied in [117] and are called the fundamental indices of \mathbf{R} . They were furthermore shown to be well behaved under branching rules and tensor products [114,115,117]. They moreover can be obtained directly from the weight system $W(\mathbf{R})$ of a representation. We first define the quantities

$$\ell_{2k}(\mathbf{R}) = \sum_{\mu \in W(\mathbf{R})} \langle \mu, \mu \rangle^k,$$

$$K(\mathbf{R}) = \frac{3}{2 + \dim(\mathfrak{g})} \left(\frac{\dim(\mathfrak{g})}{\dim(\mathbf{R})} - \frac{1}{6} \frac{\ell_2(\mathbf{adj})}{\ell_2(\mathbf{R})} \right), \quad (\text{A15})$$

with $\langle \cdot, \cdot \rangle$ the pairing on the root space—normalized such that the longest root has length two. We note that ℓ_{2n} also defines representation indices of order $2n$, but they are not fundamental in the sense that they are not independent. The fundamental indices are instead given by [114,115,117]

$$\begin{aligned} \tilde{\ell}_2(\mathbf{R}) &= \frac{\ell_2(\mathbf{R})}{2r_{\mathfrak{g}}}, \\ \tilde{\ell}_4(\mathbf{R}) &= \ell_4(\mathbf{R}) - \frac{2 + r_{\mathfrak{g}}}{3r_{\mathfrak{g}}} K(\mathbf{R}) (\ell_2(\mathbf{R}))^2, \\ \tilde{\ell}_{2,2}(\mathbf{R}) &= K(\mathbf{R}) (\tilde{\ell}_2(\mathbf{R}))^2. \end{aligned} \quad (\text{A16})$$

From there we can compute the trace relations for any representation. For quadratic traces, and using our normalization of the Killing form, one can straightforwardly show that $\tilde{\ell}_2(\mathbf{R})$ is equivalent to the usual definition of the Dynkin index

$$A_{\mathbf{R}} = \tilde{\ell}_2(\mathbf{R}) = \frac{\ell_2(\mathbf{R})}{2r_{\mathfrak{g}}} = \frac{\dim(\mathbf{R})}{2 \dim(\mathfrak{g})} \langle \Lambda, \Lambda + 2\rho \rangle, \quad (\text{A17})$$

where Λ is the highest weight of the representation, and satisfies $A_{\mathbf{R}} = h_{\mathfrak{g}}^{\vee}$, as expected. At quartic order, we need to set a reference representation, \mathcal{F} , such that $\text{tr}_{\mathcal{F}}(F^4) = \text{Tr}F^4$, i.e., $B_{\mathcal{F}} = 1$. The usual convention—which we adopt here—is to choose the reference representation to be the so-called defining representation for a classical algebra, namely the fundamental \mathbf{n} of $\mathfrak{su}(n)$, $2\mathbf{n}$ of $\mathfrak{sp}(n)$, and the vector \mathbf{n}_v of $\mathfrak{so}(n)$.²⁶ Comparing Eq. (A14) for both the desired and reference representations, we finally find that when $\mathfrak{g} \neq \mathfrak{so}_8$

$$B_{\mathbf{R}} = \frac{\tilde{\ell}_4(\mathbf{R})}{\tilde{\ell}_4(\mathcal{F})}, \quad C_{\mathbf{R}} = K(\mathbf{R}) (\tilde{\ell}_2(\mathbf{R}))^2 - B_{\mathbf{R}} K(\mathcal{F}) (\tilde{\ell}_2(\mathcal{F}))^2. \quad (\text{A18})$$

For exceptional algebras as well as $\mathfrak{su}(2)$ and $\mathfrak{su}(3)$, there is no independent quartic Casimir, and the reference representation is ill defined. However, in those cases $\tilde{\ell}_4(\mathbf{R}) = 0 = B_{\mathbf{R}}$ by construction and the formula given above for $C_{\mathbf{R}}$ also works for exceptional algebras.

Given the machinery reviewed in this appendix, it is then straightforward to compute the trace-relation indices for a given representation of any algebra, as everything can be

²⁶In our convention, $\mathfrak{sp}(k)$ has rank k , such that $\mathfrak{sp}(1) = \mathfrak{su}(2)$, and the fundamental representation has dimension $2k$.

TABLE VII. Trace-relation coefficients for representations of $\mathfrak{so}(8)$ relevant in this work.

\mathbf{R}	$\mathbf{1}$	$\mathbf{8}_v$	$\mathbf{8}_s$	$\mathbf{8}_c$	$\mathbf{28}$
$A_{\mathbf{R}}$	0	1	1	1	6
$B_{\mathbf{R}}$	0	1	$-\frac{1}{2}$	$-\frac{1}{2}$	0
$C_{\mathbf{R}}$	0	0	$\frac{3}{8}$	$\frac{3}{8}$	3

obtained from its weight lattice. It can then be achieved in a programmatic way using dedicated software such as LieART [118,119], or by finding them in tables [120]. We note that for the latter, only the values of $\ell_{2n}(\mathbf{R})$ defined in Eq. (A15) are given, not the fundamental indices.

The case of $\mathfrak{so}(8)$: due to the presence of an additional quartic Casimir, computing the fundamental indices is slightly more involved than in other cases. However, in this work we only have to deal with the adjoint, vector, and spinor representations of $\mathfrak{so}(8)$. For brevity, we have simply collated the trace relations for those cases in Table VII. Additional details on the fourth-order Casimir invariants and their trace relations can be found in, e.g., [114].

APPENDIX B: NILPOTENT ORBITS AND THEIR BRANCHING RULES

As we have used repeatedly throughout this paper, each nilpotent orbit, O , of a simple Lie algebra, \mathfrak{g} , is associated to a homomorphism $\rho_O: \mathfrak{su}(2)_X \rightarrow \mathfrak{g}$ via the Jacobson-Morozov theorem. Let \mathfrak{f} be the centralizer in \mathfrak{g} of the image of ρ_O . Then each nilpotent orbit has an associated decomposition

$$\mathfrak{g} \rightarrow \mathfrak{su}(2)_X \oplus \mathfrak{f}, \quad (\text{B1})$$

where we choose to ignore the nonsemisimple part of \mathfrak{f} . In the special case of the maximal nilpotent orbit, the homomorphism ρ_O embeds $\mathfrak{su}(2)_X$ trivially into \mathfrak{g} , and thus $\mathfrak{f} = \mathfrak{g}$; despite this subtlety in this case, we keep the notation as in Eq. (B1) for convenience. Under such a decomposition, we are interested in the branching rule of the adjoint representation

$$\mathbf{adj} \rightarrow \bigoplus_{\ell} (\mathbf{d}_{\ell}, \mathbf{R}_{\ell}), \quad (\text{B2})$$

where \mathbf{d}_{ℓ} are irreducible $\mathfrak{su}(2)_X$ representations, and \mathbf{R}_{ℓ} are (not-necessarily irreducible) representations of \mathfrak{f} .

First, we consider the case of $\mathfrak{g} = \mathfrak{su}(K)$.²⁷ Nilpotent orbits of $\mathfrak{su}(K)$ are in one-to-one correspondence with integer partitions of K . Given a nilpotent orbit O , we write the partition associated to O in the following way

²⁷When \mathfrak{g} is a classical Lie algebra, the adjoint branching rules induced by nilpotent orbits is reviewed in detail in [121].

$$[1^{m_1}, 2^{m_2}, \dots, K^{m_K}], \quad \text{where } \sum_{i=1}^K im_i = K. \quad (\text{B3})$$

The branching rule of the fundamental representation under the decomposition as in Eq. (B1) is given in terms of the partition as

$$K \rightarrow \bigoplus_{i=1}^K (i, m_i). \quad (\text{B4})$$

Here, we have used that the commutant of the image of $\mathfrak{su}(2)_X$ is

$$\mathfrak{f} = \bigoplus_{i=1}^K \mathfrak{su}(m_i), \quad (\text{B5})$$

and m_i is the representation of \mathfrak{f} obtained by taking the tensor product of the fundamental representation of $\mathfrak{su}(m_i)$ with the singlet representation of all other factors. Once the branching rule of the fundamental representation of $\mathfrak{su}(K)$ is known, the branching rules of all other irreducible representations can be determined. In particular, the branching rule of the adjoint representation can be straightforwardly derived from the tensor product

$$K \otimes \bar{K} = \mathbf{adj} \oplus \mathbf{1}. \quad (\text{B6})$$

Similarly, we can consider the case of $\mathfrak{g} = \mathfrak{usp}(K)$, for which nilpotent orbits are in one-to-one correspondence with C-partitions of K .²⁸ A C-partition of K can be written as

$$[1^{m_1}, 2^{m_2}, \dots, K^{m_K}] \quad \text{where } \sum_{i=1}^K im_i = K$$

such that $i \text{ odd} \Rightarrow m_i \text{ even}$. (B7)

The commutant of the image of $\mathfrak{su}(2)_X$ is

$$\mathfrak{f} = \bigoplus_{i=1}^K \mathfrak{j}(m_i) \quad \text{where } \mathfrak{j} = \begin{cases} \mathfrak{usp} & \text{if } i \text{ odd} \\ \mathfrak{so} & \text{if } i \text{ even,} \end{cases} \quad (\text{B8})$$

and the branching of the fundamental representation is

$$K \rightarrow \bigoplus_{i=1}^K (i, m_i). \quad (\text{B9})$$

Here, m_i is either the fundamental representation of $\mathfrak{usp}(m_i)$ (if i is odd) or the vector representation of

²⁸To avoid the proliferation of half-integer quantities, in this appendix we temporarily use the notation $\mathfrak{usp}(K)$ rather than $\mathfrak{sp}(\frac{K}{2})$, recalling that we follow the convention where $\mathfrak{usp}(2) = \mathfrak{sp}(1) = \mathfrak{su}(2)$. In the rest of the main text, the notation \mathfrak{sp} is used.

$\mathfrak{so}(m_i)$ (if i is even), tensored with the trivial representation of all other factors in \mathfrak{f} . The branching rule for the adjoint representation then follows from

$$\mathbf{adj} = \text{Sym}(K \otimes K). \quad (\text{B10})$$

Next, we can consider the case of $\mathfrak{g} = \mathfrak{so}(K)$. Each nilpotent orbit of $\mathfrak{so}(K)$ has an underlying BD-partition; a BD-partition of K can be written as

$$[1^{m_1}, 2^{m_2}, \dots, K^{m_K}] \quad \text{where } \sum_{i=1}^K im_i = K$$

such that $i \text{ even} \Rightarrow m_i \text{ even}$. (B11)

The commutant of the image of $\mathfrak{su}(2)_X$ is

$$\mathfrak{f} = \bigoplus_{i=1}^K \mathfrak{j}(m_i) \quad \text{where } \mathfrak{j} = \begin{cases} \mathfrak{so} & \text{if } i \text{ odd} \\ \mathfrak{usp} & \text{if } i \text{ even,} \end{cases} \quad (\text{B12})$$

and the branching of the vector representation is

TABLE VIII. Cartan matrices for the exceptional algebras, with our choice of ordering for the weighted Dynkin diagrams uniquely labeling every nilpotent orbit.

\mathfrak{g}	C	w
\mathfrak{g}_2	$\begin{pmatrix} 2 & -3 \\ -1 & 2 \end{pmatrix}$	$w_1 w_2$
\mathfrak{f}_4	$\begin{pmatrix} 2 & -1 & 0 & 0 \\ -1 & 2 & -2 & 0 \\ 0 & -1 & 2 & -1 \\ 0 & 0 & -1 & 2 \end{pmatrix}$	$w_1 w_2 w_3 w_4$
e_6	$\begin{pmatrix} 2 & -1 & 0 & 0 & 0 & 0 \\ -1 & 2 & -1 & 0 & 0 & 0 \\ 0 & -1 & 2 & -1 & 0 & -1 \\ 0 & 0 & -1 & 2 & -1 & 0 \\ 0 & 0 & 0 & -1 & 2 & 0 \\ 0 & 0 & -1 & 0 & 0 & 2 \end{pmatrix}$	$w_1 w_2 w_3 w_4 w_5 w_6$
e_7	$\begin{pmatrix} 2 & -1 & 0 & 0 & 0 & 0 & 0 \\ -1 & 2 & -1 & 0 & 0 & 0 & 0 \\ 0 & -1 & 2 & -1 & 0 & 0 & -1 \\ 0 & 0 & -1 & 2 & -1 & 0 & 0 \\ 0 & 0 & 0 & -1 & 2 & -1 & 0 \\ 0 & 0 & 0 & 0 & -1 & 2 & 0 \\ 0 & 0 & -1 & 0 & 0 & 0 & 2 \end{pmatrix}$	$w_1 w_2 w_3 w_4 w_5 w_6 w_7$
e_8	$\begin{pmatrix} 2 & -1 & 0 & 0 & 0 & 0 & 0 & 0 \\ -1 & 2 & -1 & 0 & 0 & 0 & 0 & 0 \\ 0 & -1 & 2 & -1 & 0 & 0 & 0 & -1 \\ 0 & 0 & -1 & 2 & -1 & 0 & 0 & 0 \\ 0 & 0 & 0 & -1 & 2 & -1 & 0 & 0 \\ 0 & 0 & 0 & 0 & -1 & 2 & -1 & 0 \\ 0 & 0 & 0 & 0 & 0 & -1 & 2 & 0 \\ 0 & 0 & -1 & 0 & 0 & 0 & 0 & 2 \end{pmatrix}$	$w_1 w_2 w_3 w_4 w_5 w_6 w_7 w_8$

TABLE IX. Nilpotent orbits of \mathfrak{g}_2 .

w	Bala-Carter	$\mathfrak{g}_2 \rightarrow \mathfrak{su}_2^{(I_{\mathcal{O}})} \oplus \mathfrak{f}^{(I)}$	$\dim \mathcal{O}$	$\mathbf{adj} \rightarrow \bigoplus_i (d_i, R_i)$
[0, 0]	0	$\mathfrak{su}_2^{(0)} \oplus \mathfrak{g}_2^{(1)}$	0	(1, 14)
[1, 0]	A_1	$\mathfrak{su}_2^{(1)} \oplus \mathfrak{su}_2^{(3)}$	6	(3, 1) \oplus (2, 4) \oplus (1, 3)
[0, 1]	\tilde{A}_1	$\mathfrak{su}_2^{(3)} \oplus \mathfrak{su}_2^{(1)}$	8	(3, 1) \oplus (4, 2) \oplus (1, 3)
[2, 0]	$G_2(a_1)$	$\mathfrak{su}_2^{(4)} \oplus \emptyset$	10	5 \oplus 3 \cdot 3
[2, 2]	G_2	$\mathfrak{su}_2^{(28)} \oplus \emptyset$	12	11 \oplus 3

$$K \rightarrow \bigoplus_{i=1}^K (i, m_i). \tag{B13}$$

Again, m_i is either the fundamental representation of $\mathfrak{u}\mathfrak{sp}(m_i)$ (if i is even) or the vector representation of $\mathfrak{so}(m_i)$ (if i is odd), tensored with the trivial representation of all other factors in \mathfrak{f} . The branching rule for the adjoint representation then follows directly from

$$\mathbf{adj} = \text{ASym}(K \otimes K). \tag{B14}$$

Finally, we turn to the cases where \mathfrak{g} is an exceptional Lie algebra, where we use both the Bala-Carter notation [70,71] and the weighted Dynkin diagrams to label the nilpotent orbits. Recall that a corollary of the Jacobson-Morozov theorem is that for each nilpotent orbit, it is always possible to uniquely define an $\mathfrak{su}(2)$ triplet (X, Y, H) of

generators such that H is in the Cartan subalgebra, and for which each of the simple roots E_i has eigenvalue $w_i = 0, 1, 2$, see Eq. (3.30). Of course, this labeling then depends on the ordering of the simple roots of the simple algebra \mathfrak{g} . We choose a basis where they correspond to the rows of the Cartan matrix, C , and the weights defining the nilpotent orbits are arranged as in Table VIII. Note that for a classical algebra, one can obtain the weighted Dynkin diagram of a nilpotent orbit given directly from its partition [67].

For exceptional algebras, the Jacobson-Morozov decomposition involves representations that go beyond the usual adjoint, and defining representations. The associated branching rules can be found in, e.g., [122–126], and have been reproduced in Tables IX–XIII. For convenience, we also included the weighted Dynkin diagram of the nilpotent orbits following the above ordering, as well as the Dynkin embedding index for each flavor factor.

TABLE X. Nilpotent orbits of \mathfrak{f}_4 .

w	Bala-Carter	$\mathfrak{f}_4 \rightarrow \mathfrak{su}_2^{(I_{\mathcal{O}})} \oplus \mathfrak{f}^{(I)}$	$\dim \mathcal{O}$	$\mathbf{adj} \rightarrow \bigoplus_i (d_i, R_i)$
[0, 0, 0, 0]	0	$\mathfrak{su}_2^{(0)} \oplus \mathfrak{f}_4^{(1)}$	0	(1, 52)
[1, 0, 0, 0]	A_1	$\mathfrak{su}_2^{(1)} \oplus \mathfrak{sp}_3^{(1)}$	16	(3, 1) \oplus (2, 14') \oplus (1, 21)
[0, 0, 0, 1]	\tilde{A}_1	$\mathfrak{su}_2^{(2)} \oplus \mathfrak{su}_4^{(1)}$	22	(3, 1) \oplus (3, 6) \oplus (2, 4) \oplus (2, $\bar{4}$) \oplus (1, 15)
[0, 1, 0, 0]	$A_1 + \tilde{A}_1$	$\mathfrak{su}_2^{(3)} \oplus (\mathfrak{su}_2^{(1)} \oplus \mathfrak{su}_4^{(2)})$	28	(1, 3, 1) \oplus (1, 1, 3) \oplus (2, 5, 2) \oplus (3, 1, 1) \oplus (3, 5, 1) \oplus (4, 1, 2)
[2, 0, 0, 0]	A_2	$\mathfrak{su}_2^{(4)} \oplus \mathfrak{su}_3^{(2)}$	30	(3, 1) \oplus (3, 6) \oplus (3, $\bar{6}$) \oplus (5, 1) \oplus (1, 8)
[0, 0, 0, 2]	\tilde{A}_2	$\mathfrak{su}_2^{(8)} \oplus \mathfrak{g}_2^{(1)}$	30	(3, 1) \oplus (5, 7) \oplus (1, 14)
[0, 0, 1, 0]	$A_2 + \tilde{A}_1$	$\mathfrak{su}_2^{(6)} \oplus \mathfrak{su}_2^{(6)}$	34	(3, 1) \oplus (3, 5) \oplus (5, 3) \oplus (4, 2) \oplus (2, 4) \oplus (1, 3)
[2, 0, 0, 1]	B_2	$\mathfrak{su}_2^{(10)} \oplus (\mathfrak{su}_2^{(1)} \oplus \mathfrak{su}_2^{(1)})$	36	(7, 1, 1) \oplus (5, 2, 2) \oplus (4, 2, 1) \oplus (4, 1, 2) \oplus (3, 1, 1) \oplus (1, 3, 1) \oplus (1, 1, 3)
[0, 1, 0, 1]	$\tilde{A}_2 + A_1$	$\mathfrak{su}_2^{(9)} \oplus \mathfrak{su}_2^{(3)}$	36	2 \cdot (3, 1) \oplus (6, 2) \oplus (5, 3) \oplus (4, 2) \oplus (2, 4) \oplus (1, 3)
[1, 0, 1, 0]	$C_3(a_1)$	$\mathfrak{su}_2^{(11)} \oplus \mathfrak{su}_2^{(1)}$	38	3 \cdot (3, 1) \oplus (7, 1) \oplus (6, 2) \oplus (5, 1) \oplus 2 \cdot (4, 2) \oplus (1, 3)
[0, 2, 0, 0]	$F_4(a_3)$	$\mathfrak{su}_2^{(12)} \oplus \emptyset$	40	2 \cdot 7 \oplus 4 \cdot 5 \oplus 6 \cdot 3
[2, 2, 0, 0]	B_3	$\mathfrak{su}_2^{(28)} \oplus \mathfrak{su}_2^{(8)}$	42	(3, 1) \oplus (11, 1) \oplus (7, 5) \oplus (1, 3)
[1, 0, 1, 2]	C_3	$\mathfrak{su}_2^{(35)} \oplus \mathfrak{su}_2^{(1)}$	42	(11, 1) \oplus (10, 2) \oplus (7, 1) \oplus (4, 2) \oplus (3, 1) \oplus (1, 3)
[0, 2, 0, 2]	$F_4(a_2)$	$\mathfrak{su}_2^{(36)} \oplus \emptyset$	44	2 \cdot 11 \oplus 9 \oplus 7 \oplus 5 \oplus 3 \cdot 3
[2, 2, 0, 2]	$F_4(a_1)$	$\mathfrak{su}_2^{(60)} \oplus \emptyset$	46	15 \oplus 2 \cdot 11 \oplus 7 \oplus 5 \oplus 3
[2, 2, 2, 2]	F_4	$\mathfrak{su}_2^{(156)} \oplus \emptyset$	48	23 \oplus 15 \oplus 11 \oplus 3

TABLE XI. Nilpotent orbits of e_6 .

w	Bala-Carter	$e_6 \rightarrow \mathfrak{su}_2^{(l_o)} \oplus \mathfrak{f}^{(l)}$	$\dim \mathcal{O}$	$\text{adj} \rightarrow \bigoplus_i (d_i, R_i)$
[0, 0, 0, 0, 0, 0]	0	$\mathfrak{su}_2^{(0)} \oplus e_6^{(1)}$	0	(1, 78)
[0, 0, 0, 0, 0, 1]	A_1	$\mathfrak{su}_2^{(1)} \oplus \mathfrak{su}_6^{(1)}$	22	(1, 35) \oplus (2, 20) \oplus (3, 1)
[1, 0, 0, 0, 1, 0]	$2A_1$	$\mathfrak{su}_2^{(2)} \oplus \mathfrak{so}_7^{(1)}$	32	(1, 21) \oplus (1, 1) \oplus 2 \cdot (2, 8) \oplus (3, 7) \oplus (3, 1)
[0, 0, 1, 0, 0, 0]	$3A_1$	$\mathfrak{su}_2^{(3)} \oplus (\mathfrak{su}_2^{(1)} \oplus \mathfrak{su}_3^{(2)})$	40	(1, 1, 8) \oplus (1, 3, 1) \oplus (2, 2, 8) \oplus (3, 1, 1) \oplus (3, 1, 8) \oplus (4, 2, 1)
[0, 0, 0, 0, 0, 2]	A_2	$\mathfrak{su}_2^{(4)} \oplus (\mathfrak{su}_3^{(1)} \oplus \mathfrak{su}_3^{(1)})$	42	(1, 8, 1) \oplus (1, 1, 8) \oplus (3, 1, 1) \oplus (3, 3, 3) \oplus (3, $\bar{3}$, $\bar{3}$) \oplus (5, 1, 1)
[1, 0, 0, 0, 1, 1]	$A_2 + A_1$	$\mathfrak{su}_2^{(5)} \oplus \mathfrak{su}_3^{(1)}$	46	(1, 1) \oplus (1, 8) \oplus (2, 3) \oplus (2, $\bar{3}$) \oplus 2 \cdot (2, 1) \oplus (3, 3) \oplus (3, $\bar{3}$) \oplus 2 \cdot (3, 1) \oplus (4, 3) \oplus (4, $\bar{3}$) \oplus (5, 1)
[2, 0, 0, 0, 2, 0]	$2A_2$	$\mathfrak{su}_2^{(8)} \oplus \mathfrak{g}_2^{(1)}$	48	(1, 14) \oplus (3, 7) \oplus (3, 1) \oplus (5, 7) \oplus (5, 1)
[0, 1, 0, 1, 0, 0]	$A_2 + 2A_1$	$\mathfrak{su}_2^{(6)} \oplus \mathfrak{su}_2^{(6)}$	50	(1, 1) \oplus (1, 3) \oplus 2 \cdot (2, 4) \oplus (3, 1) \oplus (3, 3) \oplus (3, 5) \oplus 2 \cdot (4, 2) \oplus (5, 3)
[1, 0, 1, 0, 1, 0]	$2A_2 + A_1$	$\mathfrak{su}_2^{(9)} \oplus \mathfrak{su}_2^{(3)}$	54	(1, 3) \oplus (2, 4) \oplus (2, 2) \oplus (3, 3) \oplus 2 \cdot (3, 1) \oplus 2 \cdot (4, 2) \oplus (5, 3) \oplus (5, 1) \oplus (6, 2)
[1, 0, 0, 0, 1, 2]	A_3	$\mathfrak{su}_2^{(10)} \oplus \mathfrak{sp}_2^{(1)}$	52	(1, 10) \oplus (1, 1) \oplus (3, 1) \oplus 2 \cdot (4, 4) \oplus (5, 5) \oplus (7, 1)
[0, 1, 0, 1, 0, 1]	$A_3 + A_1$	$\mathfrak{su}_2^{(11)} \oplus \mathfrak{su}_2^{(1)}$	56	(1, 1) \oplus (1, 3) \oplus (2, 2) \oplus 4 \cdot (3, 1) \oplus 3 \cdot (4, 2) \oplus 3 \cdot (5, 1) \oplus (6, 2) \oplus (7, 1)
[0, 0, 2, 0, 0, 0]	$D_4(a_1)$	$\mathfrak{su}_2^{(12)} \oplus \emptyset$	58	2 \cdot 1 \oplus 9 \cdot 3 \oplus 7 \cdot 5 \oplus 2 \cdot 7
[2, 0, 0, 0, 2, 2]	A_4	$\mathfrak{su}_2^{(20)} \oplus \mathfrak{su}_2^{(1)}$	60	(1, 3) \oplus (1, 1) \oplus 2 \cdot (3, 2) \oplus (3, 1) \oplus 3 \cdot (5, 1) \oplus 2 \cdot (7, 2) \oplus (7, 1) \oplus (9, 1)
[1, 1, 0, 1, 1, 1]	$A_4 + A_1$	$\mathfrak{su}_2^{(21)} \oplus \emptyset$	62	1 \oplus 2 \cdot 2 \oplus 2 \cdot 3 \oplus 2 \cdot 4 \oplus 3 \cdot 5 \oplus 2 \cdot 6 \oplus 7 \oplus 2 \cdot 8 \oplus 9
[0, 0, 2, 0, 0, 2]	D_4	$\mathfrak{su}_2^{(28)} \oplus \mathfrak{su}_3^{(2)}$	60	(1, 8) \oplus (3, 1) \oplus (7, 8) \oplus (11, 1)
[2, 1, 0, 1, 2, 1]	A_5	$\mathfrak{su}_2^{(35)} \oplus \mathfrak{su}_2^{(1)}$	64	(1, 3) \oplus (3, 1) \oplus (4, 2) \oplus (5, 1) \oplus (6, 2) \oplus (7, 1) \oplus (9, 1) \oplus (10, 2) \oplus (11, 1)
[1, 1, 0, 1, 1, 2]	$D_5(a_1)$	$\mathfrak{su}_2^{(30)} \oplus \emptyset$	64	1 \oplus 2 \cdot 2 \oplus 2 \cdot 3 \oplus 5 \oplus 2 \cdot 6 \oplus 2 \cdot 7 \oplus 2 \cdot 8 \oplus 9 \oplus 11
[2, 0, 2, 0, 2, 0]	$E_6(a_3)$	$\mathfrak{su}_2^{(36)} \oplus \emptyset$	66	3 \cdot 3 \oplus 3 \cdot 5 \oplus 2 \cdot 7 \oplus 2 \cdot 9 \oplus 2 \cdot 11
[2, 0, 2, 0, 2, 2]	D_5	$\mathfrak{su}_2^{(60)} \oplus \emptyset$	68	1 \oplus 3 \oplus 2 \cdot 5 \oplus 7 \oplus 9 \oplus 3 \cdot 11 \oplus 15
[2, 2, 0, 2, 2, 2]	$E_6(a_1)$	$\mathfrak{su}_2^{(84)} \oplus \emptyset$	70	3 \oplus 5 \oplus 7 \oplus 9 \oplus 2 \cdot 11 \oplus 15 \oplus 17
[2, 2, 2, 2, 2, 2]	E_6	$\mathfrak{su}_2^{(156)} \oplus \emptyset$	72	3 \oplus 9 \oplus 11 \oplus 15 \oplus 17 \oplus 23

TABLE XII. Nilpotent orbits of e_7 .

w	Bala-Carter	$e_7 \rightarrow \mathfrak{su}_2^{(l_o)} \oplus \mathfrak{f}^{(l)}$	$\dim \mathcal{O}$	$\text{adj} \rightarrow \bigoplus_i (d_i, R_i)$
[0, 0, 0, 0, 0, 0, 0]	0	$\mathfrak{su}_2^{(0)} \oplus e_7^{(1)}$	0	(1, 133)
[1, 0, 0, 0, 0, 0, 0]	A_1	$\mathfrak{su}_2^{(1)} \oplus \mathfrak{so}_{12}^{(1)}$	34	(1, 66) \oplus (2, $\bar{32}$) \oplus (3, 1)
[0, 0, 0, 0, 1, 0, 0]	$2A_1$	$\mathfrak{su}_2^{(2)} \oplus (\mathfrak{so}_9^{(1)} \oplus \mathfrak{su}_2^{(1)})$	52	(1, 1, 3) \oplus (1, 36, 1) \oplus (2, 16, 2) \oplus (3, 1, 1) \oplus (3, 9, 1)
[0, 1, 0, 0, 0, 0, 0]	$(3A_1)'$	$\mathfrak{su}_2^{(3)} \oplus (\mathfrak{sp}_3^{(1)} \oplus \mathfrak{su}_2^{(1)})$	64	(1, 1, 3) \oplus (1, 21, 1) \oplus (2, 14, 2) \oplus (3, 1, 1) \oplus (3, 14, 1) \oplus (4, 1, 2)
[0, 0, 0, 0, 0, 2, 0]	$(3A_1)''$	$\mathfrak{su}_2^{(3)} \oplus \mathfrak{f}_4^{(1)}$	54	(1, 52) \oplus (3, 1) \oplus (3, 26)
[0, 0, 0, 0, 0, 1, 1]	$4A_1$	$\mathfrak{su}_2^{(4)} \oplus \mathfrak{sp}_3^{(1)}$	70	(1, 21) \oplus (2, 6) \oplus (2, 14') \oplus 2 \cdot (3, 1) \oplus (3, 14) \oplus (4, 6)
[2, 0, 0, 0, 0, 0, 0]	A_2	$\mathfrak{su}_2^{(4)} \oplus \mathfrak{su}_6^{(1)}$	66	(1, 35) \oplus (3, 1) \oplus (3, 15) \oplus (3, $\bar{15}$) \oplus (5, 1)

(Table continued)

TABLE XII. (Continued)

w	Bala-Carter	$e_7 \rightarrow \mathfrak{su}_2^{(l_o)} \oplus \mathfrak{f}^{(l)}$	$\dim \mathcal{O}$	$\text{adj} \rightarrow \bigoplus_i (d_i, R_i)$
[1, 0, 0, 0, 1, 0, 0]	$A_2 + A_1$	$\mathfrak{su}_2^{(5)} \oplus \mathfrak{su}_4^{(1)}$	76	$(1, 1) \oplus (1, 15) \oplus 2 \cdot (2, 4) \oplus 2 \cdot (2, \bar{4}) \oplus 4 \cdot (3, 1) \oplus 2 \cdot (3, 6) \oplus (4, 4) \oplus (4, \bar{4}) \oplus (5, 1)$
[0, 0, 1, 0, 0, 0, 0]	$A_2 + 2A_1$	$\mathfrak{su}_2^{(6)} \oplus (\mathfrak{su}_2^{(1)} \oplus \mathfrak{su}_2^{(2)} \oplus \mathfrak{su}_2^{(6)})$	82	$(1, 3, 1, 1) \oplus (1, 1, 3, 1) \oplus (1, 1, 1, 3) \oplus (2, 2, 2, 4) \oplus (3, 1, 1, 1)$
[0, 0, 0, 0, 2, 0, 0]	$2A_2$	$\mathfrak{su}_2^{(8)} \oplus (\mathfrak{g}_2^{(1)} \oplus \mathfrak{su}_2^{(3)})$	84	$\oplus (3, 1, 3, 3) \oplus (3, 1, 1, 5) \oplus (4, 2, 2, 2) \oplus (5, 1, 1, 3) \oplus (1, 1, 3) \oplus (1, 14, 1) \oplus (3, 1, 1) \oplus (3, 7, 3) \oplus (5, 1, 3) \oplus (5, 7, 1)$
[0, 0, 0, 0, 0, 0, 2]	$A_2 + 3A_1$	$\mathfrak{su}_2^{(7)} \oplus \mathfrak{g}_2^{(2)}$	84	$(1, 14) \oplus (3, 1) \oplus (3, 27) \oplus (5, 7)$
[0, 1, 0, 0, 1, 0, 0]	$2A_2 + A_1$	$\mathfrak{su}_2^{(9)} \oplus (\mathfrak{su}_2^{(3)} \oplus \mathfrak{su}_2^{(3)})$	90	$(1, 3, 1) \oplus (1, 1, 3) \oplus (2, 3, 2) \oplus (2, 1, 4) \oplus 2 \cdot (3, 1, 1) \oplus (3, 3, 3) \oplus (4, 1, 2) \oplus (4, 3, 2) \oplus (5, 3, 1) \oplus (5, 1, 3) \oplus (6, 1, 2)$
[2, 0, 0, 0, 1, 0, 0]	A_3	$\mathfrak{su}_2^{(10)} \oplus (\mathfrak{so}_7^{(1)} \oplus \mathfrak{su}_2^{(1)})$	84	$(1, 1, 3) \oplus (1, 21, 1) \oplus (3, 1, 1) \oplus (4, 8, 2) \oplus (5, 7, 1) \oplus (7, 1, 1)$
[1, 0, 1, 0, 0, 0, 0]	$(A_3 + A_1)'$	$\mathfrak{su}_2^{(11)} \oplus (\mathfrak{su}_2^{(1)} \oplus \mathfrak{su}_2^{(2)} \oplus \mathfrak{su}_2^{(1)})$	92	$(1, 3, 1, 1) \oplus (1, 1, 3, 1) \oplus (1, 1, 1, 3) \oplus (2, 2, 3, 1) \oplus 2 \cdot (3, 1, 1, 1) \oplus (3, 1, 2, 2) \oplus (4, 2, 1, 1) \oplus (4, 2, 2, 2) \oplus (5, 1, 2, 2) \oplus (5, 1, 3, 1) \oplus (6, 2, 1, 1) \oplus (7, 1, 1, 1)$
[2, 0, 0, 0, 0, 2, 0]	$(A_3 + A_1)''$	$\mathfrak{su}_2^{(11)} \oplus \mathfrak{so}_7^{(1)}$	86	$(1, 21) \oplus 2 \cdot (3, 1) \oplus (3, 8) \oplus (5, 7) \oplus (5, 8) \oplus (7, 1)$
[1, 0, 0, 1, 0, 1, 0]	$A_3 + 2A_1$	$\mathfrak{su}_2^{(12)} \oplus (\mathfrak{su}_2^{(1)} \oplus \mathfrak{su}_2^{(2)})$	94	$(1, 3, 1) \oplus (1, 1, 3) \oplus (2, 1, 2) \oplus (2, 2, 3) \oplus 3 \cdot (3, 1, 1) \oplus (3, 2, 2) \oplus (4, 2, 1) \oplus 2 \cdot (4, 1, 2) \oplus (5, 2, 2) \oplus (5, 1, 3) \oplus (6, 2, 1) \oplus (6, 1, 2) \oplus (7, 1, 1)$
[0, 2, 0, 0, 0, 0, 0]	$D_4(a_1)$	$\mathfrak{su}_2^{(12)} \oplus (\mathfrak{su}_2^{(1)} \oplus \mathfrak{su}_2^{(1)} \oplus \mathfrak{su}_2^{(1)})$	94	$(1, 3, 1, 1) \oplus (1, 1, 3, 1) \oplus (1, 1, 1, 3) \oplus 3 \cdot (3, 1, 1, 1) \oplus (3, 2, 2, 1) \oplus (3, 2, 1, 2) \oplus (3, 1, 2, 2) \oplus (5, 1, 1, 1) \oplus (5, 2, 2, 1) \oplus (5, 2, 1, 2) \oplus (5, 1, 2, 2) \oplus 2 \cdot (7, 1, 1, 1)$
[0, 1, 0, 0, 0, 1, 1]	$D_4(a_1) + A_1$	$\mathfrak{su}_2^{(13)} \oplus (\mathfrak{su}_2^{(1)} \oplus \mathfrak{su}_2^{(1)})$	96	$(1, 3, 1) \oplus (1, 1, 3) \oplus (2, 2, 1) \oplus (2, 1, 2) \oplus 4 \cdot (3, 1, 1) \oplus (3, 2, 2) \oplus 2 \cdot (4, 2, 1) \oplus 2 \cdot (4, 1, 2) \oplus (5, 1, 1) \oplus (5, 2, 2) \oplus (6, 2, 1) \oplus (6, 1, 2) \oplus 2 \cdot (7, 1, 1)$
[0, 0, 1, 0, 1, 0, 0]	$A_3 + A_2$	$\mathfrak{su}_2^{(14)} \oplus \mathfrak{su}_2^{(1)}$	98	$(1, 1) \oplus (1, 3) \oplus 2 \cdot (2, 2) \oplus 8 \cdot (3, 1) \oplus 4 \cdot (4, 2) \oplus 4 \cdot (5, 1) \oplus 2 \cdot (6, 2) \oplus 3 \cdot (7, 1)$
[2, 2, 0, 0, 0, 0, 0]	D_4	$\mathfrak{su}_2^{(28)} \oplus \mathfrak{sp}_3^{(1)}$	96	$(1, 21) \oplus (3, 1) \oplus (7, 14) \oplus (11, 1)$
[0, 0, 0, 2, 0, 0, 0]	$A_3 + A_2 + A_1$	$\mathfrak{su}_2^{(15)} \oplus \mathfrak{su}_2^{(24)}$	100	$(1, 3) \oplus (3, 1) \oplus (3, 5) \oplus (3, 9) \oplus (5, 3) \oplus (5, 7) \oplus (7, 5)$
[2, 0, 0, 0, 2, 0, 0]	A_4	$\mathfrak{su}_2^{(20)} \oplus \mathfrak{su}_3^{(1)}$	100	$(1, 1) \oplus (1, 8) \oplus (3, 1) \oplus (3, 3) \oplus (3, \bar{3}) \oplus 3 \cdot (5, 1) \oplus (5, 3) \oplus (5, \bar{3}) \oplus (7, 1) \oplus (7, 3) \oplus (7, \bar{3}) \oplus (9, 1)$
[1, 0, 1, 0, 1, 0, 0]	$A_4 + A_1$	$\mathfrak{su}_2^{(21)} \oplus \emptyset$	104	$2 \cdot 1 \oplus 4 \cdot 2 \oplus 4 \cdot 3 \oplus 4 \cdot 4 \oplus 5 \cdot 5 \oplus 4 \cdot 6 \oplus 3 \cdot 7 \oplus 2 \cdot 8 \oplus 9$
[2, 1, 0, 0, 0, 1, 1]	$D_4 + A_1$	$\mathfrak{su}_2^{(29)} \oplus \mathfrak{sp}_2^{(1)}$	102	$(1, 10) \oplus (2, 4) \oplus 2 \cdot (3, 1) \oplus (6, 4) \oplus (7, 1) \oplus (7, 5) \oplus (8, 4) \oplus (11, 1)$
[2, 0, 1, 0, 1, 0, 0]	$D_5(a_1)$	$\mathfrak{su}_2^{(30)} \oplus \mathfrak{su}_2^{(1)}$	106	$(1, 1) \oplus (1, 3) \oplus 2 \cdot (2, 2) \oplus 4 \cdot (3, 1) \oplus (5, 1) \oplus 2 \cdot (6, 2) \oplus 4 \cdot (7, 1) \oplus 2 \cdot (8, 2) \oplus (9, 1) \oplus (11, 1)$
[0, 0, 2, 0, 0, 0, 0]	$A_4 + A_2$	$\mathfrak{su}_2^{(24)} \oplus \mathfrak{su}_2^{(15)}$	106	$(1, 3) \oplus (3, 1) \oplus (3, 5) \oplus (5, 3) \oplus (5, 7) \oplus (7, 5) \oplus (9, 3)$
[2, 0, 0, 0, 2, 2, 0]	A_5'	$\mathfrak{su}_2^{(35)} \oplus \mathfrak{g}_2^{(1)}$	102	$(1, 14) \oplus (3, 1) \oplus (5, 7) \oplus (7, 1) \oplus (9, 7) \oplus (11, 1)$
[1, 0, 1, 0, 1, 2, 0]	$A_5 + A_1$	$\mathfrak{su}_2^{(36)} \oplus \mathfrak{su}_2^{(3)}$	108	$(1, 3) \oplus (2, 4) \oplus 2 \cdot (3, 1) \oplus (4, 2) \oplus (5, 3) \oplus (6, 2) \oplus (7, 1) \oplus (8, 2)$

(Table continued)

TABLE XII. (Continued)

w	Bala-Carter	$e_7 \rightarrow \mathfrak{su}_2^{(I_O)} \oplus \mathfrak{f}^{(I)}$	$\dim \mathcal{O}$	$\text{adj} \rightarrow \bigoplus_i (d_i, R_i)$
[2, 0, 0, 2, 0, 0, 0]	$D_5(a_1) + A_1$	$\mathfrak{su}_2^{(31)} \oplus \mathfrak{su}_2^{(8)}$	108	$\oplus(9, 3) \oplus (10, 2) \oplus (11, 1)$ $(11, 1) \oplus (9, 3) \oplus (7, 5) \oplus (7, 3) \oplus (5, 3) \oplus (3, 5) \oplus$ $2 \cdot (3, 1) \oplus (1, 3)$
[1, 0, 1, 0, 2, 0, 0]	A'_5	$\mathfrak{su}_2^{(35)} \oplus (\mathfrak{su}_2^{(1)} \oplus \mathfrak{su}_2^{(3)})$	108	$(1, 3, 1) \oplus (1, 1, 3) \oplus (3, 1, 1) \oplus (4, 2, 1) \oplus$ $(5, 1, 3) \oplus (6, 2, 3)$ $\oplus(7, 1, 1) \oplus (9, 1, 3) \oplus (10, 2, 1) \oplus (11, 1, 1)$
[0, 1, 0, 1, 0, 2, 1]	$D_6(a_2)$	$\mathfrak{su}_2^{(38)} \oplus \mathfrak{su}_2^{(1)}$	110	$(1, 3) \oplus 3 \cdot (3, 1) \oplus 2 \cdot (4, 2) \oplus (5, 1) \oplus (6, 2) \oplus 3 \cdot$ $(7, 1) \oplus (8, 2)$ $\oplus(9, 1) \oplus (10, 2) \oplus 2 \cdot (11, 1)$
[0, 2, 0, 0, 2, 0, 0]	$E_6(a_3)$	$\mathfrak{su}_2^{(36)} \oplus \mathfrak{su}_2^{(3)}$	110	$(1, 3) \oplus 3 \cdot (3, 1) \oplus 2 \cdot (5, 3) \oplus (5, 1) \oplus (7, 3) \oplus$ $(7, 1) \oplus (9, 1)$ $\oplus(9, 3) \oplus 2 \cdot (11, 1)$
[0, 0, 2, 0, 0, 2, 0]	$E_7(a_5)$	$\mathfrak{su}_2^{(39)} \oplus \emptyset$	112	$6 \cdot 3 \oplus 4 \cdot 5 \oplus 5 \cdot 7 \oplus 3 \cdot 9 \oplus 3 \cdot 11$
[2, 2, 0, 0, 2, 0, 0]	D_5	$\mathfrak{su}_2^{(60)} \oplus (\mathfrak{su}_2^{(1)} \oplus \mathfrak{su}_2^{(2)})$	112	$(1, 3, 1) \oplus (1, 1, 3) \oplus (3, 1, 1) \oplus (5, 2, 2) \oplus$ $(7, 1, 1) \oplus (9, 1, 3)$ $\oplus(11, 1, 1) \oplus (11, 2, 2) \oplus (15, 1, 1)$
[0, 0, 2, 0, 2, 0, 0]	A_6	$\mathfrak{su}_2^{(56)} \oplus \mathfrak{su}_2^{(7)}$	114	$(1, 3) \oplus (3, 1) \oplus (5, 3) \oplus (7, 5) \oplus (9, 3) \oplus (11, 1) \oplus$ $(13, 3)$
[2, 1, 0, 1, 0, 2, 1]	$D_6(a_1)$	$\mathfrak{su}_2^{(62)} \oplus \mathfrak{su}_2^{(1)}$	114	$(1, 3) \oplus 2 \cdot (3, 1) \oplus (4, 2) \oplus (6, 2) \oplus 2 \cdot (7, 1) \oplus$ $(9, 1) \oplus (10, 2)$ $\oplus 2 \cdot (11, 1) \oplus (12, 2) \oplus (15, 1)$
[2, 1, 0, 1, 1, 0, 1]	$D_5 + A_1$	$\mathfrak{su}_2^{(61)} \oplus \mathfrak{su}_2^{(2)}$	114	$(1, 3) \oplus 2 \cdot (3, 1) \oplus (4, 2) \oplus (6, 2) \oplus (7, 1) \oplus$ $(9, 3) \oplus (10, 2)$ $\oplus(11, 1) \oplus (12, 2) \oplus (15, 1)$
[2, 0, 2, 0, 0, 2, 0]	$E_7(a_4)$	$\mathfrak{su}_2^{(63)} \oplus \emptyset$	116	$4 \cdot 3 \oplus 2 \cdot 5 \oplus 3 \cdot 7 \oplus 2 \cdot 9 \oplus 4 \cdot 11 \oplus 13 \oplus 15$
[2, 1, 0, 1, 2, 2, 1]	D_6	$\mathfrak{su}_2^{(110)} \oplus \mathfrak{su}_2^{(1)}$	118	$(1, 3) \oplus (3, 1) \oplus (6, 2) \oplus (7, 1) \oplus (10, 2) \oplus 2 \cdot$ $(11, 1) \oplus (15, 1)$ $\oplus(16, 2) \oplus (19, 1)$
[2, 0, 2, 0, 2, 0, 0]	$E_6(a_1)$	$\mathfrak{su}_2^{(84)} \oplus \emptyset$	118	$1 \oplus 3 \oplus 3 \cdot 5 \oplus 7 \oplus 3 \cdot 9 \oplus 2 \cdot 11 \oplus 2 \cdot 13 \oplus$ $15 \oplus 17$
[2, 0, 2, 0, 2, 2, 0]	$E_7(a_3)$	$\mathfrak{su}_2^{(111)} \oplus \emptyset$	120	$2 \cdot 3 \oplus 5 \oplus 2 \cdot 7 \oplus 9 \oplus 3 \cdot 11 \oplus 2 \cdot 15 \oplus 17 \oplus 19$
[2, 2, 2, 0, 2, 0, 0]	E_6	$\mathfrak{su}_2^{(156)} \oplus \mathfrak{su}_2^{(3)}$	120	$(1, 3) \oplus (3, 1) \oplus (9, 3) \oplus (11, 1) \oplus (15, 1) \oplus$ $(17, 3) \oplus (23, 1)$
[2, 2, 0, 2, 0, 2, 2]	$E_7(a_2)$	$\mathfrak{su}_2^{(159)} \oplus \emptyset$	122	$2 \cdot 3 \oplus 7 \oplus 9 \oplus 2 \cdot 11 \oplus 2 \cdot 15 \oplus 17 \oplus 19 \oplus 23$
[2, 2, 0, 2, 2, 2, 2]	$E_7(a_1)$	$\mathfrak{su}_2^{(231)} \oplus \emptyset$	124	$3 \oplus 7 \oplus 2 \cdot 11 \oplus 15 \oplus 17 \oplus 19 \oplus 23 \oplus 27$
[2, 2, 2, 2, 2, 2, 2]	E_7	$\mathfrak{su}_2^{(399)} \oplus \emptyset$	126	$3 \oplus 11 \oplus 15 \oplus 19 \oplus 23 \oplus 27 \oplus 35$

TABLE XIII. Nilpotent orbits of e_8 .

w	Bala-Carter	$e_8 \rightarrow \mathfrak{su}_2^{(I_O)} \oplus \mathfrak{f}^{(I)}$	$\dim \mathcal{O}$	$\text{adj} \rightarrow \bigoplus_i (d_i, R_i)$
[0, 0, 0, 0, 0, 0, 0, 0]	0	$\mathfrak{su}_2^{(0)} \oplus e_8^{(1)}$	0	$(1, 248)$
[0, 0, 0, 0, 0, 0, 1, 0]	A_1	$\mathfrak{su}_2^{(1)} \oplus e_7^{(1)}$	58	$(3, 1) \oplus (2, 56) \oplus (1, 133)$
[1, 0, 0, 0, 0, 0, 0, 0]	$2A_1$	$\mathfrak{su}_2^{(2)} \oplus \mathfrak{so}_{13}^{(1)}$	92	$(1, 78) \oplus (2, 64) \oplus (3, 1) \oplus (3, 13)$
[0, 0, 0, 0, 0, 1, 0, 0]	$3A_1$	$\mathfrak{su}_2^{(3)} \oplus (\mathfrak{f}_4^{(1)} \oplus \mathfrak{su}_2^{(1)})$	112	$(1, 1, 3) \oplus (1, 52, 1) \oplus (2, 26, 2) \oplus (3, 1, 1) \oplus$ $(3, 26, 1) \oplus (4, 1, 2)$

(Table continued)

TABLE XIII. (Continued)

w	Bala-Carter	$\mathfrak{e}_8 \rightarrow \mathfrak{su}_2^{(l_0)} \oplus \mathfrak{f}^{(l)}$	$\dim \mathcal{O}$	$\text{adj} \rightarrow \bigoplus_i (d_i, R_i)$
[0, 0, 0, 0, 0, 2, 0]	A_2	$\mathfrak{su}_2^{(4)} \oplus \mathfrak{e}_6^{(1)}$	114	$(1, 78) \oplus (3, 1) \oplus (3, 27) \oplus (3, \bar{27}) \oplus (5, 1)$
[0, 0, 0, 0, 0, 0, 1]	$4A_1$	$\mathfrak{su}_2^{(4)} \oplus \mathfrak{sp}_4^{(1)}$	128	$(1, 36) \oplus (2, 48) \oplus (3, 1) \oplus (3, 27) \oplus (4, 8)$
[1, 0, 0, 0, 0, 0, 1, 0]	$A_2 + A_1$	$\mathfrak{su}_2^{(5)} \oplus \mathfrak{su}_6^{(1)}$	136	$(1, 35) \oplus (2, 6) \oplus (2, \bar{6}) \oplus (2, 20) \oplus 2 \cdot (3, 1) \oplus (3, 15) \oplus (3, \bar{15}) \oplus (4, 6) \oplus (4, \bar{6}) \oplus (5, 1)$
[0, 0, 0, 0, 1, 0, 0, 0]	$A_2 + 2A_1$	$\mathfrak{su}_2^{(6)} \oplus (\mathfrak{so}_7^{(1)} \oplus \mathfrak{su}_2^{(6)})$	146	$(1, 1, 3) \oplus (1, 21, 1) \oplus (2, 8, 4) \oplus (3, 7, 3) \oplus (3, 1, 5) \oplus (3, 1, 1) \oplus (4, 8, 2) \oplus (5, 1, 3)$
[1, 0, 0, 0, 0, 0, 2, 0]	A_3	$\mathfrak{su}_2^{(10)} \oplus \mathfrak{so}_{11}^{(1)}$	148	$(1, 55) \oplus (3, 1) \oplus (4, 32) \oplus (5, 11) \oplus (7, 1)$
[0, 1, 0, 0, 0, 0, 0, 0]	$A_2 + 3A_1$	$\mathfrak{su}_2^{(7)} \oplus (\mathfrak{g}_2^{(2)} \oplus \mathfrak{su}_2^{(1)})$	154	$(1, 14, 1) \oplus (1, 1, 3) \oplus (2, 14, 2) \oplus (3, 27, 1) \oplus (3, 1, 1) \oplus (4, 7, 2) \oplus (5, 7, 1)$
[2, 0, 0, 0, 0, 0, 0, 0]	$2A_2$	$\mathfrak{su}_2^{(8)} \oplus (\mathfrak{g}_2^{(1)} \oplus \mathfrak{g}_2^{(1)})$	156	$(1, 14, 1) \oplus (1, 1, 14) \oplus (3, 7, 7) \oplus (3, 1, 1) \oplus (5, 1, 7) \oplus (5, 7, 1)$
[1, 0, 0, 0, 0, 1, 0, 0]	$2A_2 + A_1$	$\mathfrak{su}_2^{(9)} \oplus (\mathfrak{g}_2^{(1)} \oplus \mathfrak{su}_2^{(3)})$	162	$(1, 1, 3) \oplus (1, 14, 1) \oplus (2, 1, 4) \oplus (2, 7, 2) \oplus 2 \cdot (3, 1, 1) \oplus (3, 7, 3) \oplus (4, 1, 2) \oplus (4, 7, 2) \oplus (5, 1, 3) \oplus (5, 7, 1) \oplus (6, 1, 2)$
[0, 0, 0, 0, 1, 0, 1, 0]	$A_3 + A_1$	$\mathfrak{su}_2^{(11)} \oplus (\mathfrak{so}_7^{(1)} \oplus \mathfrak{su}_2^{(1)})$	164	$(1, 1, 3) \oplus (1, 21, 1) \oplus (2, 7, 2) \oplus 2 \cdot (3, 1, 1) \oplus (3, 8, 1) \oplus (4, 8, 2) \oplus (4, 1, 2) \oplus (5, 8, 1) \oplus (5, 7, 1) \oplus (6, 1, 2) \oplus (7, 1, 1)$
[0, 0, 0, 1, 0, 0, 0, 0]	$2A_2 + 2A_1$	$\mathfrak{su}_2^{(10)} \oplus \mathfrak{sp}_2^{(3)}$	168	$(1, 10) \oplus (2, 20) \oplus (3, 1) \oplus (3, 5) \oplus (3, 14) \oplus (4, 16) \oplus (5, 10) \oplus (6, 4)$
[0, 0, 0, 0, 0, 2, 0, 0]	$D_4(a_1)$	$\mathfrak{su}_2^{(12)} \oplus \mathfrak{so}_8^{(1)}$	166	$(1, 28) \oplus 3 \cdot (3, 1) \oplus (3, 8_v) \oplus (3, 8_c) \oplus (3, 8_s) \oplus (5, 1) \oplus (5, 8_v) \oplus (5, 8_c) \oplus (5, 8_s) \oplus 2 \cdot (7, 1)$
[0, 1, 0, 0, 0, 0, 1, 0]	$A_3 + 2A_1$	$\mathfrak{su}_2^{(12)} \oplus (\mathfrak{sp}_2^{(1)} \oplus \mathfrak{su}_2^{(2)})$	172	$(1, 10, 1) \oplus (1, 1, 3) \oplus (2, 4, 3) \oplus (2, 1, 2) \oplus 2 \cdot (3, 1, 1) \oplus (3, 5, 1) \oplus (3, 4, 2) \oplus (4, 1, 2) \oplus (4, 4, 1) \oplus (4, 5, 2) \oplus (5, 4, 2) \oplus (5, 1, 3) \oplus (6, 4, 1) \oplus (6, 1, 2) \oplus (7, 1, 1)$
[0, 0, 0, 0, 0, 1, 0, 1]	$D_4(a_1) + A_1$	$\mathfrak{su}_2^{(13)} \oplus (\mathfrak{su}_2^{(1)} \oplus \mathfrak{su}_2^{(1)} \oplus \mathfrak{su}_2^{(1)})$	176	$(1, 1, 1, 3) \oplus (1, 1, 3, 1) \oplus (1, 3, 1, 1) \oplus (2, 2, 2, 2) \oplus (2, 2, 1, 1) \oplus (2, 1, 1, 2) \oplus (2, 1, 2, 1) \oplus 4 \cdot (3, 1, 1, 1) \oplus (3, 1, 2, 2) \oplus (3, 2, 2, 1) \oplus (3, 2, 1, 2) \oplus 2 \cdot (4, 2, 1, 1) \oplus 2 \cdot (4, 1, 2, 1) \oplus 2 \cdot (4, 1, 1, 2) \oplus (5, 1, 1, 1) \oplus (5, 2, 2, 1) \oplus (5, 1, 2, 2) \oplus (5, 2, 1, 2) \oplus (6, 2, 1, 1) \oplus (6, 1, 2, 1) \oplus (6, 1, 1, 2) \oplus 2 \cdot (7, 1, 1, 1)$
[0, 0, 0, 0, 0, 2, 2, 0]	D_4	$\mathfrak{su}_2^{(28)} \oplus \mathfrak{f}_4^{(1)}$	168	$(1, 52) \oplus (3, 1) \oplus (7, 26) \oplus (11, 1)$
[1, 0, 0, 0, 1, 0, 0, 0]	$A_3 + A_2$	$\mathfrak{su}_2^{(14)} \oplus \mathfrak{sp}_2^{(1)}$	178	$(1, 10) \oplus (1, 1) \oplus 2 \cdot (2, 4) \oplus 6 \cdot (3, 1) \oplus 2 \cdot (3, 5) \oplus 4 \cdot (4, 4) \oplus 3 \cdot (5, 1) \oplus (5, 5) \oplus 2 \cdot (6, 4) \oplus 3 \cdot (7, 1)$
[2, 0, 0, 0, 0, 0, 2, 0]	A_4	$\mathfrak{su}_2^{(20)} \oplus \mathfrak{su}_5^{(1)}$	180	$(1, 24) \oplus (3, 1) \oplus (3, 5) \oplus (3, \bar{5}) \oplus (5, 1) \oplus (5, 10) \oplus (5, \bar{10}) \oplus (7, 1) \oplus (7, 5) \oplus (7, \bar{5}) \oplus (9, 1)$
[0, 0, 1, 0, 0, 0, 0, 0]	$A_3 + A_2 + A_1$	$\mathfrak{su}_2^{(15)} \oplus (\mathfrak{su}_2^{(24)} \oplus \mathfrak{su}_2^{(1)})$	182	$(7, 5, 1) \oplus (5, 7, 1) \oplus (5, 3, 1) \oplus (6, 3, 2) \oplus (4, 7, 2) \oplus (3, 9, 1) \oplus (3, 5, 1) \oplus (3, 1, 1) \oplus (2, 5, 2) \oplus (1, 3, 1) \oplus (1, 1, 3)$
[0, 0, 0, 0, 0, 1, 2, 1]	$D_4 + A_1$	$\mathfrak{su}_2^{(29)} \oplus \mathfrak{sp}_3^{(1)}$	184	$(1, 21) \oplus (2, 14') \oplus 2 \cdot (3, 1) \oplus (6, 6) \oplus (7, 14) \oplus (8, 6) \oplus (11, 1)$
[0, 0, 0, 0, 0, 0, 0, 2]	$D_4(a_1) + A_2$	$\mathfrak{su}_2^{(16)} \oplus \mathfrak{su}_3^{(6)}$	184	$(1, 8) \oplus (3, 1) \oplus (3, 27) \oplus (5, 10) \oplus (5, \bar{10}) \oplus (7, 8)$
[1, 0, 0, 0, 1, 0, 1, 0]	$A_4 + A_1$	$\mathfrak{su}_2^{(21)} \oplus \mathfrak{su}_3^{(1)}$	188	$(1, 1) \oplus (1, 8) \oplus (2, 3) \oplus (2, \bar{3}) \oplus 2 \cdot (2, 1) \oplus 2 \cdot (3, 1) \oplus (3, 3) \oplus (3, \bar{3}) \oplus 2 \cdot (4, 1) \oplus (4, 3) \oplus (4, \bar{3}) \oplus 3 \cdot (5, 1) \oplus (5, 3) \oplus (5, \bar{3}) \oplus (6, 3) \oplus (6, \bar{3}) \oplus 2 \cdot (6, 1) \oplus (7, 1) \oplus (7, 3)$

(Table continued)

TABLE XIII. (Continued)

w	Bala-Carter	$\mathfrak{e}_8 \rightarrow \mathfrak{su}_2^{(I_0)} \oplus \mathfrak{f}^{(I)}$	$\dim \mathcal{O}$	$\text{adj} \rightarrow \bigoplus_i (d_i, R_i)$
[1, 0, 0, 1, 0, 0, 0, 0]	$2A_3$	$\mathfrak{su}_2^{(20)} \oplus \mathfrak{sp}_2^{(2)}$	188	$\oplus(7, \bar{3}) \oplus 2 \cdot (8, 1) \oplus (9, 1)$ $(8, 4) \oplus (7, 5) \oplus (7, 1) \oplus (6, 4) \oplus (5, 10) \oplus (4, 16) \oplus$ $(3, 5) \oplus (3, 1) \oplus (2, 4) \oplus (1, 10)$
[1, 0, 0, 0, 1, 0, 2, 0]	$D_5(a_1)$	$\mathfrak{su}_2^{(30)} \oplus \mathfrak{su}_4^{(1)}$	190	$(1, 15) \oplus (2, 4) \oplus (2, \bar{4}) \oplus 2 \cdot (3, 1) \oplus (3, 6) \oplus$ $(5, 1) \oplus (6, 4)$ $\oplus(6, \bar{4}) \oplus 2 \cdot (7, 1) \oplus (7, 6) \oplus (8, 4) \oplus (8, \bar{4}) \oplus$ $(9, 1) \oplus (11, 1)$
[0, 0, 1, 0, 0, 0, 1, 0]	$A_4 + 2A_1$	$\mathfrak{su}_2^{(22)} \oplus \mathfrak{su}_2^{(2)}$	192	$(9, 1) \oplus 2 \cdot (8, 2) \oplus 5 \cdot (7, 1) \oplus 4 \cdot (6, 2) \oplus 3 \cdot (5, 1) \oplus$ $2 \cdot (5, 3)$ $\oplus 4 \cdot (4, 2) \oplus 6 \cdot (3, 1) \oplus (3, 3) \oplus 4 \cdot (2, 2) \oplus (1, 1) \oplus$ $(1, 3)$
[0, 0, 0, 0, 2, 0, 0, 0]	$A_4 + A_2$	$\mathfrak{su}_2^{(24)} \oplus (\mathfrak{su}_2^{(1)} \oplus \mathfrak{su}_2^{(15)})$	194	$(1, 3, 1) \oplus (1, 1, 3) \oplus (3, 1, 1) \oplus (3, 2, 6) \oplus (3, 1, 5) \oplus$ $(5, 1, 7)$ $\oplus(5, 1, 3) \oplus (5, 2, 2) \oplus (7, 1, 5) \oplus (7, 2, 4) \oplus (9, 1, 3)$
[0, 0, 1, 0, 0, 0, 2, 0]	$D_5(a_1) + A_1$	$\mathfrak{su}_2^{(31)} \oplus (\mathfrak{su}_2^{(1)} \oplus \mathfrak{su}_2^{(8)})$	196	$(1, 1, 3) \oplus (1, 3, 1) \oplus (2, 2, 5) \oplus (3, 1, 5) \oplus 2 \cdot$ $(3, 1, 1) \oplus (4, 2, 1)$ $\oplus(5, 1, 3) \oplus (6, 2, 3) \oplus (7, 1, 5) \oplus (7, 1, 3) \oplus (8, 2, 3)$ $\oplus(9, 1, 3) \oplus (11, 1, 1)$
[0, 1, 0, 0, 1, 0, 0, 0]	$A_4 + A_2 + A_1$	$\mathfrak{su}_2^{(25)} \oplus \mathfrak{su}_2^{(15)}$	196	$(9, 3) \oplus (8, 4) \oplus (7, 5) \oplus (6, 2) \oplus (6, 4) \oplus (5, 3) \oplus$ $(5, 7) \oplus (4, 2)$ $\oplus(4, 6) \oplus 2 \cdot (3, 1) \oplus (3, 5) \oplus (2, 6) \oplus (1, 3)$
[2, 0, 0, 0, 1, 0, 1, 0]	A_5	$\mathfrak{su}_2^{(35)} \oplus (\mathfrak{g}_2^{(1)} \oplus \mathfrak{su}_2^{(1)})$	196	$(1, 1, 3) \oplus (1, 14, 1) \oplus (3, 1, 1) \oplus (4, 1, 2) \oplus (5, 7, 1) \oplus$ $(6, 7, 2)$ $\oplus(7, 1, 1) \oplus (9, 7, 1) \oplus (10, 1, 2) \oplus (11, 1, 1)$
[0, 0, 1, 0, 0, 1, 0, 0]	$A_4 + A_3$	$\mathfrak{su}_2^{(30)} \oplus \mathfrak{su}_2^{(10)}$	200	$(10, 2) \oplus (9, 3) \oplus (8, 4) \oplus (7, 1) \oplus (7, 5) \oplus (6, 2) \oplus$ $(6, 4)$ $\oplus 2 \cdot (5, 3) \oplus (4, 2) \oplus (4, 6) \oplus (3, 5) \oplus (3, 1) \oplus$ $(2, 4) \oplus (1, 3)$
[0, 0, 0, 0, 0, 0, 2, 2]	$D_4 + A_2$	$\mathfrak{su}_2^{(32)} \oplus \mathfrak{su}_3^{(2)}$	198	$(1, 8) \oplus 2 \cdot (3, 1) \oplus (3, 6) \oplus (3, \bar{6}) \oplus (5, 1) \oplus (5, 3) \oplus$ $(5, \bar{3})$ $\oplus(7, 3) \oplus (7, \bar{3}) \oplus (7, 8) \oplus (9, 3) \oplus (9, \bar{3}) \oplus (11, 1)$
[2, 0, 0, 0, 0, 2, 0, 0]	$E_6(a_3)$	$\mathfrak{su}_2^{(36)} \oplus \mathfrak{g}_2^{(1)}$	198	$(1, 14) \oplus 3 \cdot (3, 1) \oplus (5, 1) \oplus 2 \cdot (5, 7) \oplus (7, 1) \oplus$ $(7, 7) \oplus (9, 1) \oplus (9, 7) \oplus 2 \cdot (11, 1)$
[1, 0, 1, 0, 0, 0, 1, 0]	$A_5 + A_1$	$\mathfrak{su}_2^{(36)} \oplus (\mathfrak{su}_2^{(3)} \oplus \mathfrak{su}_2^{(1)})$	202	$(1, 1, 3) \oplus (1, 3, 1) \oplus (2, 4, 1) \oplus 2 \cdot (3, 1, 1) \oplus$ $(4, 1, 2) \oplus (4, 2, 1)$ $\oplus(5, 3, 1) \oplus (5, 2, 2) \oplus (6, 2, 1) \oplus (6, 3, 2) \oplus (7, 1, 1)$ $\oplus(7, 2, 2) \oplus (8, 2, 1) \oplus (9, 3, 1) \oplus (10, 1, 2) \oplus$ $(10, 2, 1) \oplus (11, 1, 1)$
[0, 1, 0, 0, 1, 0, 1, 0]	$D_5(a_1) + A_2$	$\mathfrak{su}_2^{(34)} \oplus \mathfrak{su}_2^{(6)}$	202	$(11, 1) \oplus (10, 2) \oplus (9, 3) \oplus (8, 4) \oplus (8, 2) \oplus (7, 3) \oplus$ $(7, 1)$ $\oplus(6, 4) \oplus (6, 2) \oplus 2 \cdot (5, 3) \oplus 2 \cdot (4, 2) \oplus 2 \cdot (3, 1) \oplus$ $(3, 5) \oplus (2, 4) \oplus (1, 3)$
[1, 0, 0, 1, 0, 1, 0, 0]	$E_6(a_3) + A_1$	$\mathfrak{su}_2^{(37)} \oplus \mathfrak{su}_2^{(3)}$	204	$(1, 3) \oplus (2, 4) \oplus 4 \cdot (3, 1) \oplus 2 \cdot (4, 2) \oplus (5, 1) \oplus 2 \cdot$ $(5, 3)$ $\oplus 3 \cdot (6, 2) \oplus (7, 1) \oplus (7, 3) \oplus 2 \cdot (8, 2) \oplus (9, 1) \oplus$ $(9, 3) \oplus (10, 2) \oplus 2 \cdot (11, 1)$
[0, 1, 0, 0, 0, 1, 0, 1]	$D_6(a_2)$	$\mathfrak{su}_2^{(38)} \oplus \mathfrak{su}_2^{(4/5)}$	204	$(1, 1, 3) \oplus (1, 3, 1) \oplus 3 \cdot (3, 1, 1) \oplus 2 \cdot (4, 2, 1) \oplus 2 \cdot$ $(4, 1, 2)$ $\oplus(5, 1, 1) \oplus (5, 2, 2) \oplus (6, 1, 2) \oplus (6, 2, 1) \oplus 3 \cdot$ $(7, 1, 1)$ $\oplus(7, 2, 2) \oplus (8, 1, 2) \oplus (8, 2, 1) \oplus (9, 1, 1) \oplus$ $(10, 1, 2) \oplus (10, 2, 1) \oplus 2 \cdot (11, 1, 1)$

(Table continued)

TABLE XIII. (Continued)

w	Bala-Carter	$e_8 \rightarrow \mathfrak{su}_2^{(I_0)} \oplus \mathfrak{f}^{(I)}$	$\dim \mathcal{O}$	$\text{adj} \rightarrow \bigoplus_i (\mathbf{d}_i, \mathbf{R}_i)$
[2, 0, 0, 0, 0, 2, 2, 0]	D_5	$\mathfrak{su}_2^{(60)} \oplus \mathfrak{so}_7^{(1)}$	200	$(\mathbf{1}, \mathbf{21}) \oplus (\mathbf{3}, \mathbf{1}) \oplus (\mathbf{5}, \mathbf{8}) \oplus (\mathbf{7}, \mathbf{1}) \oplus (\mathbf{9}, \mathbf{7}) \oplus (\mathbf{11}, \mathbf{1}) \oplus (\mathbf{11}, \mathbf{8}) \oplus (\mathbf{15}, \mathbf{1})$
[0, 0, 1, 0, 1, 0, 0, 0]	$E_7(a_5)$	$\mathfrak{su}_2^{(39)} \oplus \mathfrak{su}_2^{(1)}$	206	$(\mathbf{1}, \mathbf{3}) \oplus 6 \cdot (\mathbf{3}, \mathbf{1}) \oplus 3 \cdot (\mathbf{4}, \mathbf{2}) \oplus 4 \cdot (\mathbf{5}, \mathbf{1}) \oplus 3 \cdot (\mathbf{6}, \mathbf{2}) \oplus 5 \cdot (\mathbf{7}, \mathbf{1}) \oplus 2 \cdot (\mathbf{8}, \mathbf{2}) \oplus 3 \cdot (\mathbf{9}, \mathbf{1}) \oplus (\mathbf{10}, \mathbf{2}) \oplus 3 \cdot (\mathbf{11}, \mathbf{1})$
[1, 0, 0, 1, 0, 1, 2, 0]	$D_5 + A_1$	$\mathfrak{su}_2^{(61)} \oplus (\mathfrak{su}_2^{(1)} \oplus \mathfrak{su}_2^{(2)})$	208	$(\mathbf{1}, \mathbf{1}, \mathbf{3}) \oplus (\mathbf{1}, \mathbf{3}, \mathbf{1}) \oplus (\mathbf{2}, \mathbf{2}, \mathbf{3}) \oplus 2 \cdot (\mathbf{3}, \mathbf{1}, \mathbf{1}) \oplus (\mathbf{4}, \mathbf{1}, \mathbf{2}) \oplus (\mathbf{5}, \mathbf{2}, \mathbf{2}) \oplus (\mathbf{6}, \mathbf{1}, \mathbf{2}) \oplus (\mathbf{7}, \mathbf{1}, \mathbf{1}) \oplus (\mathbf{8}, \mathbf{2}, \mathbf{1}) \oplus (\mathbf{9}, \mathbf{1}, \mathbf{3}) \oplus (\mathbf{10}, \mathbf{1}, \mathbf{2}) \oplus (\mathbf{10}, \mathbf{2}, \mathbf{1}) \oplus (\mathbf{11}, \mathbf{1}, \mathbf{1}) \oplus (\mathbf{11}, \mathbf{2}, \mathbf{2}) \oplus (\mathbf{12}, \mathbf{1}, \mathbf{2}) \oplus (\mathbf{15}, \mathbf{1}, \mathbf{1})$
[0, 0, 0, 2, 0, 0, 0, 0]	$E_8(a_7)$	$\mathfrak{su}_2^{(40)} \oplus \emptyset$	208	$4 \cdot \mathbf{11} \oplus 6 \cdot \mathbf{9} \oplus 10 \cdot \mathbf{7} \oplus 10 \cdot \mathbf{5} \oplus 10 \cdot \mathbf{3}$
[0, 1, 0, 0, 0, 1, 2, 1]	$D_6(a_1)$	$\mathfrak{su}_2^{(62)} \oplus (\mathfrak{su}_2^{(1)} \oplus \mathfrak{su}_2^{(1)})$	210	$(\mathbf{1}, \mathbf{1}, \mathbf{3}) \oplus (\mathbf{1}, \mathbf{3}, \mathbf{1}) \oplus 2 \cdot (\mathbf{3}, \mathbf{1}, \mathbf{1}) \oplus (\mathbf{3}, \mathbf{2}, \mathbf{2}) \oplus (\mathbf{4}, \mathbf{1}, \mathbf{2}) \oplus (\mathbf{4}, \mathbf{2}, \mathbf{1}) \oplus (\mathbf{6}, \mathbf{1}, \mathbf{2}) \oplus (\mathbf{6}, \mathbf{2}, \mathbf{1}) \oplus 2 \cdot (\mathbf{7}, \mathbf{1}, \mathbf{1}) \oplus (\mathbf{9}, \mathbf{1}, \mathbf{1}) \oplus (\mathbf{9}, \mathbf{2}, \mathbf{2}) \oplus (\mathbf{10}, \mathbf{1}, \mathbf{2}) \oplus (\mathbf{10}, \mathbf{2}, \mathbf{1}) \oplus 2 \cdot (\mathbf{11}, \mathbf{1}, \mathbf{1}) \oplus (\mathbf{12}, \mathbf{1}, \mathbf{2}) \oplus (\mathbf{12}, \mathbf{2}, \mathbf{1}) \oplus (\mathbf{15}, \mathbf{1}, \mathbf{1})$
[2, 0, 0, 0, 2, 0, 0, 0]	A_6	$\mathfrak{su}_2^{(56)} \oplus (\mathfrak{su}_2^{(1)} \oplus \mathfrak{su}_2^{(7)})$	210	$(\mathbf{1}, \mathbf{1}, \mathbf{3}) \oplus (\mathbf{1}, \mathbf{3}, \mathbf{1}) \oplus (\mathbf{3}, \mathbf{1}, \mathbf{1}) \oplus (\mathbf{3}, \mathbf{2}, \mathbf{2}) \oplus (\mathbf{5}, \mathbf{1}, \mathbf{3}) \oplus (\mathbf{7}, \mathbf{1}, \mathbf{5}) \oplus (\mathbf{7}, \mathbf{2}, \mathbf{4}) \oplus (\mathbf{9}, \mathbf{1}, \mathbf{3}) \oplus (\mathbf{11}, \mathbf{1}, \mathbf{1}) \oplus (\mathbf{11}, \mathbf{2}, \mathbf{2}) \oplus (\mathbf{13}, \mathbf{1}, \mathbf{3})$
[0, 0, 1, 0, 1, 0, 2, 0]	$E_7(a_4)$	$\mathfrak{su}_2^{(63)} \oplus \mathfrak{su}_2^{(1)}$	212	$(\mathbf{1}, \mathbf{3}) \oplus (\mathbf{2}, \mathbf{2}) \oplus 4 \cdot (\mathbf{3}, \mathbf{1}) \oplus 2 \cdot (\mathbf{4}, \mathbf{2}) \oplus 2 \cdot (\mathbf{5}, \mathbf{1}) \oplus (\mathbf{6}, \mathbf{2}) \oplus 3 \cdot (\mathbf{7}, \mathbf{1}) \oplus (\mathbf{8}, \mathbf{2}) \oplus 2 \cdot (\mathbf{9}, \mathbf{1}) \oplus 2 \cdot (\mathbf{10}, \mathbf{2}) \oplus 4 \cdot (\mathbf{11}, \mathbf{1}) \oplus (\mathbf{12}, \mathbf{2}) \oplus (\mathbf{13}, \mathbf{1}) \oplus (\mathbf{15}, \mathbf{1})$
[1, 0, 1, 0, 1, 0, 0, 0]	$A_6 + A_1$	$\mathfrak{su}_2^{(57)} \oplus \mathfrak{su}_2^{(7)}$	212	$(\mathbf{1}, \mathbf{3}) \oplus (\mathbf{2}, \mathbf{2}) \oplus 2 \cdot (\mathbf{3}, \mathbf{1}) \oplus (\mathbf{4}, \mathbf{2}) \oplus (\mathbf{5}, \mathbf{3}) \oplus (\mathbf{6}, \mathbf{4}) \oplus (\mathbf{7}, \mathbf{5}) \oplus (\mathbf{8}, \mathbf{4}) \oplus (\mathbf{9}, \mathbf{3}) \oplus (\mathbf{10}, \mathbf{2}) \oplus (\mathbf{11}, \mathbf{1}) \oplus (\mathbf{12}, \mathbf{2}) \oplus (\mathbf{13}, \mathbf{3})$
[2, 0, 0, 0, 2, 0, 2, 0]	$E_6(a_1)$	$\mathfrak{su}_2^{(84)} \oplus \mathfrak{su}_3^{(1)}$	214	$(\mathbf{1}, \mathbf{8}) \oplus (\mathbf{3}, \mathbf{1}) \oplus (\mathbf{5}, \mathbf{1}) \oplus (\mathbf{5}, \mathbf{3}) \oplus (\mathbf{5}, \bar{\mathbf{3}}) \oplus (\mathbf{7}, \mathbf{1}) \oplus (\mathbf{9}, \mathbf{1}) \oplus (\mathbf{9}, \mathbf{3}) \oplus (\mathbf{9}, \bar{\mathbf{3}}) \oplus 2 \cdot (\mathbf{11}, \mathbf{1}) \oplus (\mathbf{13}, \mathbf{3}) \oplus (\mathbf{13}, \bar{\mathbf{3}}) \oplus (\mathbf{15}, \mathbf{1}) \oplus (\mathbf{17}, \mathbf{1})$
[0, 0, 0, 2, 0, 0, 2, 0]	$D_5 + A_2$	$\mathfrak{su}_2^{(64)} \oplus \emptyset$	214	$\mathbf{15} \oplus 2 \cdot \mathbf{13} \oplus 7 \cdot \mathbf{11} \oplus 5 \cdot \mathbf{9} \oplus 5 \cdot \mathbf{7} \oplus 5 \cdot \mathbf{5} \oplus 8 \cdot \mathbf{3} \oplus \mathbf{1}$
[1, 0, 1, 0, 1, 0, 1, 0]	$D_7(a_2)$	$\mathfrak{su}_2^{(70)} \oplus \emptyset$	216	$\mathbf{15} \oplus 2 \cdot \mathbf{14} \oplus \mathbf{13} \oplus 2 \cdot \mathbf{12} \oplus 2 \cdot \mathbf{11} \oplus 2 \cdot \mathbf{10} \oplus 3 \cdot \mathbf{9} \oplus 4 \cdot \mathbf{8} \oplus 3 \cdot \mathbf{7} \oplus 2 \cdot \mathbf{6} \oplus 3 \cdot \mathbf{5} \oplus 2 \cdot \mathbf{4} \oplus 2 \cdot \mathbf{3} \oplus 2 \cdot \mathbf{2} \oplus \mathbf{1}$
[2, 0, 0, 0, 2, 2, 2, 0]	E_6	$\mathfrak{su}_2^{(156)} \oplus \mathfrak{g}_2^{(1)}$	216	$(\mathbf{1}, \mathbf{14}) \oplus (\mathbf{3}, \mathbf{1}) \oplus (\mathbf{9}, \mathbf{7}) \oplus (\mathbf{11}, \mathbf{1}) \oplus (\mathbf{15}, \mathbf{1}) \oplus (\mathbf{17}, \mathbf{7}) \oplus (\mathbf{23}, \mathbf{1})$
[1, 0, 1, 0, 1, 1, 0, 0]	A_7	$\mathfrak{su}_2^{(84)} \oplus \mathfrak{su}_2^{(4)}$	218	$(\mathbf{16}, \mathbf{2}) \oplus (\mathbf{15}, \mathbf{1}) \oplus (\mathbf{13}, \mathbf{3}) \oplus (\mathbf{12}, \mathbf{2}) \oplus (\mathbf{11}, \mathbf{1}) \oplus (\mathbf{10}, \mathbf{2}) \oplus (\mathbf{9}, \mathbf{3}) \oplus (\mathbf{8}, \mathbf{4}) \oplus (\mathbf{7}, \mathbf{1}) \oplus (\mathbf{6}, \mathbf{2}) \oplus (\mathbf{5}, \mathbf{3}) \oplus (\mathbf{4}, \mathbf{2}) \oplus (\mathbf{3}, \mathbf{1}) \oplus (\mathbf{1}, \mathbf{3})$
[1, 0, 1, 0, 1, 0, 2, 0]	$E_6(a_1) + A_1$	$\mathfrak{su}_2^{(85)} \oplus \emptyset$	218	$\mathbf{17} \oplus \mathbf{15} \oplus 2 \cdot \mathbf{14} \oplus 2 \cdot \mathbf{13} \oplus 2 \cdot \mathbf{12} \oplus 2 \cdot \mathbf{11} \oplus 2 \cdot \mathbf{10} \oplus 3 \cdot \mathbf{9} \oplus 2 \cdot \mathbf{8} \oplus 7 \oplus 2 \cdot \mathbf{6} \oplus 3 \cdot \mathbf{5} \oplus 2 \cdot \mathbf{4} \oplus 2 \cdot \mathbf{3} \oplus 2 \cdot \mathbf{2} \oplus \mathbf{1}$
[0, 0, 2, 0, 0, 0, 2, 0]	$E_8(b_6)$	$\mathfrak{su}_2^{(88)} \oplus \emptyset$	220	$\mathbf{17} \oplus 3 \cdot \mathbf{15} \oplus 2 \cdot \mathbf{13} \oplus 6 \cdot \mathbf{11} \oplus 3 \cdot \mathbf{9} \oplus 5 \cdot \mathbf{7} \oplus 4 \cdot \mathbf{5} \oplus 4 \cdot \mathbf{3}$
[2, 1, 0, 0, 0, 1, 2, 1]	D_6	$\mathfrak{su}_2^{(110)} \oplus \mathfrak{sp}_2^{(1)}$	216	$(\mathbf{1}, \mathbf{10}) \oplus (\mathbf{3}, \mathbf{1}) \oplus (\mathbf{6}, \mathbf{4}) \oplus (\mathbf{7}, \mathbf{1}) \oplus (\mathbf{10}, \mathbf{4}) \oplus (\mathbf{11}, \mathbf{1}) \oplus (\mathbf{11}, \mathbf{5}) \oplus (\mathbf{15}, \mathbf{1}) \oplus (\mathbf{16}, \mathbf{4}) \oplus (\mathbf{19}, \mathbf{1})$
[2, 0, 1, 0, 1, 0, 2, 0]	$E_7(a_3)$	$\mathfrak{su}_2^{(111)} \oplus \mathfrak{su}_2^{(1)}$	220	$(\mathbf{1}, \mathbf{3}) \oplus (\mathbf{2}, \mathbf{2}) \oplus 2 \cdot (\mathbf{3}, \mathbf{1}) \oplus (\mathbf{5}, \mathbf{1}) \oplus (\mathbf{6}, \mathbf{2}) \oplus 2 \cdot (\mathbf{7}, \mathbf{1}) \oplus (\mathbf{9}, \mathbf{1})$

(Table continued)

TABLE XIII. (Continued)

w	Bala-Carter	$\mathfrak{e}_8 \rightarrow \mathfrak{su}_2^{(I_0)} \oplus \mathfrak{f}^{(I)}$	$\dim \mathcal{O}$	$\text{adj} \rightarrow \bigoplus_i (\mathbf{d}_i, \mathbf{R}_i)$
[2, 0, 0, 2, 0, 0, 2, 0]	$D_7(a_1)$	$\mathfrak{su}_2^{(112)} \oplus \emptyset$	222	$\oplus 2 \cdot (\mathbf{10}, \mathbf{2}) \oplus 3 \cdot (\mathbf{11}, \mathbf{1}) \oplus (\mathbf{12}, \mathbf{2}) \oplus 2 \cdot (\mathbf{15}, \mathbf{1}) \oplus (\mathbf{16}, \mathbf{2}) \oplus (\mathbf{17}, \mathbf{1}) \oplus (\mathbf{19}, \mathbf{1})$ $\mathbf{19} \oplus 2 \cdot \mathbf{17} \oplus 3 \cdot \mathbf{15} \oplus \mathbf{13} \oplus 6 \cdot \mathbf{11} \oplus 3 \cdot \mathbf{9} \oplus 3 \cdot \mathbf{7} \oplus 2 \cdot \mathbf{5} \oplus 4 \cdot \mathbf{3} \oplus \mathbf{1}$
[1, 0, 1, 0, 1, 2, 2, 0]	$E_6 + A_1$	$\mathfrak{su}_2^{(157)} \oplus \mathfrak{su}_2^{(3)}$	222	$(\mathbf{23}, \mathbf{1}) \oplus (\mathbf{18}, \mathbf{2}) \oplus (\mathbf{17}, \mathbf{3}) \oplus (\mathbf{16}, \mathbf{2}) \oplus (\mathbf{15}, \mathbf{1}) \oplus (\mathbf{11}, \mathbf{1})$ $\oplus (\mathbf{10}, \mathbf{2}) \oplus (\mathbf{9}, \mathbf{3}) \oplus (\mathbf{8}, \mathbf{2}) \oplus 2 \cdot (\mathbf{3}, \mathbf{1}) \oplus (\mathbf{2}, \mathbf{4}) \oplus (\mathbf{1}, \mathbf{3})$
[0, 1, 0, 1, 0, 2, 2, 1]	$E_7(a_2)$	$\mathfrak{su}_2^{(159)} \oplus \mathfrak{su}_2^{(1)}$	224	$(\mathbf{23}, \mathbf{1}) \oplus (\mathbf{19}, \mathbf{1}) \oplus (\mathbf{18}, \mathbf{2}) \oplus (\mathbf{17}, \mathbf{1}) \oplus (\mathbf{16}, \mathbf{2}) \oplus 2 \cdot (\mathbf{15}, \mathbf{1})$ $\oplus 2 \cdot (\mathbf{11}, \mathbf{1}) \oplus (\mathbf{10}, \mathbf{2}) \oplus (\mathbf{9}, \mathbf{1}) \oplus (\mathbf{8}, \mathbf{2}) \oplus (\mathbf{7}, \mathbf{1}) \oplus (\mathbf{4}, \mathbf{2}) \oplus 2 \cdot (\mathbf{3}, \mathbf{1}) \oplus (\mathbf{1}, \mathbf{3})$
[0, 0, 2, 0, 0, 2, 0, 0]	$E_8(a_6)$	$\mathfrak{su}_2^{(120)} \oplus \emptyset$	224	$2 \cdot (\mathbf{19}, \mathbf{1}) \oplus (\mathbf{17}, \mathbf{1}) \oplus 3 \cdot \mathbf{15} \oplus 3 \cdot \mathbf{13} \oplus 3 \cdot \mathbf{11} \oplus 3 \cdot \mathbf{9}$ $\oplus 5 \cdot \mathbf{7} \oplus 5 \cdot \mathbf{3} \oplus \mathbf{3}$
[2, 1, 0, 1, 1, 0, 1, 1]	D_7	$\mathfrak{su}_2^{(182)} \oplus \mathfrak{su}_2^{(2)}$	226	$(\mathbf{23}, \mathbf{1}) \oplus (\mathbf{22}, \mathbf{2}) \oplus (\mathbf{19}, \mathbf{1}) \oplus (\mathbf{16}, \mathbf{2}) \oplus (\mathbf{15}, \mathbf{1}) \oplus (\mathbf{13}, \mathbf{3})$ $\oplus (\mathbf{12}, \mathbf{2}) \oplus (\mathbf{11}, \mathbf{1}) \oplus (\mathbf{10}, \mathbf{2}) \oplus (\mathbf{7}, \mathbf{1}) \oplus (\mathbf{4}, \mathbf{2}) \oplus (\mathbf{3}, \mathbf{1}) \oplus (\mathbf{1}, \mathbf{3})$
[0, 0, 2, 0, 0, 2, 2, 0]	$E_8(b_5)$	$\mathfrak{su}_2^{(160)} \oplus \emptyset$	226	$\mathbf{23} \oplus 2 \cdot \mathbf{19} \oplus 3 \cdot \mathbf{17} \oplus 3 \cdot \mathbf{15} \oplus 3 \cdot \mathbf{11} \oplus 3 \cdot \mathbf{9} \oplus 2 \cdot \mathbf{7} \oplus \mathbf{5} \oplus 4 \cdot \mathbf{3}$
[2, 1, 0, 1, 0, 2, 2, 1]	$E_7(a_1)$	$\mathfrak{su}_2^{(231)} \oplus \mathfrak{su}_2^{(1)}$	228	$(\mathbf{27}, \mathbf{1}) \oplus (\mathbf{23}, \mathbf{1}) \oplus (\mathbf{22}, \mathbf{2}) \oplus (\mathbf{19}, \mathbf{1}) \oplus (\mathbf{17}, \mathbf{1}) \oplus (\mathbf{16}, \mathbf{2}) \oplus (\mathbf{15}, \mathbf{1})$ $\oplus (\mathbf{12}, \mathbf{2}) \oplus 2 \cdot (\mathbf{11}, \mathbf{1}) \oplus (\mathbf{7}, \mathbf{1}) \oplus (\mathbf{6}, \mathbf{2}) \oplus (\mathbf{3}, \mathbf{1}) \oplus (\mathbf{1}, \mathbf{3})$
[2, 0, 2, 0, 0, 2, 0, 0]	$E_8(a_5)$	$\mathfrak{su}_2^{(184)} \oplus \emptyset$	228	$2 \cdot \mathbf{23} \oplus \mathbf{21} \oplus \mathbf{19} \oplus \mathbf{17} \oplus 3 \cdot \mathbf{15} \oplus 2 \cdot \mathbf{13} \oplus 4 \cdot \mathbf{11} \oplus \mathbf{9} \oplus \mathbf{7} \oplus 5 \oplus 3 \cdot \mathbf{3}$
[2, 0, 2, 0, 0, 2, 2, 0]	$E_8(b_4)$	$\mathfrak{su}_2^{(232)} \oplus \emptyset$	230	$\mathbf{27} \oplus 2 \cdot \mathbf{23} \oplus \mathbf{21} \oplus \mathbf{19} \oplus 2 \cdot \mathbf{17} \oplus 2 \cdot \mathbf{15} \oplus \mathbf{13} \oplus 3 \cdot \mathbf{11} \oplus 2 \cdot \mathbf{7} \oplus 5 \oplus 2 \cdot \mathbf{3}$
[2, 1, 0, 1, 2, 2, 2, 1]	E_7	$\mathfrak{su}_2^{(399)} \oplus \mathfrak{su}_2^{(1)}$	232	$(\mathbf{35}, \mathbf{1}) \oplus (\mathbf{28}, \mathbf{2}) \oplus (\mathbf{27}, \mathbf{1}) \oplus (\mathbf{23}, \mathbf{1}) \oplus (\mathbf{19}, \mathbf{1}) \oplus (\mathbf{18}, \mathbf{2}) \oplus (\mathbf{15}, \mathbf{1}) \oplus (\mathbf{11}, \mathbf{1}) \oplus (\mathbf{10}, \mathbf{2}) \oplus (\mathbf{3}, \mathbf{1}) \oplus (\mathbf{1}, \mathbf{3})$
[2, 0, 2, 0, 2, 0, 2, 0]	$E_8(a_4)$	$\mathfrak{su}_2^{(280)} \oplus \emptyset$	232	$\mathbf{29} \oplus \mathbf{27} \oplus 2 \cdot \mathbf{23} \oplus 2 \cdot \mathbf{19} \oplus \mathbf{17} \oplus 3 \cdot \mathbf{15} \oplus 2 \cdot \mathbf{11} \oplus \mathbf{9} \oplus \mathbf{7} \oplus 5 \oplus \mathbf{3}$
[2, 0, 2, 0, 2, 2, 2, 0]	$E_8(a_3)$	$\mathfrak{su}_2^{(400)} \oplus \emptyset$	234	$\mathbf{35} \oplus \mathbf{29} \oplus 2 \cdot \mathbf{27} \oplus \mathbf{23} \oplus 2 \cdot \mathbf{19} \oplus \mathbf{17} \oplus \mathbf{15} \oplus 2 \cdot \mathbf{11} \oplus \mathbf{9} \oplus 2 \cdot \mathbf{3}$
[2, 2, 0, 2, 0, 2, 2, 2]	$E_8(a_2)$	$\mathfrak{su}_2^{(520)} \oplus \emptyset$	236	$\mathbf{39} \oplus \mathbf{35} \oplus \mathbf{29} \oplus \mathbf{27} \oplus 2 \cdot \mathbf{23} \oplus \mathbf{19} \oplus \mathbf{17} \oplus \mathbf{15} \oplus \mathbf{11} \oplus \mathbf{7} \oplus \mathbf{3}$
[2, 2, 0, 2, 2, 2, 2, 2]	$E_8(a_1)$	$\mathfrak{su}_2^{(760)} \oplus \emptyset$	238	$\mathbf{47} \oplus \mathbf{39} \oplus \mathbf{35} \oplus \mathbf{29} \oplus \mathbf{27} \oplus \mathbf{23} \oplus \mathbf{19} \oplus \mathbf{15} \oplus \mathbf{11} \oplus \mathbf{3}$
[2, 2, 2, 2, 2, 2, 2, 2]	E_8	$\mathfrak{su}_2^{(1240)} \oplus \emptyset$	240	$\mathbf{59} \oplus \mathbf{47} \oplus \mathbf{39} \oplus \mathbf{35} \oplus \mathbf{27} \oplus \mathbf{23} \oplus \mathbf{15} \oplus \mathbf{3}$

APPENDIX C: HASSE DIAGRAMS

For completeness, in this appendix we collate the Hasse diagrams of the nilpotent orbits associated with the Lie algebras appearing in long quivers of exceptional types in Figs. 2–6. For each orbit, we give the weighted Dynkin diagram and the Jacobson-Morozov decomposition $\mathfrak{g} \rightarrow \mathfrak{su}(2)_X \oplus \mathfrak{f}$. The superscripts indicate the Dynkin embedding index of each factor. For the reader’s convenience, individual versions of all the Hasse diagrams can be found as ancillary files in the arXiv version of this work.

For completeness, we have also included the name of the transverse Slodowy slices between nilpotent orbits, following the notation introduced by Kraft and Procesi [72],

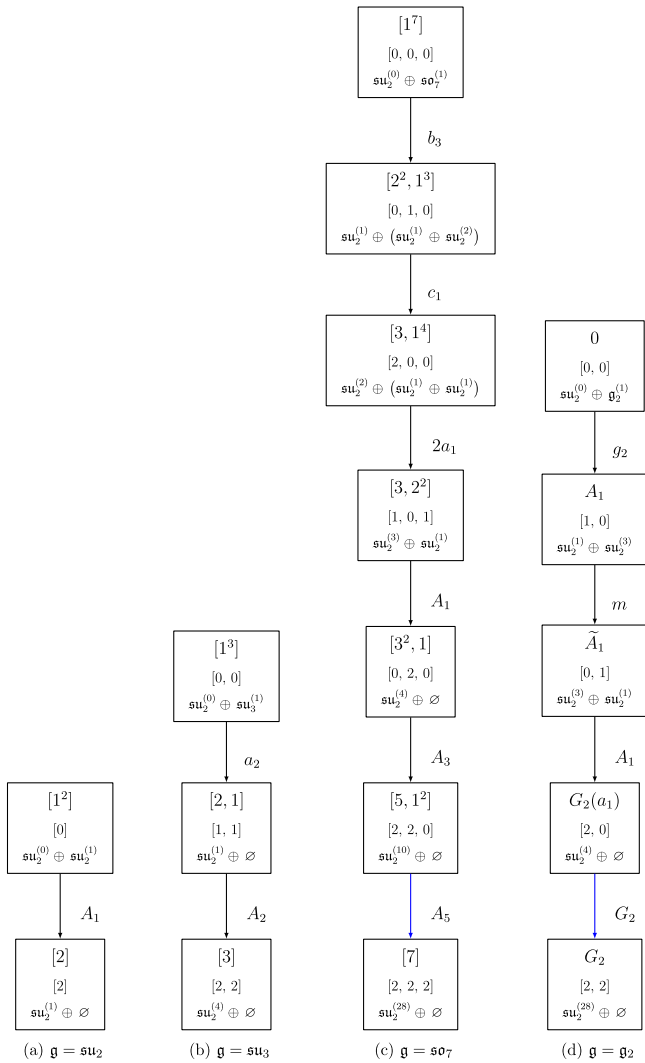


FIG. 2. Hasse diagram for the nilpotent orbit of various low-rank algebras. Each orbit is labeled by its partition or Bala-Carter label for classical or exceptional algebras, respectively.

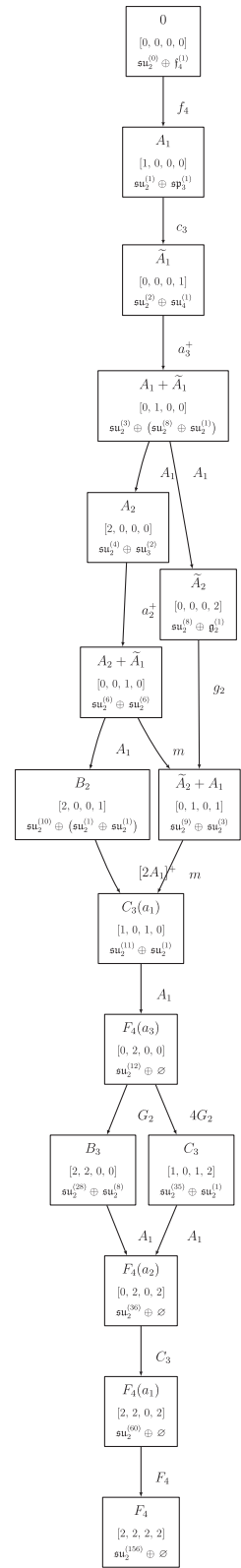


FIG. 3. Hasse diagram for the nilpotent orbits of \mathfrak{f}_4 . Each orbit is labeled by its Bala-Carter label.

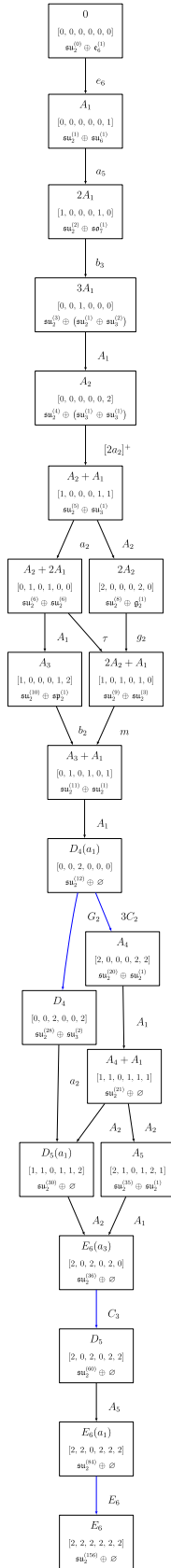


FIG. 4. Hasse diagram for the nilpotent orbits of e_6 . Each orbit is labeled by its Bala-Carter label.

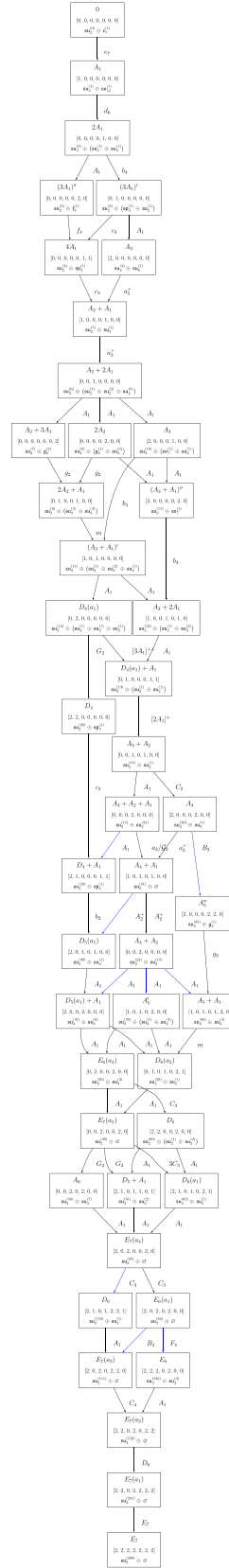


FIG. 5. Hasse diagram for the nilpotent orbits of e_7 . Each orbit is labeled by its Bala-Carter label.

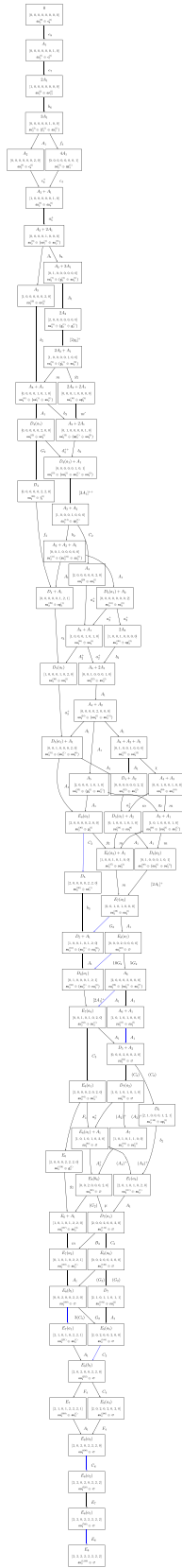


FIG. 6. Hasse diagram for the nilpotent orbits of e_8 . Each orbit is labeled by its Bala-Carter label.

see also [73] for exceptional cases. Transitions colored in blue indicate that in the associated quiver, another minimal conformal matter is affected, and the transition is not allowed if the quiver is too short.

APPENDIX D: FROM A NILPOTENT ORBIT TO A TENSOR BRANCH

While our main result is that the anomaly polynomial of long quivers rely only on a few parameters that do not depend on the details of the geometric engineering, the tensor branch effective field theory of a 6D (1, 0) SCFT associated to a particular noncompact elliptically fibered Calabi-Yau threefold is a pivotal component underlying our analysis. As was noted already in [15] (see also [22]), the tensor branch configurations appear to organize themselves into families associated to nilpotent orbits of simple Lie algebras. In this appendix, we provide a comprehensive mapping between the nilpotent orbits and the tensor branch descriptions that they are purported to be associated to.

In the main body of this paper, we show that the difference in the anomaly polynomials for the theories with the tensor branch configurations associated to the maximal nilpotent orbit and any other nilpotent orbit is precisely what we would expect from a bottom-up Higgsing by giving a vacuum expectation value valued in the nilpotent orbit to the moment map of the flavor symmetry associated to the maximal nilpotent orbit.

It is important to note that the correspondence described in the previous literature does not directly relate a nilpotent orbit to a tensor branch. First, one needs to pick a parent theory of the family with a \mathfrak{g} flavor symmetry factor, and then, for certain choices of parent theory, one notices that there is a family of descendant theories that are in one-to-one correspondence with the nilpotent orbits of \mathfrak{g} .²⁹ The parent theories for such families were enumerated in [22], and in this appendix we give the correspondence between nilpotent orbits and descendant tensor branch configurations for each family.

1. A-series

We start by considering parent SCFTs with an $\mathfrak{su}(K)$ flavor algebra and a tensor branch configuration that takes the form

$$\frac{\mathfrak{su}_K}{2} \cdots \frac{\mathfrak{su}_K}{2} \cdots, \tag{D1}$$

where the \cdots on the right indicates any attached collection of curves and algebras. To satisfy the long quiver condition, which we assume throughout this paper, it is sufficient to take the number of $\frac{\mathfrak{su}_K}{2}$ on the left to be at least $K + 1$. Let O

²⁹In fact, one defines the notion of a parent theory in this way.

be a nilpotent orbit of $\mathfrak{su}(K)$; O can be written uniquely as an integer partition of K

$$[1^{m_1}, 2^{m_2}, \dots, K^{m_K}], \quad \text{such that } \sum_{i=1}^K i m_i = K. \quad (\text{D2})$$

Then, the tensor branch effective field theory associated to the nilpotent orbit O can be described as [47]

$$\begin{array}{ccccccc} \mathfrak{su}_{k_1} & \mathfrak{su}_{k_2} & \mathfrak{su}_{k_3} & \dots & \mathfrak{su}_{k_K} & \mathfrak{su}_K & \dots \\ 2 & 2 & 2 & \dots & 2 & 2 & \dots \end{array} \quad (\text{D3})$$

The rightmost-written $\mathfrak{su}(K)$ gauge algebra is always present when we consider long quivers. The k_i are fixed in terms of the exponents of the partition by the anomaly cancellation conditions

$$2k_i - k_{i-1} - k_{i+1} = m_i, \quad (\text{D4})$$

where, for convenience, we have defined $k_0 = 0$ and $k_{K+1} = K$. This system of equations can be solved to yield an exact expression for k_i . Taking into account that the coefficients m_i define a partition of K , it is straightforward to show that

$$k_i = K - \sum_{j=1}^{K-i} j m_{i+j}. \quad (\text{D5})$$

Thus, we have determined the putative tensor branch description of the 6D (1, 0) SCFT associated to the parent SCFT in Eq. (D1) and the nilpotent orbit in Eq. (D2).

2. C-series

Next, we consider the tensor branch descriptions associated to parent theories which take the form

$$\begin{array}{ccccccc} \mathfrak{so}_{2K+8} & \mathfrak{sp}_K & \mathfrak{so}_{2K+8} & \dots & \mathfrak{sp}_K & \mathfrak{so}_{2K+8} & \dots \\ 4 & 1 & 4 & \dots & 1 & 4 & \dots \end{array}, \quad (\text{D6})$$

and a choice of nilpotent orbit of $\mathfrak{sp}(K)$. The \dots on the right in Eq. (D6) represents any combinations of curves and algebras that can be consistently attached. In this case, the long quiver condition is satisfied if we have at least $K + 1$ copies of \mathfrak{so}_{2K+8} on the left in Eq. (D6). A nilpotent orbit of $\mathfrak{sp}(K)$ is given by a C-partition of $2K$, as described around Eq. (B7).

It was proposed that the descendant of the parent theory in Eq. (D6) associated to the nilpotent orbit in Eq. (B7) has the tensor branch description

$$\begin{array}{ccccccc} \mathfrak{so}_{k_1} & \mathfrak{sp}_{k_2} & \mathfrak{so}_{k_3} & \dots & \mathfrak{sp}_{k_{2K}} & \mathfrak{so}_{2K+8} & \dots \\ 4 & 1 & 4 & \dots & 1 & 4 & \dots \end{array} \quad (\text{D7})$$

The k_i are again fixed in terms of the C-partition via the anomaly cancellation conditions. We have

$$\begin{aligned} k_i - 8 - k_{i-1} - k_{i+1} &= \frac{m_i}{2} & \text{if } i \text{ odd,} \\ 4k_i + 16 - k_{i-1} - k_{i+1} &= m_i & \text{if } i \text{ even.} \end{aligned} \quad (\text{D8})$$

Note that the right-hand side (rhs) is always guaranteed to be an integer from the C-partition condition, and we have defined $k_0 = 0$ and $k_{2K+1} = 2K + 8$. Again, as for the A-series, we can solve for k_i and find a compact expression

$$\begin{aligned} k_i &= 2(K + 4) - \sum_{j=1}^{2K-i} j m_{i+j} & \text{if } i \text{ odd,} \\ k_i &= K - \sum_{j=1}^{2K-i} \frac{j}{2} m_{i+j} & \text{if } i \text{ even.} \end{aligned} \quad (\text{D9})$$

3. D-series

The next set of families of 6D (1, 0) SCFTs that we consider are those progenated from a parent theory of the form

$$\begin{array}{ccccccc} \mathfrak{sp}_{K-4} & \mathfrak{so}_{2K} & \mathfrak{sp}_{K-4} & \dots & \mathfrak{so}_{2K} & \mathfrak{sp}_{K-4} & \dots \\ 1 & 4 & 1 & \dots & 4 & 1 & \dots \end{array} \quad (\text{D10})$$

Such a parent theory has an $\mathfrak{so}(2K)$ flavor symmetry. Each nilpotent orbit O has an underlying D-partition, as in Eq. (B11).

As we have already discussed, the association of a nilpotent orbit to be D-partition is not unique. In this paper, we determine the anomaly polynomials of the relevant 6D SCFTs from both a top-down tensor branch perspective, and from a bottom-up nilpotent Higgsing perspective, where the latter depends only on the parent theory and the choice of nilpotent orbit. For parent theories with an $\mathfrak{so}(2K)$ flavor algebra, the anomaly polynomial is actually agnostic to the precise nilpotent orbit, and instead only depends on the underlying D-partition. The dependence of the tensor branch description on the choice of nilpotent orbit itself has been discussed in detail in [69], however, for our purposes, we only need to know the tensor branch as depending on the D-partition; while this would appear to give two distinct SCFTs with the same tensor branch, there are in fact choices of discrete θ -angles by which the tensor branch effective field theories differ. We do not write the θ -angles here and refer the reader to [69] for the full details.

Given a parent theory of the form in Eq. (D10) and a nilpotent orbit associated to a D-partition as in Eq. (B11), the descendant theory is proposed to have the tensor branch effective descriptions

$$\begin{array}{ccccccc} \mathfrak{sp}_{k_1} & \mathfrak{so}_{k_2} & \mathfrak{sp}_{k_3} & \dots & \mathfrak{so}_{k_{2K}} & \mathfrak{sp}_{K-4} & \dots \\ 1 & 4 & 1 & \dots & 4 & 1 & \dots \end{array} \quad (\text{D11})$$

As usual, the anomaly cancellation conditions fix the ranks of the various gauge algebras in terms of the multiplicities

specifying the D-partition. We must have

$$\begin{aligned} k_i - 8 - k_{i-1} - k_{i+1} &= \frac{m_i}{2} & \text{if } i \text{ even,} \\ 4k_i + 16 - k_{i-1} - k_{i+1} &= m_i & \text{if } i \text{ odd.} \end{aligned} \quad (\text{D12})$$

The D-partition condition now guarantees that m_i is an even integer for i even, and thus the rhs is always an integer. We have defined $k_0 = 0$ and $k_{2K+1} = K - 4$ for convenience. As for the C-series, a closed expression can be found

$$\begin{aligned} k_i &= 2K - \sum_{j=1}^{2K-i} j m_{i+j} & \text{if } i \text{ even,} \\ k_i &= (K - 4) - \sum_{j=1}^{2K-i} \frac{j}{2} m_{i+j} & \text{if } i \text{ odd.} \end{aligned} \quad (\text{D13})$$

Interestingly, the k_i that one obtains in this way are sometimes inconsistent with the allowed F-theory configurations. For example, one may obtain a $k_i = 7$ for i even, which would indicate that the tensor description is of the form $\cdots 4 \cdots$, which cannot be engineered from a non-compact elliptically fibered Calabi-Yau threefold in the F-theory construction of 6D (1, 0) SCFTs. In fact, when the ranks of the gauge algebras are “too small,” the prescription for the tensor branch geometry associated to the nilpotent orbit, which we gave in Eq. (D11) needs to be modified. The modification can be summarized in the following short list of replacement rules

$$\begin{aligned} \begin{array}{c} \mathfrak{sp}_{-3} \mathfrak{so}_3 \mathfrak{sp}_{-2} \mathfrak{so}_5 \mathfrak{sp}_{-1} \mathfrak{so}_7 \\ 1 \quad 4 \quad 1 \quad 4 \quad 1 \quad 4 \quad \cdots \end{array} &\longrightarrow \begin{array}{c} \mathfrak{su}_2 \mathfrak{g}_2 \\ 2 \quad 2 \quad 3 \quad \cdots \end{array}, \\ \begin{array}{c} \mathfrak{sp}_{-3} \mathfrak{so}_4 \mathfrak{sp}_{-1} \mathfrak{so}_7 \\ 1 \quad 4 \quad 1 \quad 4 \quad \cdots \end{array} &\longrightarrow \begin{array}{c} \mathfrak{su}_2 \mathfrak{g}_2 \\ 2 \quad 3 \quad \cdots \end{array}, \\ \begin{array}{c} \mathfrak{sp}_{-3} \mathfrak{so}_4 \mathfrak{sp}_{-1} \mathfrak{so}_8 \\ 1 \quad 4 \quad 1 \quad 4 \quad \cdots \end{array} &\longrightarrow \begin{array}{c} \mathfrak{su}_2 \mathfrak{so}_7 \\ 2 \quad 3 \quad \cdots \end{array}, \\ \begin{array}{c} \mathfrak{sp}_{-2} \mathfrak{so}_5 \mathfrak{sp}_{-1} \mathfrak{so}_7 \\ 1 \quad 4 \quad 1 \quad 4 \quad \cdots \end{array} &\longrightarrow \begin{array}{c} \mathfrak{su}_2 \mathfrak{so}_7 \\ 2 \quad 3 \quad \cdots \end{array}, \\ \begin{array}{c} \mathfrak{sp}_{-2} \mathfrak{so}_6 \\ 1 \quad 4 \quad \cdots \end{array} &\longrightarrow \begin{array}{c} \mathfrak{su}_3 \\ 3 \quad \cdots \end{array}, \\ \begin{array}{c} \mathfrak{sp}_{-2} \mathfrak{so}_7 \\ 1 \quad 4 \quad \cdots \end{array} &\longrightarrow \begin{array}{c} \mathfrak{g}_2 \\ 3 \quad \cdots \end{array}, \\ \begin{array}{c} \mathfrak{sp}_{-2} \mathfrak{so}_8 \\ 1 \quad 4 \quad \cdots \end{array} &\longrightarrow \begin{array}{c} \mathfrak{so}_7 \\ 3 \quad \cdots \end{array}, \\ \begin{array}{c} \mathfrak{sp}_{-1} \mathfrak{g} \\ 1 \quad 4 \quad \cdots \end{array} &\longrightarrow \begin{array}{c} \mathfrak{g} \\ 3 \quad \cdots \end{array}. \end{aligned} \quad (\text{D14})$$

In this way, we have specified a way of assigning to a parent theory of the form in Eq. (D10) and a choice of nilpotent orbit of $\mathfrak{so}(2K)$ as in Eq. (B11) a 6D (1, 0) tensor branch.

4. E-series

Finally, we turn to what we call the “E-series” of tensor branch descriptions. These will be long quivers whose spine contains a repeating pattern of exceptional conformal matter.

TABLE XIV. The tensor branch descriptions associated to nilpotent Higgsing of the \mathfrak{su}_3 flavor symmetry for a long quiver associated to e_6 conformal matter with fraction number $f = \frac{1}{2}$.

Nilpotent orbit	\mathfrak{f}	Tensor branch
$[1^3]$	\mathfrak{su}_3	e_6 $16 \cdots$
$[2, 1]$	\emptyset	e_6 $5 \cdots$
$[3]$	\emptyset	f_4 $5 \cdots$

Note that when the fractions $f \neq 1$, the tensor branch translations that we describe herein do *not* all involve a nilpotent orbit of an exceptional Lie algebra as $\mathfrak{g}_f \subseteq \mathfrak{g}$.

Due to the sporadic nature of this series, we present the dictionary between parent theory with flavor symmetry factor \mathfrak{g} plus each nilpotent orbit of \mathfrak{g} and the tensor branch description in the form of tables, which were first described explicitly in [20] when $f = 1$. These are Tables XIV and XV for e_6 , Tables XVI–XIX for e_7 , and Tables XX–XXV for e_8 . In each table, the nilpotent orbit labelled as either $[1^K]$ or 0 —and appearing on the first row—provides the form of the tensor branch description of the parent theory. Subsequent rows provide the tensor branch effective field theory corresponding to that parent theory plus each nilpotent of the given flavor algebra of the parent theory.

TABLE XV. The tensor branch descriptions associated to nilpotent Higgsing of the e_6 flavor symmetry for a long quiver associated to e_6 conformal matter with fraction number $f = 1$.

Nilpotent orbit	\mathfrak{f}	Tensor branch
0	e_6	$\mathfrak{su}_3 \ e_6 \ \mathfrak{su}_3 \ e_6 \ \mathfrak{su}_3 \ e_6 \ \mathfrak{su}_3 \ e_6$ $1 \ 3 \ 161 \ 3 \ 161 \ 3 \ 161 \ 3 \ 16 \cdots$
A_1	\mathfrak{su}_6	$\mathfrak{su}_3 \ e_6 \ \mathfrak{su}_3 \ e_6 \ \mathfrak{su}_3 \ e_6 \ \mathfrak{su}_3 \ e_6$ $2 \ 161 \ 3 \ 161 \ 3 \ 161 \ 3 \ 16 \cdots$
$2A_1$	\mathfrak{so}_7	$\mathfrak{su}_2 \ e_6 \ \mathfrak{su}_3 \ e_6 \ \mathfrak{su}_3 \ e_6 \ \mathfrak{su}_3 \ e_6$ $2 \ 161 \ 3 \ 161 \ 3 \ 161 \ 3 \ 16 \cdots$
$3A_1$	$\mathfrak{su}_2 \oplus \mathfrak{su}_3$	$e_6 \ \mathfrak{su}_3 \ e_6 \ \mathfrak{su}_3 \ e_6 \ \mathfrak{su}_3 \ e_6$ $2161 \ 3 \ 161 \ 3 \ 161 \ 3 \ 16 \cdots$
A_2	$\mathfrak{su}_3 \oplus \mathfrak{su}_3$	1 $e_6 \ \mathfrak{su}_3 \ e_6 \ \mathfrak{su}_3 \ e_6 \ \mathfrak{su}_3 \ e_6$ $161 \ 3 \ 161 \ 3 \ 161 \ 3 \ 16 \cdots$
$A_2 + A_1$	\mathfrak{su}_3	$e_6 \ \mathfrak{su}_3 \ e_6 \ \mathfrak{su}_3 \ e_6 \ \mathfrak{su}_3 \ e_6$ $151 \ 3 \ 161 \ 3 \ 161 \ 3 \ 16 \cdots$
$2A_2$	\mathfrak{g}_2	$f_4 \ \mathfrak{su}_3 \ e_6 \ \mathfrak{su}_3 \ e_6 \ \mathfrak{su}_3 \ e_6$ $151 \ 3 \ 161 \ 3 \ 161 \ 3 \ 16 \cdots$
$A_2 + 2A_1$	\mathfrak{su}_2	$e_6 \ \mathfrak{su}_3 \ e_6 \ \mathfrak{su}_3 \ e_6 \ \mathfrak{su}_3 \ e_6$ $41 \ 3 \ 161 \ 3 \ 161 \ 3 \ 16 \cdots$
$2A_2 + A_1$	\mathfrak{su}_2	$f_4 \ \mathfrak{su}_3 \ e_6 \ \mathfrak{su}_3 \ e_6 \ \mathfrak{su}_3 \ e_6$ $41 \ 3 \ 161 \ 3 \ 161 \ 3 \ 16 \cdots$
A_3	\mathfrak{sp}_2	$\mathfrak{so}_{10} \ \mathfrak{su}_3 \ e_6 \ \mathfrak{su}_3 \ e_6 \ \mathfrak{su}_3 \ e_6$ $4 \ 1 \ 3 \ 161 \ 3 \ 161 \ 3 \ 16 \cdots$
$A_3 + A_1$	\mathfrak{su}_2	$\mathfrak{so}_9 \ \mathfrak{su}_3 \ e_6 \ \mathfrak{su}_3 \ e_6 \ \mathfrak{su}_3 \ e_6$ $4 \ 1 \ 3 \ 161 \ 3 \ 161 \ 3 \ 16 \cdots$
$D_4(a_1)$	\emptyset	$\mathfrak{so}_8 \ \mathfrak{su}_3 \ e_6 \ \mathfrak{su}_3 \ e_6 \ \mathfrak{su}_3 \ e_6$ $4 \ 1 \ 3 \ 161 \ 3 \ 161 \ 3 \ 16 \cdots$
A_4	\mathfrak{su}_2	$\mathfrak{so}_7 \ \mathfrak{su}_2 \ e_6 \ \mathfrak{su}_3 \ e_6 \ \mathfrak{su}_3 \ e_6$ $3 \ 2 \ 161 \ 3 \ 161 \ 3 \ 16 \cdots$
$A_4 + A_1$	\emptyset	$\mathfrak{g}_2 \ \mathfrak{su}_2 \ e_6 \ \mathfrak{su}_3 \ e_6 \ \mathfrak{su}_3 \ e_6$ $3 \ 2 \ 161 \ 3 \ 161 \ 3 \ 16 \cdots$

(Table continued)

TABLE XX. The tensor branch descriptions associated to nilpotent Higgsing of the \mathfrak{su}_2 flavor symmetry for a long quiver associated to e_8 conformal matter with fraction number $f = \frac{1}{4}$.

Nilpotent orbit	\mathfrak{f}	Tensor branch
$[1^2]$	\mathfrak{su}_2	$21(12) \dots$
$[2]$	\emptyset	$1(12) \dots$

TABLE XXI. The tensor branch descriptions associated to nilpotent Higgsing of the \mathfrak{g}_2 flavor symmetry for a long quiver associated to e_8 conformal matter with fraction number $f = \frac{1}{3}$.

Nilpotent orbit	\mathfrak{f}	Tensor branch
0	\mathfrak{g}_2	$2 \overset{e_8}{21(12)} 12 \overset{e_8}{2} \overset{e_8}{3} \overset{e_8}{1513} \overset{e_8}{2} \overset{e_8}{21(12)} \dots$
A_1	\mathfrak{su}_2	$221(12) \overset{e_8}{12} \overset{e_8}{2} \overset{e_8}{3} \overset{e_8}{1513} \overset{e_8}{2} \overset{e_8}{21(12)} \dots$
\tilde{A}_1	\mathfrak{su}_2	$21(12) \overset{1}{e_8} 12 \overset{e_8}{2} \overset{e_8}{3} \overset{e_8}{1513} \overset{e_8}{2} \overset{e_8}{21(12)} \dots$
$G_2(a_1)$	\emptyset	$1(12) \overset{1}{e_8} 12 \overset{e_8}{2} \overset{e_8}{3} \overset{e_8}{1513} \overset{e_8}{2} \overset{e_8}{21(12)} \dots$
G_2	\emptyset	$81 \overset{e_7}{2} \overset{e_7}{3} \overset{e_7}{1513} \overset{e_7}{2} \overset{e_7}{21(12)} \dots$

TABLE XXII. The tensor branch descriptions associated to nilpotent Higgsing of the \mathfrak{f}_4 flavor symmetry for a long quiver associated to e_8 conformal matter with fraction number $f = \frac{1}{2}$.

Nilpotent orbit	\mathfrak{f}	Tensor branch
0	\mathfrak{f}_4	$13 \overset{e_8}{2} \overset{e_8}{21(12)} 12 \overset{e_8}{2} \overset{e_8}{3} \overset{e_8}{1513} \overset{e_8}{2} \overset{e_8}{21(12)} \dots$
A_1	\mathfrak{sp}_3	$2 \overset{e_8}{2} \overset{e_8}{21(12)} 12 \overset{e_8}{2} \overset{e_8}{3} \overset{e_8}{1513} \overset{e_8}{2} \overset{e_8}{21(12)} \dots$
\tilde{A}_1	\mathfrak{su}_4	$2 \overset{e_8}{2} \overset{e_8}{21(12)} 12 \overset{e_8}{2} \overset{e_8}{3} \overset{e_8}{1513} \overset{e_8}{2} \overset{e_8}{21(12)} \dots$
$A_1 + \tilde{A}_1$	$\mathfrak{su}_2 \oplus \mathfrak{su}_2$	$2 \overset{e_8}{2} \overset{e_8}{21(12)} 12 \overset{e_8}{2} \overset{e_8}{3} \overset{e_8}{1513} \overset{e_8}{2} \overset{e_8}{21(12)} \dots$
A_2	\mathfrak{su}_3	$2 \overset{e_8}{2} \overset{e_8}{21(12)} 12 \overset{e_8}{2} \overset{e_8}{3} \overset{e_8}{1513} \overset{e_8}{2} \overset{e_8}{21(12)} \dots$
\tilde{A}_2	\mathfrak{g}_2	$2 \overset{1}{e_8} 21(12) 12 \overset{e_8}{2} \overset{e_8}{3} \overset{e_8}{1513} \overset{e_8}{2} \overset{e_8}{21(12)} \dots$
$A_2 + \tilde{A}_1$	\mathfrak{su}_2	$2221(12) \overset{e_8}{12} \overset{e_8}{2} \overset{e_8}{3} \overset{e_8}{1513} \overset{e_8}{2} \overset{e_8}{21(12)} \dots$
B_2	$\mathfrak{su}_2 \oplus \mathfrak{su}_2$	$21(12) \overset{1}{e_8} 12 \overset{e_8}{2} \overset{e_8}{3} \overset{e_8}{1513} \overset{e_8}{2} \overset{e_8}{21(12)} \dots$
$\tilde{A}_2 + A_1$	\mathfrak{su}_2	$221(12) \overset{1}{e_8} 12 \overset{e_8}{2} \overset{e_8}{3} \overset{e_8}{1513} \overset{e_8}{2} \overset{e_8}{21(12)} \dots$
$C_3(a_1)$	\mathfrak{su}_2	$21(12) \overset{1}{e_8} 12 \overset{e_8}{2} \overset{e_8}{3} \overset{e_8}{1513} \overset{e_8}{2} \overset{e_8}{21(12)} \dots$
$F_4(a_3)$	\emptyset	$1 \overset{1}{e_8} 12 \overset{e_8}{2} \overset{e_8}{3} \overset{e_8}{1513} \overset{e_8}{2} \overset{e_8}{21(12)} \dots$
B_3	\mathfrak{su}_2	$81 \overset{e_7}{2} \overset{e_7}{3} \overset{e_7}{1513} \overset{e_7}{2} \overset{e_7}{21(12)} \dots$
C_3	\mathfrak{su}_2	$181 \overset{e_7}{2} \overset{e_7}{3} \overset{e_7}{1513} \overset{e_7}{2} \overset{e_7}{21(12)} \dots$
$F_4(a_2)$	\emptyset	$71 \overset{e_7}{2} \overset{e_7}{3} \overset{e_7}{1513} \overset{e_7}{2} \overset{e_7}{21(12)} \dots$
$F_4(a_1)$	\emptyset	$61 \overset{e_6}{3} \overset{e_6}{1513} \overset{e_6}{2} \overset{e_6}{21(12)} \dots$
F_4	\emptyset	$51 \overset{1}{e_8} 3 \overset{1}{e_8} 21(12) \dots$

TABLE XXV. (Continued)

Table with columns: Nilpotent orbit, f, Tensor branch. Rows include 2A3, D5(a1), A4+2A1, A4+A2, D5(a1)+A1, A4+A2+A1, A5, A4+A3, D4+A2, E6(a3), A5+A1, D5(a1)+A2, E6(a3)+A1, D6(a2), D5, E7(a5), D5+A1, E8(a7), D6(a1), A6, E7(a4), A6+A1, E6(a1), D5+A2, D7(a2), E6, A7, E6(a1)+A1, E8(b6), D6.

(Table continued)

TABLE XXV. (Continued)

Nilpotent orbit	\mathfrak{f}	Tensor branch
$E_7(a_3)$	\mathfrak{su}_2	$\mathfrak{so}_{10} \mathfrak{su}_2 \mathfrak{so}_9 \mathfrak{q}_2 \mathfrak{su}_2 \quad \mathfrak{e}_8 \quad \mathfrak{su}_2 \mathfrak{q}_2 \quad \mathfrak{f}_4 \mathfrak{q}_2 \mathfrak{su}_2 \quad \mathfrak{e}_8 \quad \mathfrak{su}_2 \mathfrak{q}_2 \quad \mathfrak{f}_4 \mathfrak{q}_2 \mathfrak{su}_2 \quad \mathfrak{e}_8 \quad \mathfrak{su}_2 \mathfrak{q}_2 \quad \mathfrak{f}_4 \mathfrak{q}_2 \mathfrak{su}_2 \quad \mathfrak{e}_8 \dots$ $4 \quad 1 \quad 4 \quad 13 \quad 2 \quad 21(12)12 \quad 2 \quad 3 \quad 1513 \quad 2 \quad 21(12)12 \quad 2 \quad 3 \quad 1513 \quad 2 \quad 21(12)12 \quad 2 \quad 3 \quad 1513 \quad 2 \quad 21(12)12 \quad 2 \quad 3 \quad 1513 \quad 2 \quad 21(12) \dots$
$D_7(a_1)$	\emptyset	$\mathfrak{so}_9 \mathfrak{su}_2 \mathfrak{so}_9 \mathfrak{q}_2 \mathfrak{su}_2 \quad \mathfrak{e}_8 \quad \mathfrak{su}_2 \mathfrak{q}_2 \quad \mathfrak{f}_4 \mathfrak{q}_2 \mathfrak{su}_2 \quad \mathfrak{e}_8 \quad \mathfrak{su}_2 \mathfrak{q}_2 \quad \mathfrak{f}_4 \mathfrak{q}_2 \mathfrak{su}_2 \quad \mathfrak{e}_8 \quad \mathfrak{su}_2 \mathfrak{q}_2 \quad \mathfrak{f}_4 \mathfrak{q}_2 \mathfrak{su}_2 \quad \mathfrak{e}_8 \dots$ $4 \quad 1 \quad 4 \quad 13 \quad 2 \quad 21(12)12 \quad 2 \quad 3 \quad 1513 \quad 2 \quad 21(12)12 \quad 2 \quad 3 \quad 1513 \quad 2 \quad 21(12)12 \quad 2 \quad 3 \quad 1513 \quad 2 \quad 21(12)12 \quad 2 \quad 3 \quad 1513 \quad 2 \quad 21(12) \dots$
$E_6 + A_1$	\mathfrak{su}_2	$\mathfrak{f}_4 \mathfrak{q}_2 \mathfrak{su}_2 \quad \mathfrak{e}_8 \quad \mathfrak{su}_2 \mathfrak{q}_2 \quad \mathfrak{f}_4 \mathfrak{q}_2 \mathfrak{su}_2 \quad \mathfrak{e}_8 \quad \mathfrak{su}_2 \mathfrak{q}_2 \quad \mathfrak{f}_4 \mathfrak{q}_2 \mathfrak{su}_2 \quad \mathfrak{e}_8 \quad \mathfrak{su}_2 \mathfrak{q}_2 \quad \mathfrak{f}_4 \mathfrak{q}_2 \mathfrak{su}_2 \quad \mathfrak{e}_8 \dots$ $413 \quad 2 \quad 21 \quad 1 \quad 12 \quad 2 \quad 3 \quad 1513 \quad 2 \quad 21(12)12 \quad 2 \quad 3 \quad 1513 \quad 2 \quad 21(12)12 \quad 2 \quad 3 \quad 1513 \quad 2 \quad 21(12) \dots$
$E_7(a_2)$	\mathfrak{su}_2	$\mathfrak{so}_9 \mathfrak{q}_2 \mathfrak{su}_2 \quad \mathfrak{e}_8 \quad \mathfrak{su}_2 \mathfrak{q}_2 \quad \mathfrak{f}_4 \mathfrak{q}_2 \mathfrak{su}_2 \quad \mathfrak{e}_8 \quad \mathfrak{su}_2 \mathfrak{q}_2 \quad \mathfrak{f}_4 \mathfrak{q}_2 \mathfrak{su}_2 \quad \mathfrak{e}_8 \quad \mathfrak{su}_2 \mathfrak{q}_2 \quad \mathfrak{f}_4 \mathfrak{q}_2 \mathfrak{su}_2 \quad \mathfrak{e}_8 \dots$ $4 \quad 13 \quad 2 \quad 21 \quad 1 \quad 12 \quad 2 \quad 3 \quad 1513 \quad 2 \quad 21(12)12 \quad 2 \quad 3 \quad 1513 \quad 2 \quad 21(12)12 \quad 2 \quad 3 \quad 1513 \quad 2 \quad 21(12) \dots$
$E_8(a_6)$	\emptyset	$\mathfrak{so}_8 \mathfrak{so}_8 \mathfrak{q}_2 \mathfrak{su}_2 \quad \mathfrak{e}_8 \quad \mathfrak{su}_2 \mathfrak{q}_2 \quad \mathfrak{f}_4 \mathfrak{q}_2 \mathfrak{su}_2 \quad \mathfrak{e}_8 \quad \mathfrak{su}_2 \mathfrak{q}_2 \quad \mathfrak{f}_4 \mathfrak{q}_2 \mathfrak{su}_2 \quad \mathfrak{e}_8 \quad \mathfrak{su}_2 \mathfrak{q}_2 \quad \mathfrak{f}_4 \mathfrak{q}_2 \mathfrak{su}_2 \quad \mathfrak{e}_8 \dots$ $4 \quad 1 \quad 4 \quad 13 \quad 2 \quad 21(12)12 \quad 2 \quad 3 \quad 1513 \quad 2 \quad 21(12)12 \quad 2 \quad 3 \quad 1513 \quad 2 \quad 21(12)12 \quad 2 \quad 3 \quad 1513 \quad 2 \quad 21(12) \dots$
D_7	\mathfrak{su}_2	$\frac{2}{1}$ $\mathfrak{q}_2 \mathfrak{su}_2 \quad \mathfrak{e}_8 \quad \mathfrak{su}_2 \mathfrak{q}_2 \quad \mathfrak{f}_4 \mathfrak{q}_2 \mathfrak{su}_2 \quad \mathfrak{e}_8 \quad \mathfrak{su}_2 \mathfrak{q}_2 \quad \mathfrak{f}_4 \mathfrak{q}_2 \mathfrak{su}_2 \quad \mathfrak{e}_8 \quad \mathfrak{su}_2 \mathfrak{q}_2 \quad \mathfrak{f}_4 \mathfrak{q}_2 \mathfrak{su}_2 \quad \mathfrak{e}_8 \dots$ $3 \quad 2 \quad 21(12)12 \quad 2 \quad 3 \quad 1513 \quad 2 \quad 21(12)12 \quad 2 \quad 3 \quad 1513 \quad 2 \quad 21(12)12 \quad 2 \quad 3 \quad 1513 \quad 2 \quad 21(12)12 \quad 2 \quad 3 \quad 1513 \quad 2 \quad 21(12) \dots$
$E_8(b_5)$	\emptyset	$\frac{1}{1}$ $\mathfrak{so}_8 \mathfrak{q}_2 \mathfrak{su}_2 \quad \mathfrak{e}_8 \quad \mathfrak{su}_2 \mathfrak{q}_2 \quad \mathfrak{f}_4 \mathfrak{q}_2 \mathfrak{su}_2 \quad \mathfrak{e}_8 \quad \mathfrak{su}_2 \mathfrak{q}_2 \quad \mathfrak{f}_4 \mathfrak{q}_2 \mathfrak{su}_2 \quad \mathfrak{e}_8 \quad \mathfrak{su}_2 \mathfrak{q}_2 \quad \mathfrak{f}_4 \mathfrak{q}_2 \mathfrak{su}_2 \quad \mathfrak{e}_8 \dots$ $4 \quad 13 \quad 2 \quad 21(12)12 \quad 2 \quad 3 \quad 1513 \quad 2 \quad 21(12)12 \quad 2 \quad 3 \quad 1513 \quad 2 \quad 21(12)12 \quad 2 \quad 3 \quad 1513 \quad 2 \quad 21(12)12 \quad 2 \quad 3 \quad 1513 \quad 2 \quad 21(12) \dots$
$E_7(a_1)$	\mathfrak{su}_2	$\mathfrak{so}_7 \mathfrak{su}_2 \quad \mathfrak{e}_7 \quad \mathfrak{su}_2 \mathfrak{q}_2 \quad \mathfrak{f}_4 \mathfrak{q}_2 \mathfrak{su}_2 \quad \mathfrak{e}_8 \quad \mathfrak{su}_2 \mathfrak{q}_2 \quad \mathfrak{f}_4 \mathfrak{q}_2 \mathfrak{su}_2 \quad \mathfrak{e}_8 \quad \mathfrak{su}_2 \mathfrak{q}_2 \quad \mathfrak{f}_4 \mathfrak{q}_2 \mathfrak{su}_2 \quad \mathfrak{e}_8 \dots$ $3 \quad 2 \quad 181 \quad 2 \quad 3 \quad 1513 \quad 2 \quad 21(12)12 \quad 2 \quad 3 \quad 1513 \quad 2 \quad 21(12)12 \quad 2 \quad 3 \quad 1513 \quad 2 \quad 21(12) \dots$
$E_8(a_5)$	\emptyset	$\frac{1}{1}$ $\mathfrak{q}_2 \mathfrak{su}_2 \quad \mathfrak{e}_8 \quad \mathfrak{su}_2 \mathfrak{q}_2 \quad \mathfrak{f}_4 \mathfrak{q}_2 \mathfrak{su}_2 \quad \mathfrak{e}_8 \quad \mathfrak{su}_2 \mathfrak{q}_2 \quad \mathfrak{f}_4 \mathfrak{q}_2 \mathfrak{su}_2 \quad \mathfrak{e}_8 \quad \mathfrak{su}_2 \mathfrak{q}_2 \quad \mathfrak{f}_4 \mathfrak{q}_2 \mathfrak{su}_2 \quad \mathfrak{e}_8 \dots$ $3 \quad 2 \quad 21(12)12 \quad 2 \quad 3 \quad 1513 \quad 2 \quad 21(12)12 \quad 2 \quad 3 \quad 1513 \quad 2 \quad 21(12)12 \quad 2 \quad 3 \quad 1513 \quad 2 \quad 21(12) \dots$
$E_8(b_4)$	\emptyset	$\frac{1}{1}$ $\mathfrak{q}_2 \mathfrak{su}_2 \quad \mathfrak{e}_7 \quad \mathfrak{su}_2 \mathfrak{q}_2 \quad \mathfrak{f}_4 \mathfrak{q}_2 \mathfrak{su}_2 \quad \mathfrak{e}_8 \quad \mathfrak{su}_2 \mathfrak{q}_2 \quad \mathfrak{f}_4 \mathfrak{q}_2 \mathfrak{su}_2 \quad \mathfrak{e}_8 \quad \mathfrak{su}_2 \mathfrak{q}_2 \quad \mathfrak{f}_4 \mathfrak{q}_2 \mathfrak{su}_2 \quad \mathfrak{e}_8 \dots$ $3 \quad 2 \quad 181 \quad 2 \quad 3 \quad 1513 \quad 2 \quad 21(12)12 \quad 2 \quad 3 \quad 1513 \quad 2 \quad 21(12)12 \quad 2 \quad 3 \quad 1513 \quad 2 \quad 21(12)12 \quad 2 \quad 3 \quad 1513 \quad 2 \quad 21(12) \dots$
E_7	\mathfrak{su}_2	$\frac{1}{1}$ $\mathfrak{q}_2 \mathfrak{f}_4 \mathfrak{q}_2 \mathfrak{su}_2 \quad \mathfrak{e}_8 \quad \mathfrak{su}_2 \mathfrak{q}_2 \quad \mathfrak{f}_4 \mathfrak{q}_2 \mathfrak{su}_2 \quad \mathfrak{e}_8 \quad \mathfrak{su}_2 \mathfrak{q}_2 \quad \mathfrak{f}_4 \mathfrak{q}_2 \mathfrak{su}_2 \quad \mathfrak{e}_8 \quad \mathfrak{su}_2 \mathfrak{q}_2 \quad \mathfrak{f}_4 \mathfrak{q}_2 \mathfrak{su}_2 \quad \mathfrak{e}_8 \dots$ $3 \quad 1513 \quad 2 \quad 21(12)12 \quad 2 \quad 3 \quad 1513 \quad 2 \quad 21(12)12 \quad 2 \quad 3 \quad 1513 \quad 2 \quad 21(12) \dots$
$E_8(a_4)$	\emptyset	$\mathfrak{su}_3 \quad \mathfrak{e}_6 \quad \mathfrak{su}_3 \quad \mathfrak{f}_4 \mathfrak{q}_2 \mathfrak{su}_2 \quad \mathfrak{e}_8 \quad \mathfrak{su}_2 \mathfrak{q}_2 \quad \mathfrak{f}_4 \mathfrak{q}_2 \mathfrak{su}_2 \quad \mathfrak{e}_8 \quad \mathfrak{su}_2 \mathfrak{q}_2 \quad \mathfrak{f}_4 \mathfrak{q}_2 \mathfrak{su}_2 \quad \mathfrak{e}_8 \dots$ $3 \quad 161 \quad 3 \quad 1513 \quad 2 \quad 21(12)12 \quad 2 \quad 3 \quad 1513 \quad 2 \quad 21(12)12 \quad 2 \quad 3 \quad 1513 \quad 2 \quad 21(12) \dots$
$E_8(a_3)$	\emptyset	$\frac{1}{1}$ $\mathfrak{su}_3 \quad \mathfrak{f}_4 \mathfrak{q}_2 \mathfrak{su}_2 \quad \mathfrak{e}_8 \quad \mathfrak{su}_2 \mathfrak{q}_2 \quad \mathfrak{f}_4 \mathfrak{q}_2 \mathfrak{su}_2 \quad \mathfrak{e}_8 \quad \mathfrak{su}_2 \mathfrak{q}_2 \quad \mathfrak{f}_4 \mathfrak{q}_2 \mathfrak{su}_2 \quad \mathfrak{e}_8 \quad \mathfrak{su}_2 \mathfrak{q}_2 \quad \mathfrak{f}_4 \mathfrak{q}_2 \mathfrak{su}_2 \quad \mathfrak{e}_8 \dots$ $3 \quad 1513 \quad 2 \quad 21(12)12 \quad 2 \quad 3 \quad 1513 \quad 2 \quad 21(12)12 \quad 2 \quad 3 \quad 1513 \quad 2 \quad 21(12) \dots$
$E_8(a_2)$	\emptyset	$\mathfrak{su}_2 \mathfrak{so}_7 \mathfrak{su}_2 \quad \mathfrak{e}_7 \quad \mathfrak{su}_2 \mathfrak{q}_2 \quad \mathfrak{f}_4 \mathfrak{q}_2 \mathfrak{su}_2 \quad \mathfrak{e}_8 \quad \mathfrak{su}_2 \mathfrak{q}_2 \quad \mathfrak{f}_4 \mathfrak{q}_2 \mathfrak{su}_2 \quad \mathfrak{e}_8 \quad \mathfrak{su}_2 \mathfrak{q}_2 \quad \mathfrak{f}_4 \mathfrak{q}_2 \mathfrak{su}_2 \quad \mathfrak{e}_8 \dots$ $2 \quad 3 \quad 2 \quad 181 \quad 2 \quad 3 \quad 1513 \quad 2 \quad 21(12)12 \quad 2 \quad 3 \quad 1513 \quad 2 \quad 21(12) \dots$
$E_8(a_1)$	\emptyset	$\frac{1}{1}$ $\mathfrak{su}_2 \mathfrak{q}_2 \quad \mathfrak{f}_4 \mathfrak{q}_2 \mathfrak{su}_2 \quad \mathfrak{e}_8 \quad \mathfrak{su}_2 \mathfrak{q}_2 \quad \mathfrak{f}_4 \mathfrak{q}_2 \mathfrak{su}_2 \quad \mathfrak{e}_8 \quad \mathfrak{su}_2 \mathfrak{q}_2 \quad \mathfrak{f}_4 \mathfrak{q}_2 \mathfrak{su}_2 \quad \mathfrak{e}_8 \dots$ $2 \quad 3 \quad 1513 \quad 2 \quad 21(12)12 \quad 2 \quad 3 \quad 1513 \quad 2 \quad 21(12) \dots$
E_8	\emptyset	$\frac{1}{1}$ $\mathfrak{su}_2 \mathfrak{q}_2 \quad \mathfrak{f}_4 \mathfrak{q}_2 \mathfrak{su}_2 \quad \mathfrak{e}_8 \quad \mathfrak{su}_2 \mathfrak{q}_2 \quad \mathfrak{f}_4 \mathfrak{q}_2 \mathfrak{su}_2 \quad \mathfrak{e}_8 \quad \mathfrak{su}_2 \mathfrak{q}_2 \quad \mathfrak{f}_4 \mathfrak{q}_2 \mathfrak{su}_2 \quad \mathfrak{e}_8 \dots$ $2 \quad 2 \quad 3 \quad 1513 \quad 2 \quad 21(12) \dots$

[1] W. Nahm, Supersymmetries and their representations, *Nucl. Phys.* **B135**, 149 (1978).
 [2] C. Cordova, T. T. Dumitrescu, and K. Intriligator, Anomalies, renormalization group flows, and the a-theorem in six-dimensional (1, 0) theories, *J. High Energy Phys.* **10** (2016) 080.
 [3] J. Louis and S. Lüst, Supersymmetric AdS₇ backgrounds in half-maximal supergravity and marginal operators of (1, 0) SCFTs, *J. High Energy Phys.* **10** (2015) 120.
 [4] C. Cordova, T. T. Dumitrescu, and K. Intriligator, Deformations of superconformal theories, *J. High Energy Phys.* **11** (2016) 135.
 [5] C. Cordova, T. T. Dumitrescu, and K. Intriligator, Multiplets of superconformal symmetry in diverse dimensions, *J. High Energy Phys.* **03** (2019) 163.
 [6] M. Buican, J. Hayling, and C. Papageorgakis, Aspects of superconformal multiplets in $D > 4$, *J. High Energy Phys.* **11** (2016) 091.
 [7] E. Witten, Some comments on string dynamics, in *STRINGS 95: Future Perspectives in String Theory* (World Scientific, Singapore, 1995), pp. 501–523, [arXiv:hep-th/9507121](https://arxiv.org/abs/hep-th/9507121).
 [8] A. Strominger, Open p-branes, *Phys. Lett. B* **383**, 44 (1996).
 [9] N. Seiberg, Nontrivial fixed points of the renormalization group in six-dimensions, *Phys. Lett. B* **390**, 169 (1997).
 [10] P. C. Argyres, J. J. Heckman, K. Intriligator, and M. Martone, Snowmass white paper on SCFTs, [arXiv:2202.07683](https://arxiv.org/abs/2202.07683).
 [11] C. Vafa, Evidence for F theory, *Nucl. Phys.* **B469**, 403 (1996).
 [12] D. R. Morrison and C. Vafa, Compactifications of F theory on Calabi-Yau threefolds. 1, *Nucl. Phys.* **B473**, 74 (1996).
 [13] D. R. Morrison and C. Vafa, Compactifications of F theory on Calabi-Yau threefolds. 2, *Nucl. Phys.* **B476**, 437 (1996).

- [14] J.J. Heckman, D.R. Morrison, and C. Vafa, On the classification of 6D SCFTs and generalized ADE orbifolds, *J. High Energy Phys.* **05** (2014) 028; **06** (2015) 017(E).
- [15] J.J. Heckman, D.R. Morrison, T. Rudelius, and C. Vafa, Atomic classification of 6D SCFTs, *Fortschr. Phys.* **63**, 468 (2015).
- [16] N. Nakayama, On Weierstrass models, in *Algebraic Geometry and Commutative Algebra* (Kinokuniya, Tokyo, 1988), Vol. II, pp. 405–431, [10.1016/B978-0-12-348032-3.50004-9](https://doi.org/10.1016/B978-0-12-348032-3.50004-9).
- [17] J.J. Heckman and T. Rudelius, Top down approach to 6D SCFTs, *J. Phys. A* **52**, 093001 (2019).
- [18] C. Lawrie and L. Mansi, The Higgs branch of 6D (1, 0) SCFTs & LSTs with DE-type SUSY enhancement, [arXiv:2406.02670](https://arxiv.org/abs/2406.02670).
- [19] M. Del Zotto, J.J. Heckman, A. Tomasiello, and C. Vafa, 6d conformal matter, *J. High Energy Phys.* **02** (2015) 054.
- [20] J.J. Heckman, T. Rudelius, and A. Tomasiello, 6D RG flows and nilpotent hierarchies, *J. High Energy Phys.* **07** (2016) 082.
- [21] F. Hassler, J.J. Heckman, T.B. Rochais, T. Rudelius, and H. Y. Zhang, T-branes, string junctions, and 6D SCFTs, *Phys. Rev. D* **101**, 086018 (2020).
- [22] J.J. Heckman, T. Rudelius, and A. Tomasiello, Fission, fusion, and 6D RG flows, *J. High Energy Phys.* **02** (2019) 167.
- [23] F. Baume, J.J. Heckman, and C. Lawrie, 6D SCFTs, 4D SCFTs, conformal matter, and spin chains, *Nucl. Phys.* **B967**, 115401 (2021).
- [24] J.J. Heckman, Qubit construction in 6D SCFTs, *Phys. Lett. B* **811**, 135891 (2020).
- [25] S. S. Razamat, E. Sabag, and G. Zafrir, From 6d flows to 4d flows, *J. High Energy Phys.* **12** (2019) 108.
- [26] O. Bergman, M. Fazzi, D. Rodríguez-Gómez, and A. Tomasiello, Charges and holography in 6d (1, 0) theories, *J. High Energy Phys.* **05** (2020) 138.
- [27] F. Baume, J.J. Heckman, and C. Lawrie, Super-spin chains for 6D SCFTs, *Nucl. Phys.* **B992**, 116250 (2023).
- [28] J. Distler, M. J. Kang, and C. Lawrie (to be published).
- [29] D. D. Frey and T. Rudelius, 6D SCFTs and the classification of homomorphisms $\Gamma_{ADE} \rightarrow E_8$, *Adv. Theor. Math. Phys.* **24**, 709 (2020).
- [30] C. Lawrie, T. Lepper, and A. Mininno (to be published).
- [31] M. J. Duff, J. T. Liu, and R. Minasian, Eleven-dimensional origin of string-string duality: A one loop test, *Nucl. Phys.* **B452**, 261 (1995).
- [32] E. Witten, Five-brane effective action in M theory, *J. Geom. Phys.* **22**, 103 (1997).
- [33] D. Freed, J. A. Harvey, R. Minasian, and G. W. Moore, Gravitational anomaly cancellation for M theory five-branes, *Adv. Theor. Math. Phys.* **2**, 601 (1998).
- [34] J. A. Harvey, R. Minasian, and G. W. Moore, Non-Abelian tensor multiplet anomalies, *J. High Energy Phys.* **09** (1998) 004.
- [35] K. A. Intriligator, Anomaly matching and a Hopf-Wess-Zumino term in 6d, $N = (2, 0)$ field theories, *Nucl. Phys.* **B581**, 257 (2000).
- [36] P. Yi, Anomaly of (2, 0) theories, *Phys. Rev. D* **64**, 106006 (2001).
- [37] K. Ohmori, H. Shimizu, Y. Tachikawa, and K. Yonekura, Anomaly polynomial of general 6d SCFTs, *Prog. Theor. Exp. Phys.* **2014**, 103B07 (2014).
- [38] S.-J. Lee, D. Regalado, and T. Weigand, 6d SCFTs and $U(1)$ flavour symmetries, *J. High Energy Phys.* **11** (2018) 147.
- [39] F. Apruzzi, M. Fazzi, J. J. Heckman, T. Rudelius, and H. Y. Zhang, General prescription for global $U(1)$'s in 6D SCFTs, *Phys. Rev. D* **101**, 086023 (2020).
- [40] G. 't Hooft, Naturalness, chiral symmetry, and spontaneous chiral symmetry breaking, *NATO Sci. Ser. B* **59**, 135 (1980).
- [41] K. Ohmori, H. Shimizu, and Y. Tachikawa, Anomaly polynomial of E-string theories, *J. High Energy Phys.* **08** (2014) 002.
- [42] K. Intriligator, 6d, $\mathcal{N} = (1, 0)$ Coulomb branch anomaly matching, *J. High Energy Phys.* **10** (2014) 162.
- [43] F. Baume, M. J. Kang, and C. Lawrie, Two 6D origins of 4D SCFTs: Class S and 6D (1, 0) on a torus, *Phys. Rev. D* **106**, 086003 (2022).
- [44] C.-M. Chang and Y.-H. Lin, Carving out the end of the world or (superconformal bootstrap in six dimensions), *J. High Energy Phys.* **08** (2017) 128.
- [45] F. Baume, M. Fuchs, and C. Lawrie, Superconformal blocks for mixed 1/2-BPS correlators with $SU(2)$ R-symmetry, *J. High Energy Phys.* **11** (2019) 164.
- [46] F. Baume and C. Lawrie, Bootstrapping (D, D) conformal matter, *Phys. Rev. D* **105**, 046006 (2022).
- [47] N. Mekareeya, T. Rudelius, and A. Tomasiello, T-branes, anomalies and moduli spaces in 6D SCFTs, *J. High Energy Phys.* **10** (2017) 158.
- [48] N. Mekareeya, K. Ohmori, H. Shimizu, and A. Tomasiello, Small instanton transitions for M5 fractions, *J. High Energy Phys.* **10** (2017) 055.
- [49] N. Mekareeya, K. Ohmori, Y. Tachikawa, and G. Zafrir, E_8 instantons on type-A ALE spaces and supersymmetric field theories, *J. High Energy Phys.* **09** (2017) 144.
- [50] H.-C. Kim, S. S. Razamat, C. Vafa, and G. Zafrir, Compactifications of ADE conformal matter on a torus, *J. High Energy Phys.* **09** (2018) 110.
- [51] M. Del Zotto and G. Lockhart, Universal features of BPS strings in six-dimensional SCFTs, *J. High Energy Phys.* **08** (2018) 173.
- [52] J. Chen, B. Haghighat, S. Liu, and M. Sperling, 4d $N = 1$ from 6d D-type $N = (1, 0)$, *J. High Energy Phys.* **01** (2020) 152.
- [53] D. R. Morrison and W. Taylor, Classifying bases for 6D F-theory models, *Central Eur. J. Phys.* **10**, 1072 (2012).
- [54] M. B. Green and J. H. Schwarz, Anomaly cancellation in supersymmetric $D = 10$ gauge theory and superstring theory, *Phys. Lett. B* **149**, 117 (1984).
- [55] M. B. Green, J. H. Schwarz, and P. C. West, Anomaly free chiral theories in six-dimensions, *Nucl. Phys.* **B254**, 327 (1985).
- [56] A. Sagnotti, A note on the Green-Schwarz mechanism in open string theories, *Phys. Lett. B* **294**, 196 (1992).

- [57] J. de Boer, R. Dijkgraaf, K. Hori, A. Keurentjes, J. Morgan, D.R. Morrison, and S. Sethi, Triples, fluxes, and strings, *Adv. Theor. Math. Phys.* **4**, 995 (2002).
- [58] E. Witten, Toroidal compactification without vector structure, *J. High Energy Phys.* **02** (1998) 006.
- [59] Y. Tachikawa, Frozen singularities in M and F theory, *J. High Energy Phys.* **06** (2016) 128.
- [60] K. Ohmori, H. Shimizu, Y. Tachikawa, and K. Yonekura, 6d $\mathcal{N} = (1, 0)$ theories on T^2 and class S theories: Part I, *J. High Energy Phys.* **07** (2015) 014.
- [61] K. Ohmori, H. Shimizu, Y. Tachikawa, and K. Yonekura, 6d $\mathcal{N} = (1, 0)$ theories on S^1/T^2 and class S theories: Part II, *J. High Energy Phys.* **12** (2015) 131.
- [62] A. Hanany and A. Zaffaroni, Issues on orientifolds: On the brane construction of gauge theories with $SO(2n)$ global symmetry, *J. High Energy Phys.* **07** (1999) 009.
- [63] A. Hanany and B. Kol, On orientifolds, discrete torsion, branes and M theory, *J. High Energy Phys.* **06** (2000) 013.
- [64] D.R. Morrison and T. Rudelius, F-theory and unpaired tensors in 6D SCFTs and LSTs, *Fortschr. Phys.* **64**, 645 (2016).
- [65] P.R. Merks, Classifying global symmetries of 6D SCFTs, *J. High Energy Phys.* **03** (2018) 163.
- [66] O. Chacaltana, J. Distler, and Y. Tachikawa, Nilpotent orbits and codimension-two defects of 6d $N = (2, 0)$ theories, *Int. J. Mod. Phys. A* **28**, 1340006 (2013).
- [67] D. H. Collingwood and W. M. McGovern, *Nilpotent Orbits in Semisimple Lie Algebras* (Routledge, London, 2017), [10.1201/9780203745809-5](https://doi.org/10.1201/9780203745809-5).
- [68] J. Distler, B. Ergun, and A. Shehper, Distinguishing $d = 4$ $N = 2$ SCFTs, [arXiv:2012.15249](https://arxiv.org/abs/2012.15249).
- [69] J. Distler, M. J. Kang, and C. Lawrie, Distinguishing 6D $(1, 0)$ SCFTs: An extension to the geometric construction, *Phys. Rev. D* **106**, 066011 (2022).
- [70] P. Bala and R. W. Carter, Classes of unipotent elements in simple algebraic groups. II, in *Mathematical Proceedings of the Cambridge Philosophical Society* (Cambridge University Press, Cambridge, England, 1976), Vol. 80, pp. 1–18, [10.1017/S0305004100052610](https://doi.org/10.1017/S0305004100052610).
- [71] P. Bala and R. W. Carter, Classes of unipotent elements in simple algebraic groups. I, in *Mathematical Proceedings of the Cambridge Philosophical Society* (Cambridge University Press, Cambridge, England, 1976), Vol. 79, pp. 401–425, [10.1017/S0305004100052403](https://doi.org/10.1017/S0305004100052403).
- [72] H. Kraft and C. Procesi, Minimal singularities in GLn, *Inventiones Math.* **62**, 503 (1981).
- [73] B. Fu, D. Juteau, P. Levy, and E. Sommers, Generic singularities of nilpotent orbit closures, *Adv. Math.* **305**, 1 (2017).
- [74] L. Alvarez-Gaume and E. Witten, Gravitational anomalies, *Nucl. Phys.* **B234**, 269 (1984).
- [75] M. Fazzi, S. Giacomelli, and S. Giri, Hierarchies of RG flows in 6d $(1, 0)$ massive E-strings, *J. High Energy Phys.* **03** (2023) 089.
- [76] M. Fazzi and S. Giri, Hierarchy of RG flows in 6d $(1, 0)$ orbi-instantons, *J. High Energy Phys.* **12** (2022) 076.
- [77] H. Shimizu, Y. Tachikawa, and G. Zafrir, Anomaly matching on the Higgs branch, *J. High Energy Phys.* **12** (2017) 127.
- [78] Y. Tachikawa, A review of the T_N theory and its cousins, *Prog. Theor. Exp. Phys.* **2015**, 11B102 (2015).
- [79] M. Esole and M. J. Kang, Matter representations from geometry: Under the spell of Dynkin, [arXiv:2012.13401](https://arxiv.org/abs/2012.13401).
- [80] J. Distler and G. Elliot, Two applications of nilpotent Higgsing in class-S, [arXiv:2203.05040](https://arxiv.org/abs/2203.05040).
- [81] J. Distler, G. Elliot, M. J. Kang, and C. Lawrie, Isomorphisms of 4D $N = 2$ SCFTs from 6D, *Phys. Rev. D* **107**, 106005 (2023).
- [82] H. Osborn and A. Petkou, Implications of conformal invariance in field theories for general dimensions, *Ann. Phys. (N.Y.)* **231**, 311 (1994).
- [83] C. Córdova, T.T. Dumitrescu, and K. Intriligator, $\mathcal{N} = (1, 0)$ anomaly multiplet relations in six dimensions, *J. High Energy Phys.* **07** (2020) 065.
- [84] S. Deser and A. Schwimmer, Geometric classification of conformal anomalies in arbitrary dimensions, *Phys. Lett. B* **309**, 279 (1993).
- [85] M. J. Duff, Twenty years of the Weyl anomaly, *Classical Quantum Gravity* **11**, 1387 (1994).
- [86] D. Poland and D. Simmons-Duffin, Snowmass white paper: The numerical conformal bootstrap, in *Snowmass 2021* (2022), [arXiv:2203.08117](https://arxiv.org/abs/2203.08117).
- [87] T. Hartman, D. Mazac, D. Simmons-Duffin, and A. Zhiboedov, Snowmass white paper: The analytic conformal bootstrap, in *Snowmass 2021* (2022), [arXiv:2202.11012](https://arxiv.org/abs/2202.11012).
- [88] D. Gaiotto and E. Witten, S-duality of boundary conditions in $N = 4$ Super Yang-Mills theory, *Adv. Theor. Math. Phys.* **13**, 721 (2009).
- [89] A. B. Zamolodchikov, Irreversibility of the flux of the renormalization group in a 2D field theory, *JETP Lett.* **43**, 730 (1986).
- [90] Z. Komargodski and A. Schwimmer, On renormalization group flows in four dimensions, *J. High Energy Phys.* **12** (2011) 099.
- [91] H. Elvang, D. Z. Freedman, L.-Y. Hung, M. Kiermaier, R. C. Myers, and S. Theisen, On renormalization group flows and the a-theorem in 6d, *J. High Energy Phys.* **10** (2012) 011.
- [92] F. Baume and B. Keren-Zur, The dilaton Wess-Zumino action in higher dimensions, *J. High Energy Phys.* **11** (2013) 102.
- [93] A. Stergiou, D. Stone, and L. G. Vitale, Constraints on perturbative RG flows in six dimensions, *J. High Energy Phys.* **08** (2016) 010.
- [94] J. J. Heckman, S. Kundu, and H. Y. Zhang, Effective field theory of 6D SUSY RG flows, *Phys. Rev. D* **104**, 085017 (2021).
- [95] J. J. Heckman and T. Rudelius, Evidence for C-theorems in 6D SCFTs, *J. High Energy Phys.* **09** (2015) 218.
- [96] C. Cordova, T. T. Dumitrescu, and K. Intriligator, 2-group global symmetries and anomalies in six-dimensional quantum field theories, *J. High Energy Phys.* **04** (2021) 252.
- [97] K. Ohmori, Y. Tachikawa, and G. Zafrir, Compactifications of 6d $N = (1, 0)$ SCFTs with non-trivial Stiefel-Whitney classes, *J. High Energy Phys.* **04** (2019) 006.

- [98] S. Giacomelli, C. Meneghelli, and W. Peelaers, New $\mathcal{N} = 2$ superconformal field theories from \mathcal{S} -folds, *J. High Energy Phys.* **01** (2021) 022.
- [99] J.J. Heckman, C. Lawrie, L. Lin, H. Y. Zhang, and G. Zoccarato, 6D SCFTs, center-flavor symmetries, and Stiefel-Whitney compactifications, *Phys. Rev. D* **106**, 066003 (2022).
- [100] L. Bhardwaj, M. Del Zotto, J. J. Heckman, D. R. Morrison, T. Rudelius, and C. Vafa, F-theory and the classification of little strings, *Phys. Rev. D* **93**, 086002 (2016).
- [101] M. Del Zotto, M. Liu, and P.-K. Oehlmann, 6D heterotic little string theories and F-theory geometry: An introduction, *Proc. Symp. Pure Math.* **107**, 179 (2024).
- [102] M. Del Zotto, M. Liu, and P.-K. Oehlmann, Back to heterotic strings on ALE spaces. Part I. Instantons, 2-groups and T-duality, *J. High Energy Phys.* **01** (2023) 176.
- [103] M. Del Zotto, M. Liu, and P.-K. Oehlmann, Back to heterotic strings on ALE spaces: Part II—Geometry of T-dual little strings, *J. High Energy Phys.* **01** (2024) 109.
- [104] M. Del Zotto, M. Fazzi, and S. Giri, The Higgs branch of heterotic ALE instantons, *J. High Energy Phys.* **01** (2024) 167.
- [105] M. Del Zotto, M. Fazzi, and S. Giri, A new vista on the heterotic moduli space from six and three dimensions, *Phys. Rev. D* **109**, L021903 (2024).
- [106] H. Ahmed, P.-K. Oehlmann, and F. Ruehle, T-duality and flavor symmetries in little string theories, [arXiv:2311.02168](https://arxiv.org/abs/2311.02168).
- [107] C. Lawrie and L. Mansi, The Higgs branch of heterotic LSTs: Hasse diagrams and generalized symmetries, *Phys. Rev. D* **110**, 026016 (2024).
- [108] F. Baume, P.-K. Oehlmann, and F. Ruehle, Bounds and dualities of type II little string theories, [arXiv:2405.03877](https://arxiv.org/abs/2405.03877).
- [109] E. B. Dynkin, Semisimple subalgebras of semisimple Lie algebras, *Trans. Am. Math. Soc. Ser. 2* **6**, 111 (1957).
- [110] J. Patera, R. T. Sharp, and P. Winternitz, Higher indices of group representations, *J. Math. Phys. (N.Y.)* **17**, 1972 (1976); **18**, 1519(E) (1977).
- [111] P. Cvitanovic, *Group Theory: Birdtracks, Lie's, and Exceptional Groups* (Princeton University Press, 2020), ISBN 978-0-691-20298-3.
- [112] T. van Ritbergen, A. N. Schellekens, and J. A. M. Vermaseren, Group theory factors for Feynman diagrams, *Int. J. Mod. Phys. A* **14**, 41 (1999).
- [113] J. Erler, Anomaly cancellation in six-dimensions, *J. Math. Phys. (N.Y.)* **35**, 1819 (1994).
- [114] S. Okubo, Modified fourth order Casimir invariants and indices for simple Lie algebras, *J. Math. Phys. (N.Y.)* **23**, 8 (1982).
- [115] S. Okubo and J. Patera, General indices of representations and Casimir invariants, *J. Math. Phys. (N.Y.)* **25**, 219 (1984).
- [116] S. Okubo and J. Patera, On cancellation of higher order anomalies, *Phys. Rev. D* **31**, 2669 (1985).
- [117] S. Okubo, Quartic trace identity for exceptional Lie algebras, *J. Math. Phys. (N.Y.)* **20**, 586 (1979).
- [118] R. Feger and T. W. Kephart, LieART—A *Mathematica* application for Lie algebras and representation theory, *Comput. Phys. Commun.* **192**, 166 (2015).
- [119] R. Feger, T. W. Kephart, and R. J. Saskowski, LieART 2.0—A *Mathematica* application for Lie algebras and representation theory, *Comput. Phys. Commun.* **257**, 107490 (2020).
- [120] W. McKay, J. Patera, and D. Sankoff, The computation of branching rules for representations of semisimple lie algebras, in *Computers in Nonassociative Rings and Algebras* (Elsevier, New York, 1977), pp. 235–277.
- [121] C. Couzens, M. J. Kang, C. Lawrie, and Y. Lee, Holographic duals of Higgsed $\mathcal{D}_p^2(BCD)$, [arXiv:2312.12503](https://arxiv.org/abs/2312.12503).
- [122] O. Chacaltana, J. Distler, and A. Trimm, Tinkertoys for the E_6 theory, *J. High Energy Phys.* **09** (2015) 007.
- [123] O. Chacaltana, J. Distler, and A. Trimm, Tinkertoys for the twisted E_6 theory, [arXiv:1501.00357](https://arxiv.org/abs/1501.00357).
- [124] O. Chacaltana, J. Distler, and A. Trimm, Tinkertoys for the Z3-twisted D4 theory, [arXiv:1601.02077](https://arxiv.org/abs/1601.02077).
- [125] O. Chacaltana, J. Distler, A. Trimm, and Y. Zhu, Tinkertoys for the E_7 theory, *J. High Energy Phys.* **05** (2018) 031.
- [126] O. Chacaltana, J. Distler, A. Trimm, and Y. Zhu, Tinkertoys for the E_8 theory, [arXiv:1802.09626](https://arxiv.org/abs/1802.09626).